Charles University in Prague

Faculty of Science

Department of Plant Experimental Biology

Master Thesis

Characterization of eukaryotic translation initiation factor 3 subunits (eIF3) in *A. thaliana* male gametophyte

Bc. Filip Linhart

Supervisor: Said S. Hafidh, Ph.D.

Consultant: doc. RNDr. David Honys, Ph.D.

Prague, 2017

Experimental tasks presented in this work have been carried out at the Laboratory of Pollen Biology, Institute of Experimental Botany of Czech Academy of Science (ASCR, v.v.i.), Prague 6, Lysolaje, Czech Republic.

Prohlášení:

Tímto prohlašuji, že jsem vyhotovil tuto magisterskou diplomovou práci nezávisle pod školením pana Saida S. Hafidha, Ph.D., s doc. RNDr. Davidem Honysem, Ph.D. v roli poradce. Data a dokumenty jsou výsledkem vlastní práce, v opačném případě je to výslovně uvedeno a veškeré použité zdroje řádně citovány. Tato práce není předmětem obhajoby jakýchkoliv jiných akademických titulů.

Declaration:

I hereby state that I have completed this master thesis as an independent work, under the supervision of Said S. Hafidh, Ph.D. and with consultation of doc. RNDr. David Honys, Ph.D. Data and documents are from my own work, unless otherwise explicitly mentioned, in which case all used sources are formally cited. This thesis is not subject of any other defending academic titles.

Filip Linhart

Prague, August 2nd 2017

Acknowledgements

I would like to acknowledge my supervisor Said S. Hafidh. Ph.D. for his professional help and guidance through global work elaboration, scientific advice, technical assistance and organizational coaching for my investigations and experiments. I am also thankful for his assistance in formal and linguistic finalization of this thesis. I am also very grateful to my consultant and principle investigator of Laboratory of Pollen Biology, doc. RNDr. David Honys, Ph.D, for giving me the opportunity to achieve this work in his laboratory and for his precious advises. I would like to express my gratitude to the whole team of Laboratory of Pollen Biology, for having assisted me in my first practical laboratory experience and having created a motivating, professional and friendly atmosphere. Finally, I would like to acknowledge the support of my family and friends during this period.

This project offered a huge learning opportunity in time management, dealing with messy T-DNA lines, tidiness and most unforgettable pleasing an army type supervisor, and I am very grateful for that!

ABSTRACT

From RNA-to-protein, translation initiation and protein synthesis is mediated by trans-acting factors that recognize mRNA features common to almost all eukaryotes. Eukaryotic translation initiation factor 3 complex (eIF3) is a highly conserved protein complex that recognizes 5'-CAP elements of the mRNA to initiate translation. eIF3 consists of nine subunits, three of them having two isoforms: eIF3A, eIF2B1, eIF3B2, eIF3C1, eIF3C2, eIF3D, eIF3E, eIF3F, eIF3G1, eIF3G2, eIF3H and eIF3K. This work deals with functional characterization, expression and subcellular localization of eIF3B1, eIF3B2 and eIF3E in *Arabidopsis thaliana* male gametophyte and interaction of eIF3E with the Constitutive photomorphogenesis 9 (COP9) complex as a regulatory complex of eIF3E post-translational control. Here we show that depletion of *eif3b1* or *eif3b2* is not gametophytic lethal and that the two protein might function redundantly, whereas, knockout of eIF3E causes male gametophyte lethality. Interestingly, *eif3b1* show post-fertilization defects during embryogenesis, suggesting that its redundancy with eIF3B2 is restricted to the gametophyte. Gene expression studies revealed high expression of eIF3 subunits in actively dividing zones of leaf primordia, root meristem and root elongation zones as well as in the vegetative cell and sperm cells of the male gametophyte. The localization of the all three subunits was prominent around the vegetative cell membrane, in the vegetative cytosol in punctuate form as well as potentially in sperm cell membranes or sperm cells cytosol but not in any of the cells nuclei. Most intriguing, it was established that COP9 core subunit CSN7 (FUS5) and CSN1 (FUS6) are not essential in the male gametophyte and that the mechanism of eIF3E post-translational turnover by COP9 is not conserved in pollen.

Key words: plants, *Arabidopsis thaliana*, gametophyte, male gametophyte, pollen, pollen grain, pollen tube, silique, translation, mRNA, eukaryotic initiation factor 3, translation initiation factor 3, eIF3, constitutive photomorphogenesis, COP9 signalosome, CSN, transmission, expression, protein localization, knockout mutation

ABSTRACT IN CZECH

Od RNA k proteinu je iniciace translace a proteosyntéza zprostředkovávaná trans-vazebnými faktory, jež rozeznávají charakteristiky nRNA, společná téměř všem eukaryotům. Komplex tvořící eukaryotický translační iniciační faktor 3 (eIF3) je vysoce konzervovaným proteinovým komplexem, který rozpoznává složky 5' čepičky mRNA za cílem iniciace translace. eIF3 se skládá z devíti podjednotek, z nich tři mají dvě izoformy: eIF3A, eIF2B1, eIF3B2, eIF3C1, eIF3C2, eIF3D, eIF3E, eIF3F, eIF3G1, eIF3G2, eIF3H a eIF3K. Tato práce se zabývá funkční charakterizací, expresí a subcelulární lokalizací eIF3B1, eIF3B2 a eIF3E v samčím gametofytu *Arabidopsis thaliana* a interakcí eIF3E s komplexem Constitutive photomorphogenesis 9 (COP9) ve funkci regulačního komplexu posttranslační kontroly eIF3E. Ukazujeme, že ztráta funkce *eif3b1* či *eif3b2* se neprojevuje gametofytickou letalitou a že tyto dva proteiny se zřejmě funkčně doplňují, zatímco mutace *eif3e* má za důsledek letalitu samčího gametofytu. Pouze *eif3b1* projevuje defekty následně po oplodnění, během vývoje semene. Studie genové exprese, užívající veřejně dostupná data o expresi a promotorové aktivitě prokazují vysokou úroveň exprese podjednotek eIF3 v zónách s intenzivním buněčným dělením, tedy listového primodia, kořenového meristému a elongační zóny, taktéž jako ve vegetační buňce a spermatických buňkách samčího gametofytu. Lokalizace všech tří podjednotek se význačně projevila kolem membrány vegetativní buňky a v granulárním uspořádání v cytosolu, taktéž jako na úrovni spermatických buněk, kolem membrán a/nebo v jejich cytosolu. V žádném z buněčných jader nebyl výskyt detekován. Pozoruhodnějším faktem je konstatování, které se týká COP9 komplexu, jehož esenciální podjednotky CSN7 (Fus 5) a CSN1 (Fus 6) nejsou nezbytné v gametofytu. Rovněž chybí v pylu normálně přítomný mechanismus rychlého posttranslačního obratu eIF3E, zprostředkovávaný COP9.

Klíčová slova: rostliny, huseníček, *Arabidopsis thaliana*, gametofyt, samčí gametofyt, pyl, pylové zrno, pylová láčka, šešule, translace, mRNA, eukaryotický iniciační faktor 3, translační iniciační faktor 3, eIF3, konstitutivní fotomorfogeneze, COP9 signalozom, CSN, přenos, exprese, proteinová lokalizace, knockout mutace

CONTENTS

List of used abbreviations

ATP	Adenosine triphosphate
cDNA	Complementary DNA (reverse-transcripted)
Col-0	Columbia-0 ecotype
COP9	Constitutive photomorphogenesis 9 signalosome
CSN	Other name for COP9 signalosome
DABS	Decolorized aniline blue solution
DAPI	4',6-diamidino-2-phenylindole (DNA-binding stain)
DNA	Desoxyribonucleic acid
eIF	Eukaryotic translation initiation factor
ER	Endoplasmic reticulum
Fus	Fusca (purple phenotype mutation, here related to COP9)
GFP	Green fluorescent protein
GTP	Guanosine triphosphate
HM	Homozygous mutant
HT	Heterozygous mutant
LB	E.Coli cultivation medium/Left border T-DNA specific primer
Ler	Landsberg ecotype
LP/RP	Left primer/Right primer (gene specific)
MS	Murashige and Skoog medium
ms1	Male sterile mutant plants
ORF	mRNA open reading frame
PABP	PolyA binding protein
PCR	Polymerase chain reaction
RFP	Red fluorescent protein
RNA	Ribonucleic acid (mRNA: messenger, tRNA: transport, rRNA: ribosomal)
S	Svedberg (sedimentation coefficient)
Semi Q-RT	Semi quantitative reverse transcription
T-DNA	Target DNA (insertion)
UTR	mRNA untranslated region
UV	Ultraviolet
WT	Wild type (non mutant)
YEB	Agrobacteria cultivation medium

INTRODUCTION

Proteins are encoded by genes and ensure most of vital cellular chemical and structural processes. Regulation of their synthesis involves a polymorphic set of complex mechanisms that are widely studied, although far away of being fully characterized. After DNA transcription to messenger RNA, next important and complex mechanism is the translation of obtained transcript to a polypeptide of amino acids, which will become a functional protein. The initiation step of this translation process offers multiple regulation possibilities and is the subject of present work.

Several protein complexes are implicated in the assembly of translation initiation complex, allowing proper translational initiation and subsequent protein synthesis mediated by ribosomal subunits. One of these units is eukaryotic translational initiation factor 3, called eIF3, which plays a major mediating and structural function in the translation initiation process. Multitask function of this large complex is not yet fully characterized. The complexity of this unit is an important reason on investigating its specific functionalities, in a global way and specifically by characterization of the multiple subunits constituting the eIF3 complex.

This work is specifically focused on characterization of three eIF3 complex subunits in plants, precisely subunit eIF3B and its two isoforms eIF3B1 and eIF3B2, and subunit eIF3E. Major experiments are based on studying knockout mutant phenotype with focus on male gametophyte maturation and pollen tube viability. The second part of the thesis is dedicated to the characterization of cellular and subcellular localization of these essential proteins in the sporophyte, mature pollen and in growing pollen tubes. Their potential unique role in the male gametophyte with respect to mass mRNA storage and limited translation is an important subject of present and future investigation. Beyond that, present studies also incorporate COP9 signalosome regulatory complex, to investigate whether the mode of eIF3E protein modulation by COP9 is conserved in the male gametophyte.

AIMS OF THE THESIS

The objectives of this work are focused on understanding the mechanisms of eukaryotic translation initiation factor 3 (eIF3), more specifically its subunits eIF3B1, eIF3B2 and eIF3E in *Arabidopsis thaliana* male gametophyte, and include:

1. Characterization of *eif3b1*, *eif3b2* and *eif3e* knock-out mutant lines by phenotypic screening and transmission analysis.
2. Investigate promoter activities of eIF3B1, eIF3B2 and eIF3E by plant transformation and fluorescent microscopy as well as publicly available expression data.
3. Investigate subcellular localization of eIF3B1, eIF3B2 and eIF3E by plant transformation and fluorescent microscopy, colocalization with ER and PABP.
4. Analyze possible regulation of eIF3E by COP9 signalosome in the male gametophyte using knock-out mutant lines and fluorescent reporters.

Obtained results are aimed to increase the understanding of partially known information on the role of eIF3B1, eIF3B2 and eIF3E subunits in plant germ line particularly in respect to transcripts storage and mechanisms of translational activation.

I. GENERAL INFORMATION AND LITERATURE SURVEY

1. Studied organism features

Although mechanisms of translation initiation is highly conserved throughout eukaryotes, plants are organisms featuring specific characteristics and particularities in their life phases and in many occasions involved specialized mechanisms that deserve interest in specific and general context. Among plants, *Arabidopsis thaliana* is one of the preferred research model organisms.

1.1 Plant characteristics and life cycle

1.1.1 Introduction to plants particularities

Plants are sessile autotrophic organisms, producing organic compounds by photosynthesis, implicating carbon dioxide reduction by light energy-induced reaction. Plants are commonly characterized by their modularity and capacity of adaptation, which compensates their immobility. Plant cell is characterized by the presence of chloroplast organelle, which main role is to ensure the photosynthetic function, and by presence of pectocellulosic cell wall.

Like many eukaryotes, flowering plants massively use sexual reproduction, haploid phase of the plant life cycle termed a gametophyte, and a diploid phase called the sporophyte. Gametophyte is extremely reduced in higher plants, represented by pollen and an ovule, fully dependent on sporophyte in their development. After seed germination, the sporophyte develop as a vegetative phase, until producing generative organs (flowering) induced by age and perception of environmental factors. In most flowering plants (angiosperms), male and female organs are present in the same flower, anthers (andraeceum) producing pollen and pistil (gynaeceum) producing embryo sac containing two synergid cells, an egg cell, a diploid central cell and three antipodal cells. After fertilization, in selfed plant or between different individuals of same species, fused gametes develop to an embryo protected by a seed coat, mature seed later allowing starting of the new life cycle for the next generation.

1.1.2 *Arabidopsis thaliana* characteristics and life cycle

For our study, the model organism is *Arabidopsis thaliana*, an annual plant from Brassicaceae family. This reference organism in biological studies is appreciated for its easy cultivation, small size, quick life cycle (2 months from seeds to seeds) and simple, relatively small diploid genome with only five chromosomes and a total of approximately 135 megabase pairs, which

has been fully sequenced. Plants are usually cultivated on sterile peat Jiffy tablets, sometimes *in-vitro* or on nutritive medium. Arabidopsis is self-pollinating, preventing contaminations between lines. Each pistil contains about 60 embryo sacs. General appearance and life cycle aspect of Arabidopsis thaliana is shown in Figure 1.

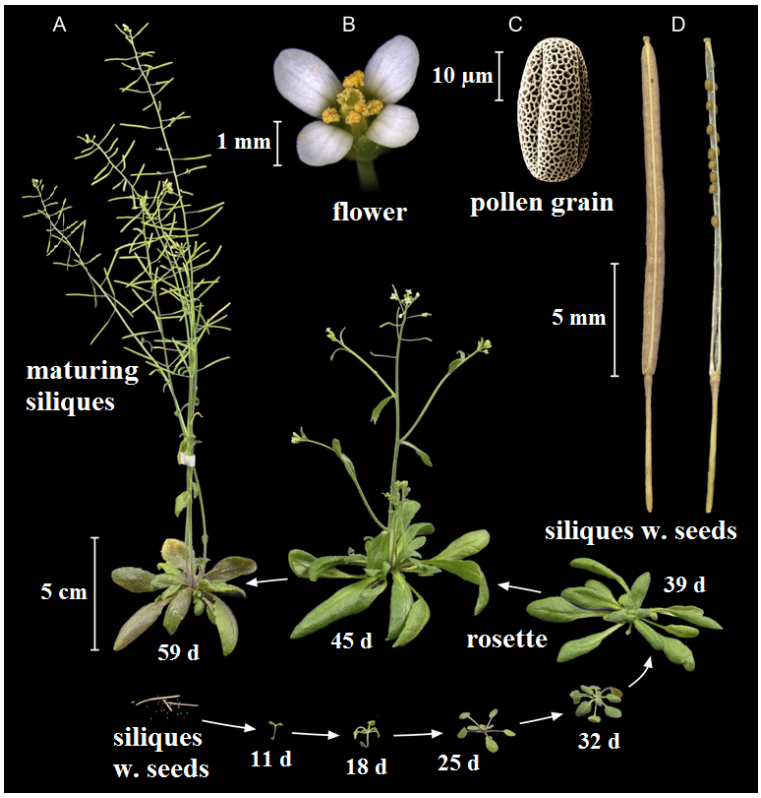

Figure 1. Life cycle steps and main organs of *Arabidopsis thaliana*. General aspect and cycle speed can vary between ecotypes. Source: modified from www.researchgate.net

1.2 *Arabidopsis* male gametophyte as a model

1.2.1 Attractive aspects of the male gametophyte as a model

Plant male gametophyte, commonly called pollen, is an extremely reduced and physiologically very active haploid organism with characteristics allowing multiple investigations in a simple way. Haploid state implicates that gametophytic mutants are carriers of a unique mutant allele after meiosis, allowing a direct phenotypical interpretation following knockout of the gene, which occurs in 50% of pollen grains, as well as a simple quantification of induced impairment by phenotypic observations and transmission frequency (Mccormick, 2004).

Multiple factors of interest motivating study of male gametophyte will not be exhaustively cited here. To mention few, we can cite for example mRNA storage, cytoskeleton dynamics, role of ionic gradients and intercellular interactions (Lin *et al.*, 2014), all of which show unique

characteristics compared to other plant tissues. For our work, one fact has to be evoked as being particularly relevant is; in growing pollen tube, stored messenger RNA translation plays a capital role in quick protein synthesis immediately after imbibition and in growing pollen tube (Honys *et al.*, 2000; Honys *et al.*, 2009; Rutley and Twell, 2015), a major reason to focus on this organism.

1.2.2 Male gametogenesis and maturation

Within the anthers of flowering plants, first developmental phase of pollen grain starts with microsporogenesis, which is similar to the process occurring in lower plants (*Cryptogamae*), where, generally, male gametophyte is constituted by a haploid microspore. As Figure 2 shows, microsporogenesis consists mainly of meiotic division, each pair of bi-chromatide chromosomes (after DNA replication) being segregated randomly in one of two cells after first divisions (meiosis I), each of those two cells then dividing into two identical cells containing monochromatide chromosomes (meiosis II). Obtained tetrad then dissociates, producing free microspores.

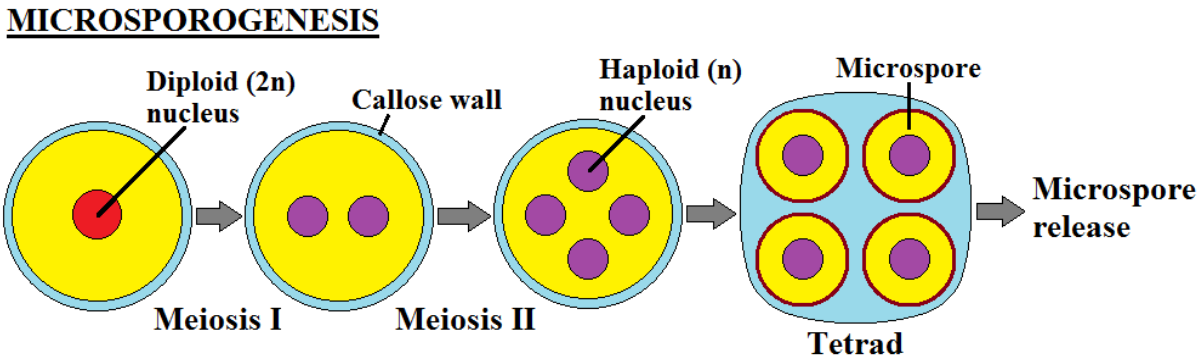

Figure 2. Steps of microsporogenesis, starting from diploid cell, leading to tetrad of haploid microspores after meiosis I and II.

After, each cell is vacuolised, polarized and the haploid nucleus divides in two identical nuclei during mitosis I, one becoming a vegetative nucleus, the second one enclosed into a second cell, called generative cell, internalized to the first larger vegetative cell, (Figure 3). Only the generative cell then goes through mitosis II (for most plants, already before maturation, sometimes after pollination), leading to two sperm cells, which will later ensure double fertilization of the female gametophyte (Figure 3). Whole pollen grain complete synthesis of a resistant exine coat, goes through de-vacuolisation, and then desiccates. Dry pollen grain, allowing water-independent fecundation and sperm cells delivery in recipient flower female gametophyte, is then released.

(Bedinger, 1992; Twell, 2011)

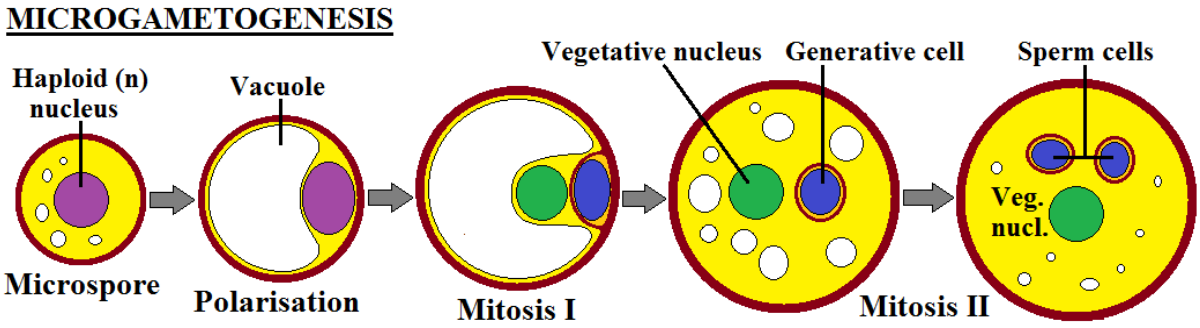

Figure 3. Steps of microgametogenesis, from microspores leading to pollen maturation and production of two sperm cells in anthers of angiosperms after two mitotic divisions

1.2.3 Pollination, pollen tube growth and fertilization

After microsporogenesis, microgametogenesis and dessication, pollen grain is released and lands on stigma of the gynoecium (female organ) of the flower, it undergoes rehydration, which is followed by pollen tube germination (Figure 4). A pollen tube grows through the pistil and reaches the embryo sac (the female gametophyte), penetrating it at the micropyle entry (Figure 4). Embryo sac contains one haploid egg cell, as well as two haploid polar nuclei. Egg cell is surrounded by two synergid cells, which are important in mediating the process of pollen tube attraction, guidance and sperm cells release. The male gametophyte sperm cells carried by the pollen tube are released and one of them fuses with egg cell, producing diploid zygote which will later develop to an embryo (Figure 4). The second sperm cell fuses with both polar nuclei, leading to the development of triploid endosperm, which play a role as nutritive tissue for the future embryo. This process, characteristic of angiosperms, is called double fertilization and leads to the development of a mature seed (Mccormick, 2004; Hamamura *et al.*, 2012; Dresselhaus and Franklin-Tong, 2013)

.

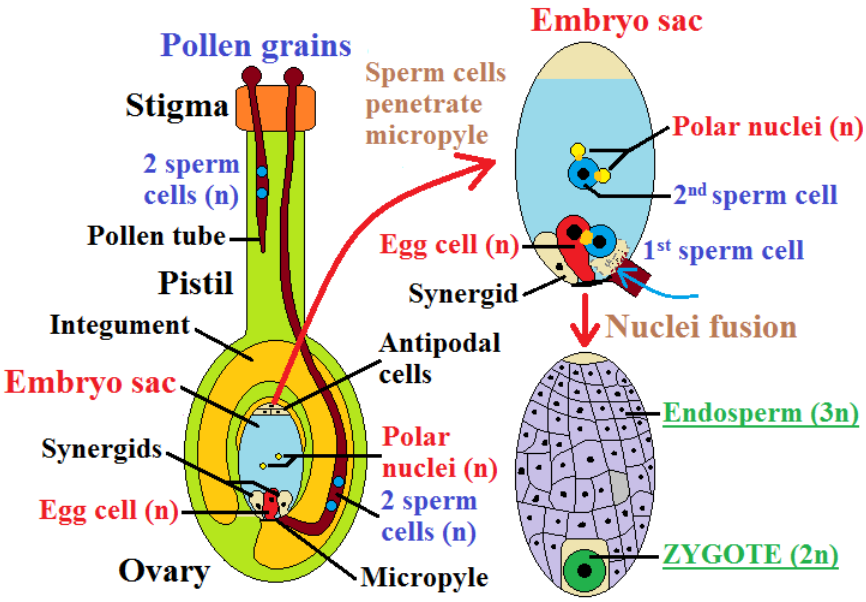

Figure 4. Common scheme of events following pollination and double fertilization process in angiosperms. Pollen grain lands on stigma and germinates, pollen tube grow through the pistil and penetrate the embryo sac at the micropyle through one of synergids. After sperm cells release by the pollen tube, we can see the sperm cells migration and subsequent fusion with egg cell and polar nuclei.

2. Translation of mRNA general description

2.1 From gene to protein, translational selectivity examples

In eukaryotic cell, a gene is first transcribed into pre-mRNA, which is stabilized by 5' methylguanosine capping, then 3' end receives poly(A) tail of multiple adenosine monophosphates. The RNA is then spliced, intervening sequences (introns) being removed in order to conserve final expressed sequence (exons). Obtained messenger RNA (mRNA) is exported to cytoplasm, waiting for the process of translation into a polypeptide chain to produce a functional protein.

However, translation do not systematically follow after the maturation and exportation of the mRNA; for example, in plants, mRNA transcripts can be stored for a long time in ribonucleoprotein complexes, allowing later quick intense protein synthesis. this is notable in case of abiotic stress, requiring energy saving, then quick metabolic restoration on recovery (Stuger *et al.*, 1999). Another case, which interests us particularly, is storage of transcripts in mature pollen grain, allowing quick metabolic processes starting immediately after rehydration of the pollen grain (Honys *et al.*, 2000; Honys *et al.*, 2009). This process is associated with notable selectivity between specific transcripts and show similarities as well as variability

between species (Hulzink *et al.*, 2002; Lin *et al.*, 2014; Rutley and Twell, 2015). This is also the case during seed imbibition and subsequent germination process (Galland *et al.*, 2014).

2.2 Translational initiation

2.2.1 Two separate complexes for mRNA and small ribosomal subunit

In eukaryotes, translational initiation follows an important number of initiation steps. First, mRNA transcript is circularized by the association of eukaryotic initiation factors 4 (eIF4), binding 5' cap through eIF4E and PolyA tail through PolyA binding proteins – PABP, eIF4G being a core structural factor of the complex and eIF4A having the helicase. Obtained complex is then ready for translational initiation, by the 43S pre-initiation complex described below (Figure 5A).

Ribosomes are implicated in the separate assembly of the second pre-initiation complex. More precisely, small 40S ribosomal subunit is bound by eIF1, eIF1A and eIF3 subunits, joined by eIF2 associated with met-tRNA (first initiation-specific transport RNA, bound with methionine aminoacid and guanosine triphosphate - GTP) (Figure 5B). We will not describe in details the precise characteristics of each initiation factor, but we will focus in this work on eIF3, the largest of all pre-initiation complexes.

2.2.2 Initiation complex assembly and translational initiation

Assembly of both described pre-initiation complexes (Figure 5C), mainly mediated by eIF3E from 43S complex binding with eIF4B and eIF4G bound with mRNA (giving rise to 48S translational initiation complex) occurs and is followed by mRNA scanning, with eIF4A serving as a molecular motor for this purpose and removing mRNA secondary structures (Figure 5C). 5' untranslated region (UTR) is scanned, then the first AUG start codon is identified, signaling the beginning of the open reading frame (ORF) which will actually be translated.

With the help of eIF5 and of hydrolysis of eIF2-bound GTP, the initiation complex bound to 40S ribosomal subunit dissociates and 60S large ribosomal subunit binds to the 40S, ribosome being assembled and translational elongation is initiated.

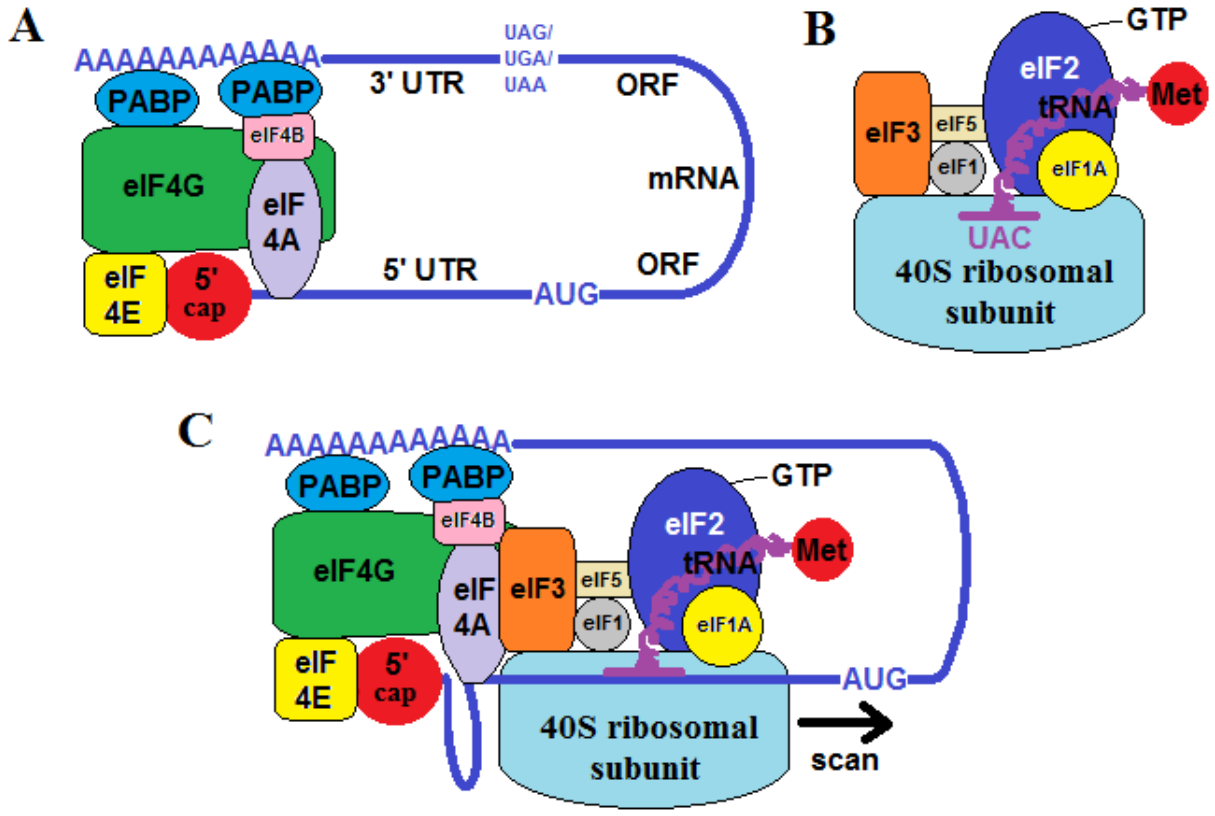

Figure 5. (A) mRNA with 5' cap and polyA tail, circularized by binding with eIF4 initiation factors. (B) 43S pre-initiation complex consisting in 40S ribosomal subunit bound with initiation factors and initiation tRNA with methionine. (C) Assembled 48S translational initiation complex, mRNA 5'UTR scanning phase occuring.

2.3 Translational elongation and termination

After translational initiation, the synthesis of the polypeptide from mRNA transcript begins. A complete ribosome assembly, constituted of pre-cited 40S and 60S subunits, and ribosomal RNA forms the catalytic complex. Transfer RNA (tRNA) with specific triplets codon supplies appropriate amino acids (after a catalyzation, leading to aminoacyl-tRNA) to the initiated polypeptide extension by binding with mRNA complementary triplets codons at A-site (aminoacyl-tRNA binding site) of ribosome. Peptidyl bond is catalyzed to add already synthetized polypeptide to the new amino acid.

The tRNA, now carrying the whole polypeptide, is translocated to central P-site position (peptidyl-tRNA binding site), while previous tRNA leaves ribosome at E (exit) site. The A site is free again with next triplet exposed for new specific aminoacyl-tRNA binding. This continues step by step until a STOP codon of mRNA appears on A site, binding with a release factor, leading to translation termination. The whole process is catalyzed by reactions taking energy from guanosine triphosphate (GTP) and adenosine triphosphate (ATP) hydrolysis, with the participation of elongations factors (eEF). (M.W.King, 2015)

A single transcript which is bound and translated simultaneously by multiple ribosomes is called polysome. Depending on the destination of synthetized protein, translation can occur in several cytoplasmatic locations, generally bound with endoplasmatic reticulum, but also freely in cytoplasm or bound with other structures as cytoskeleton (Kosowska *et al.*, 2004).

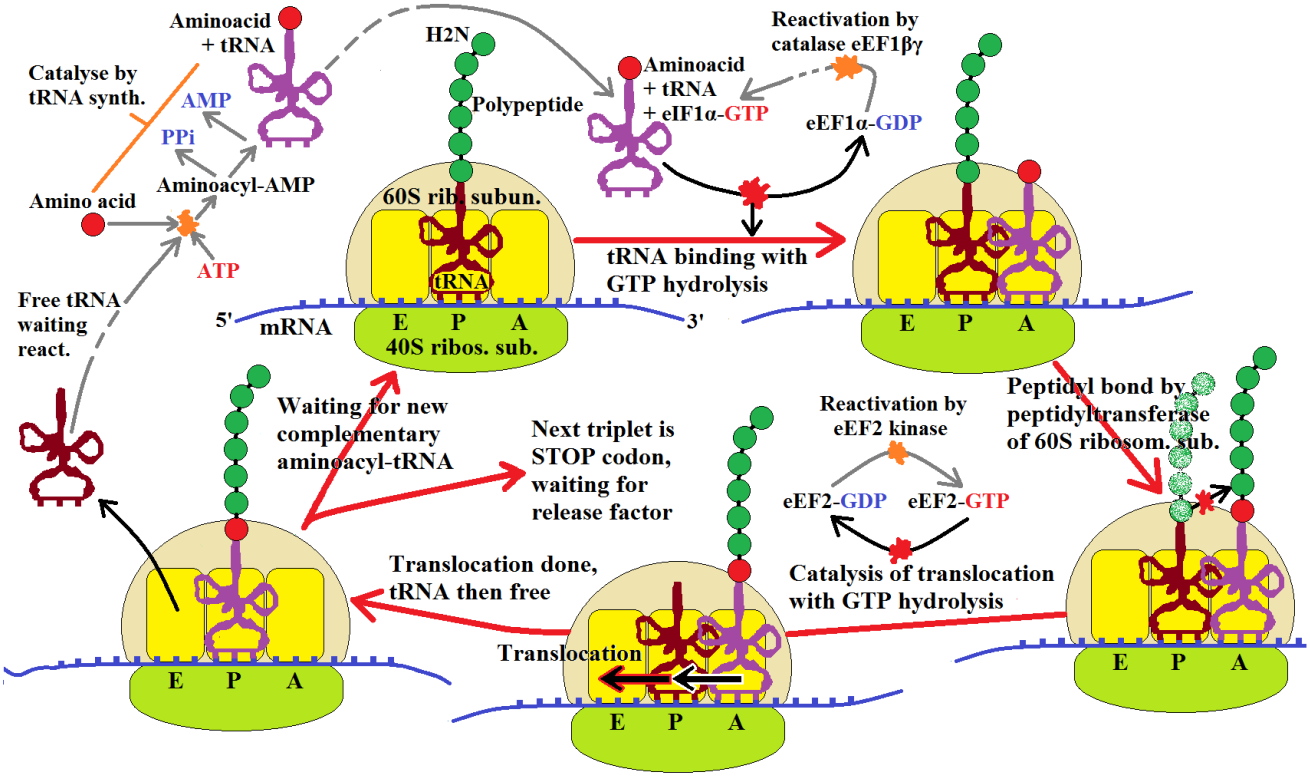

Figure 6. Schematically represented translational cycle which happens during each amino acid addition, following mRNA triplets sequence pattern. This scheme represents implicated mechanisms inside and outside ribosome. The starting of cycle is figured on the first representation of ribosome on the top-left, following steps being represented clockwise. Red arrows represent direction of the cycle; black arrows represent chemical reactions pathways of the process itself and grey arrows subsidiary related reactions.

3. Translational initiation factor 3 and its subunits

In this section, we will present a review about eukaryotic translational initiation factor 3 (eIF3), with focus on higher eukaryotes and, whenever possible, in plants.

3.1 General function and characteristics

3.1.1 Function and interactions

Eukaryotic translational initiation factor 3 (eIF3) is a multifunctional factor, playing roles in translational pre-initiation and initiation. This large protein complex promotes 43S complex assembly by binding with 40S small ribosomal subunit, eIF1 and eIF5, then promotes 48S

complex assembly through interaction with eIF4B, eIF4G and mRNA recruitment to the pre-assembled 48S complex (Burks *et al.*, 2001; Hinnebusch, 2006; Aitken and Lorsch, 2012). It also inhibits 60 ribosomal subunit association at this stage (Hinnebusch, 2006). eIF3 stays bound with 40S subunit during elongation and plays a role in ribosomal dissociation and translational reinitiation (Kolupaeva *et al.*, 2005; Mohammad *et al.*, 2017). However, exact involved mechanisms are far away from being fully understood.

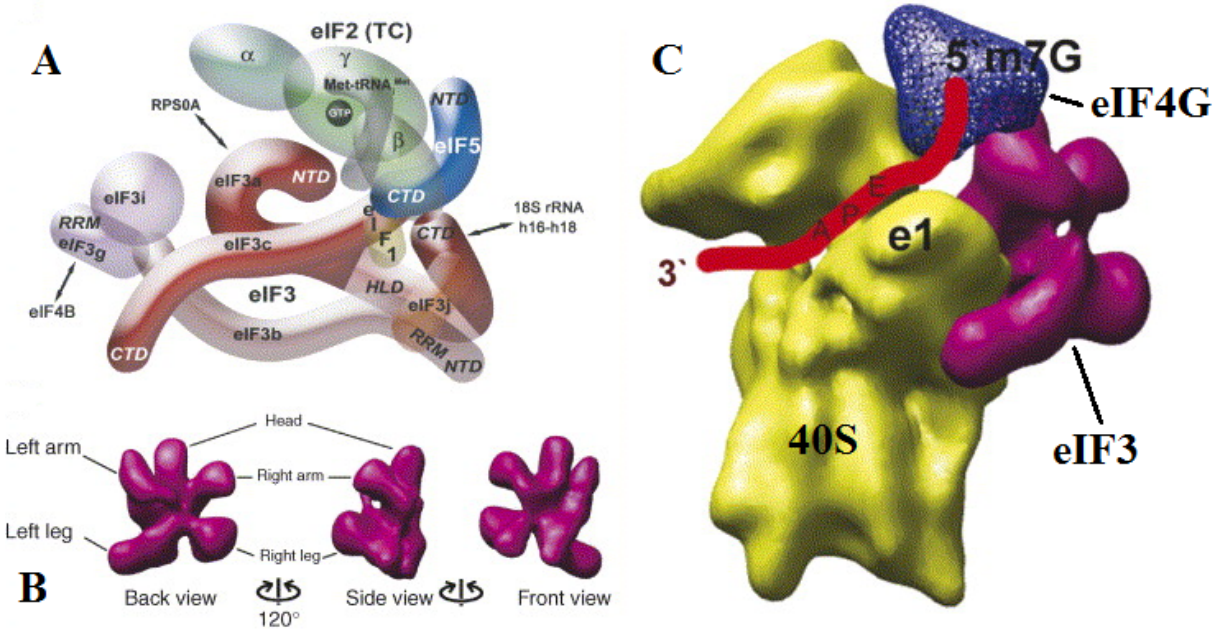

Figure 7. (A) Illustrative scheme of eIF3 interactions with other initiation factors in yeast. (B) Model giving an idea of spatial configuration of eIF3. (C) Model based on higher eukaryotes, showing eIF3 interaction with 40S ribosomal subunit (with mRNA) and with eIF4G. (Hinnebusch, 2006)

3.1.2 Structure and specificities in eukaryotes

eIF3 factor is a multiprotein complex, composed of 13 non-identical subunits in higher eukaryotes (Kolupaeva *et al.*, 2005). Some of these subunits are essential for translational initiation, referred as core subunits, others are non-essential (accessory) subunits and play regulation role (Hinnebusch, 2006), which is yet to be fully characterized . There are only minor differences between plant eIF3 complex and mammalian eIF3 complex, with the main differences concerning some accessory subunits (Burks *et al.*, 2001). eIF3A, eIF3B and eIF3C are conserved core subunits between eukaryotes while eIF3E, eIF3F and eIF3H become core subunits in higher eukaryotes, other subunits which may be essential in some organisms (such as eIF3I and eIF3G in budding yeast) are accessory in other organisms (Masutani *et al.*, 2007).

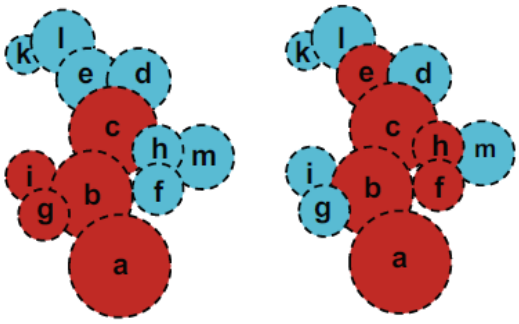

Figure 8. Illustration showing eIF3 core subunits in red and accessory subunits in blue in fission yeast (left) and mammals/plants (right), illustrating conservation and divergences. (Roy, 2010)

3.2 eIF3 subunit B

3.2.1 eIF3B general functions

eIF3B subunit has a major scaffolding function, in yeast as well as in higher eukaryotes, by interacting with at least four other eIF3 subunits, particularly eIF3A (Elantak *et al.*, 2007). It also plays a role in eIF3 complex interaction with 40S ribosomal subunit (Liu *et al.*, 2014). This interaction appears to be an interaction with ribosomal RNA (rRNA) as well as protein-protein interaction. eIF3B protein contains a RNA recognition motif, as well as a WD-40 β-propeller seemingly playing a role in interaction with uS4 ribosomal protein (Liu *et al.*, 2014). The contribution of eIF3B subunit (together with the contribution of eIF3A and eIF3C) to eIF3 affinity for 40S ribosomal subunit is quite important and the subunit also indirectly cooperates into mRNA recruitment function presented by eIF3 (Aitken *et al.*, 2016).

3.2.2 eIF3B isoforms in *Arabidopsis*

In *Arabidopsis thaliana*, eIF3B has two paralogs, eIF3B1 and eIF3B2. Protein of eIF3B1 is coded by gene AT5G27640 consisting of 11 exons and 10 introns, with an overall length of the Open reading frame (ORF) of the spliced mature mRNA being 2136 bp or 2214 bp for alternatively spliced isoform excluding the STOP codon (Figure 9). This translated sequence leading to a polypeptide constituted of 712 aa's and 738 aa's respectively. Protein of eIF3B2 is coded by gene AT5G25780 consisting of 11 exons and 10 introns. The overall length of the ORF is 2142 bp, leading to a polypetide chain of 714 amino acids (Figure 9).

Data obtained from The Arabidopsis Information Resource (TAIR) and alignment of the protein sequences showed more than 90% similarity in protein identity between eIF3B1 and eIF3B2 variants, suggesting a likely functional conservation. Another important fact is the existence of two isoforms for eIF3B1 protein, identified and available on TAIR database. This is a case of

alternative RNA splicing; in the longer isoform, a part of intron 2 becomes a part of an exon 3. When we aligned amino acids sequences of eIF3B1 longer isoform and eIF3B2 proteins, a main difference appears in RNA recognition motif domain, which is shorter in eIF3B2 compared to eIF3B1, due to an omission of 26 amino-acids present in eIF3B1 (Figure 9).

However, when we consider eIF3B1 protein shorter isoform, it is interesting to note that the missing part is located in RNA recognition motif domain and is practically the same as the "lost" sequence of eIF3B2 compared to eIF3B1 longer isoform (Figure 9). Thus, shorter eIF3B1 isoform has practically similar RNA recognition motif domain as eIF3B2, with only two omitted amino acids compared to the domain in eIF3B2.

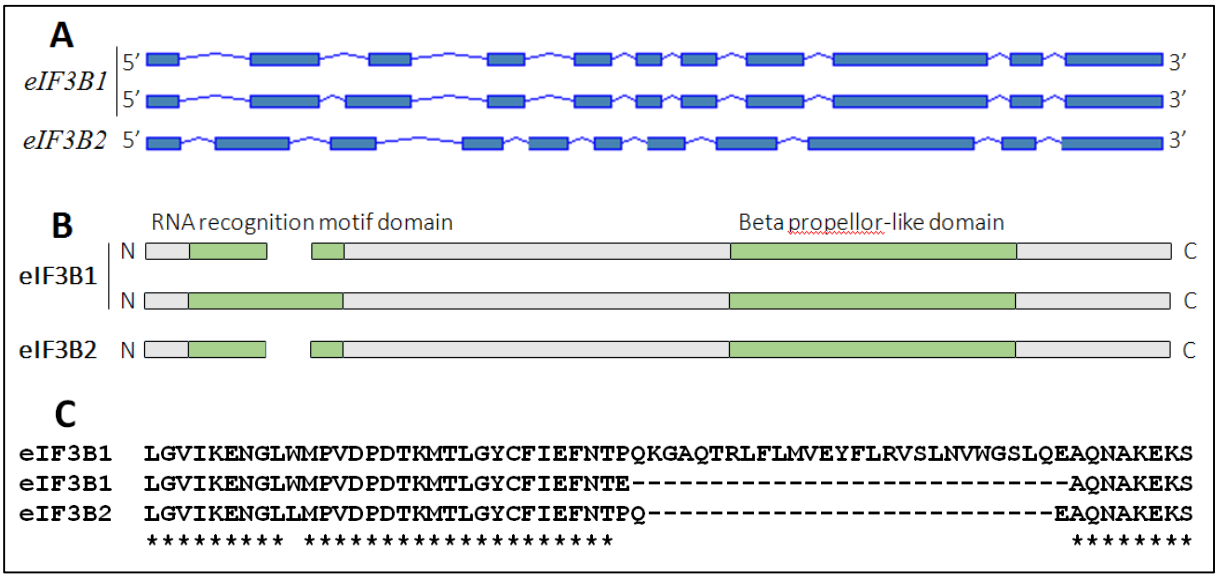

Figure 9. (A) Alignment of eif3b1 and eif3b2 genes, with alternative splicing for eif3b1. (B) General representation of the alignment of amino acid sequences of eIF3B1 isoforms and eIF3B2. We can see RNA recognition motif domain and Beta propellor-like domain, important for 40S ribosomal subunit binding function. (C) Alignment of amino acid sequences inside RNA recognition motif domain in eIF3B1 protein longer and shorter isoforms, and in eIF3B2 protein. This alignment has been done with M-Coffee sequence alignment tool. Note the extremely high conservation between eIF3B1 and eIF3B2 protein.

3.3 eIF3 subunit E

The next subunit of interest for this study is the eIF3E subunit, sometimes called Int6, divergent from eIF3B by sequence and features and having no direct physical interaction with eIF3B (Elantak *et al.*, 2007). In *Arabidopsis thaliana*, the gene coding eIF3E subunit is referenced AT3G57290 and is located on chromosome 3. It has 8 exons and 7 introns. Length of ORF is 1323 bp, translation producing a polypeptide of 441 amino acids (Figure 10). There are evolutionarily conserved similarities between eIF3E, Constitutive photomorphogenesis

signalosome (COP9) and proteasome lid subcomplex (Von Arnim and Chamovitz, 2003). It is important to mention the proteasome component (PCI) domain of the eIF3E located near C-terminal end of the polypeptide, facilitate multiple interactions.

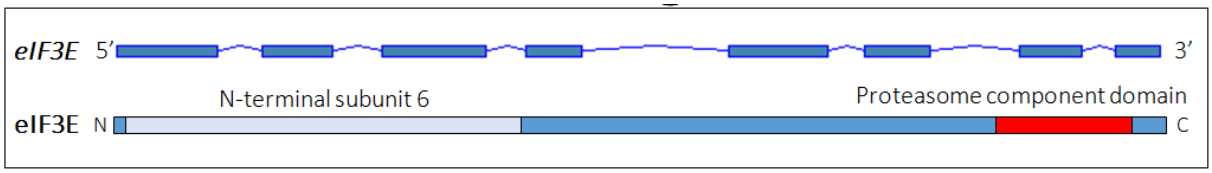

Figure 10. eif3e gene and eIF3E polypeptide chain, showing position of PCI domain.

Overall, eIF3E ensures eIF3 complex binding with mRNA cap binding protein eIF4G, this being an important function in 48S translational initiation complex assembly (Lefebvre *et al.*, 2006). Another notable fact is that subunit eIF3E is involved in general and specific protein synthesis rate modulation by regulating eIF4G phosphorylation status via an interaction with MNK1 kinase (Walsh and Mohr, 2014). In a general way, the importance of potential regulatory functions of eIF3E is known for several years (Von Arnim and Chamovitz, 2003) and has been studied in different contexts. It is interesting to observe eIF3E relatively high transcriptional abundance and its possible localization in different locations. What could be expected for a member of translation mediating complex, for example in nucleus (Yahalom *et al.*, 2001), which shows the putative functional multiplicity. Interaction with COP9 is a well-known example, as we will be described below. Furthermore, a direct influence on cell cycle through activation of cyclins has been reported at least in mammals (Morris and Jalinot, 2005; Sesen *et al.*, 2017).

4. COP9 signalosome and relation with eIF3E

4.1 Function and characteristics

COP9 is a multiprotein complex which is highly conserved between eukaryotic organisms and regulates target proteins through ubiquitin-proteasome pathway (Schwechheimer, 2004). The degradation of a target protein in the 26S proteasome is usually preceded by ubiquitination, conjugation and ligation by the E3 ubiquitin ligase. COP9 regulates the most important family of E3 ubiquitin ligases, the cullin-RING-ubiquitin ligases (CRLs), by deactivating them through dennedylation and sometimes preventing neddylation enzyme activity by remaining bound (Schwechheimer, 2004). This allows regulating the stability and turnover of proteins which are subjected to CRLs mediated turnover (Schwechheimer, 2004; Chung and Dellaire, 2015). In plants (and mammals), COP9 signalosome consists of 9 subunits, CSN1 to CSN8 and recently

discovered CSN acidic protein (Figure 11) (Rozen *et al.*, 2015). The subunit responsible for the dennedylation and possess isopeptidase activity, is CSN5 (Wei *et al.*, 2008).

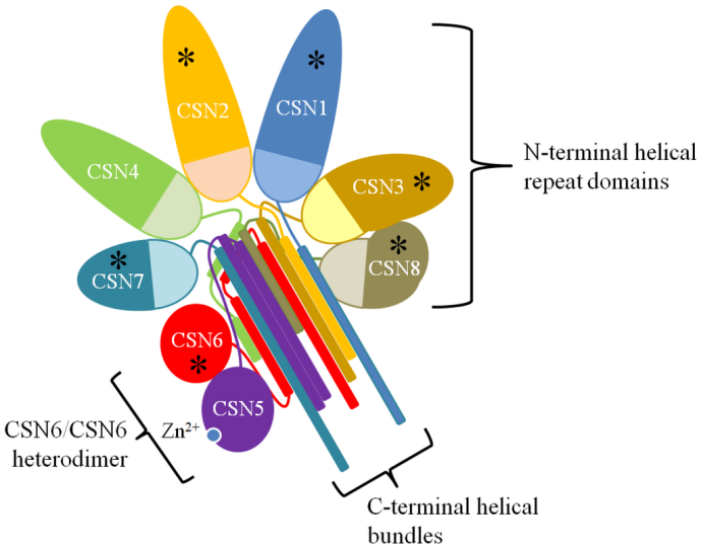

Figure 11. Schematic bidimensional representation of COP9 complex. Asterisk represents phosphorylation sites in some of the subunits, suggesting multiple levels of regulation of the individual subunits activities. Source: Chung and Dellaire, 2015.

CSN subunits 1 to 8 are all essential in *Arabidopsis thaliana,* as loss of function of any of these subunits leads to similar severe developmental defects during early stages of seed germination and result in seedling lethal phenotype (Wei *et al.*, 2008). These defects are very numerous, we can observe for example reduced germination, accumulation of anthocyanins (Kang *et al.*, 2000), altered light response (Karniol and Chamovitz, 2000) or meristem maintenance problems (Franciosini *et al.*, 2015), highlighting the essential requirement of the signalosome activities during seed germination and early seedling development.

4.2 Interaction with eIF3E

In this work, we selected to investigate further COP9 signalosome because of its known interaction with eIF3E (Yahalom *et al.*, 2008), more specifically in the context of the male gametophyte during the establishment of the male germline. First, we can say that the over-representation of eIF3E transcriptional level compared to other subunits of eIF3 is an interesting fact (see next chapter). Furthermore, it has been shown that eIF3E proteins accumulates in *Arabidopsis thaliana* COP9 signalosome mutants (Yahalom *et al.*, 2008). The consequence of an eIF3E over-accumulation appearing in or out of the context of COP9 knockdown is a global translational repression (Yahalom *et al.*, 2008), one important mechanism being association of free eIF3E proteins with eIF4G binding site, competing with whole complex association and preventing 48S initiation complex formation (Lefebvre *et al.*, 2006).

The extent of interactions between eIF3E and COP9 is seemingly larger than degradation promotion through the basic function of COP9 function. It is interesting that eIF3E and COP9 presents structural and evolutional similarities (Karniol and Chamovitz, 2000). It is proven that COP9 colocalizes at subcellular level with eIF3E and its CSN7 subunit can physically interact with eIF3E (Yahalom *et al.*, 2001). However, lack of recent studies in the continuation of cited projects makes the knowledge about this regulation pathway very poor and speculative and it is important to gather more information on the topic, by studying COP9 mutants and effect on eIF3E distribution in *Arabidopsis* sporophyte and the gametophytes.

II. MATERIALS AND METHODS

1. Plant material

1.1 In soil cultivation conditions

Arabidopsis thaliana plants were cultivated on plates and on Jiffy peat sterile tablets, under neon or LED lighting in a cultivation room, with a temperature of 20-22°C, with moderate humidity and 12 hours photoperiod. Startup fertilizer was given at seedling/early rosette stage, flower and fruit fertilizer at the beginning of generative growth. At advanced flowering and maturation stage, watering was reduced and plants going through senescence were put in maturation room. Seeds were collected from dry plants into Eppendorf tubes and let to completely dry by air for a few days to prevent mould development. Before planting, seeds were kept at -20°C for two days for stratification and for killing parasites.

1.2 *In vitro* cultivation protocol

Plants were sometimes cultivated on nutritive medium on petri dishes. This was necessary for antibiotic selections (for transformants and other mutants selection), during massive genotypings (segregation data) and for phenotypical comparisons at early stages. A laminar air flow cabinet (Flowbox) was used for manipulations for sterile working conditions.

1.2.1 Seeds sterilization

Sterilization by ethanol appeared to be insufficient to prevent occasional bacterial contamination. For this reason, it was decided to use more rigorous Savo with Igepal seeds sterilization technique. Seeds were placed in 1,5ml tubes, submerged by 1ml of 70% ethanol, than shaken for 5 minutes. Ethanol was then removed and replaced by similar volume of 10% Savo, which is a chlorine-based commercial disinfectant, with an addition of 0,1% Igepal® detergent. After 20 minutes of shaking, seeds were rinsed 5 times with distillate water in flowbox, and then the seeds were submerged in ethanol to allow pipetting into previously sterilized paper, to allow drying and subsequent plating.

1.2.2 Cultivation on ½ MS medium

Half strength Murashige and Skoog medium (½ MS medium) was used for *in vitro* plant growth. It is a medium based on agar, sucrose, macro and micronutrients, vitamins and organic compounds. After melting down, MS medium was spread on sterile petri dishes in flowbox, if necessary after mixing with antibiotic (after cooling down to prevent antibiotic degradation),

and let to solidify. Sterilized seeds on previously ethanol-imbibed papers were spread on the medium once dried, or deposed one by one when regular disposition was required (as for vertical culture growing experiments). Petri dishes were closed by Micropore™ tape, allowing gas exchanges while preventing pathogens penetration. Cultivation followed under LED cultivation lamps in controlled environment.

1.3 Pollination and pollen tube cultivation

1.3.1 Pollination, in vivo pollen tube growth

Male sterile plants, *ms1*, which present a specific mutation preventing them from producing viable pollen, were used for pollination with mutant pollen. Pollination was manually achieved under binocular microscope with the use of a forceps to depose pollen grains from exposed anthers on recipient plant stigma. One of the two usages of *ms1* plants was for crosses, particularly in order to study transmission through male gametophyte or to outcross background phenotype from T-DNA mutant lines.

As *ms1*plants are from Landsberg ecotype, while mutants to cross were mostly Columbia-0 ecotype (hybrids are not ideal for proper phenotyping), and, more important, to allow investigations on mutation transmission ratio through female gametophyte with wild type pollen donor, a more difficult alternative technique was also used for selective pollination: recipient flowers were emasculated by manual removing of anthers from an immature flower, which was subsequently pollinated two days later after recovery from emasculation.

When pollination was not done for crossing, but for *in vivo* pollen tube observations (with *ms1* plants in this case), a period of 20 to 22 hours was given to allow pollen germination and pollen growing through pistil. After this period, flowers were cut for fixation and further treatment (see section 4.2.2 for Aniline blue staining).

1.3.2 *In vitro* pollen tube growth

Pollen tubes of transformed plants were also grown *in vitro* on a solidified medium following a protocol allowing reliable pollen germination and pollen tubes observations by confocal microscopy (Boavida and Mccormick, 2007). Medium consists of 0.01% H_3BO_3, 5mM $CaCl_2$, 5mM KCl, 1mM $MgSO_4$, 10% sucrose and 1,5% low-melting agarose and its pH is adjusted to 7,5 with KOH. Liquid medium, stored in liquid state at 50°C incubator, was aliquoted on microscope slides to form a 2-3mm thick layer. Pollen was deposed on it once solidified, directly from an opened flower. Prepared slides were put in a glass petri dish, on wet absorbing paper to create humid environment, and petri dishes were sealed with Micropore™ film and

put in darkness at 22°C according to Boavida and McCormick, 2007. Observations of the pollen tubes were usually done after four hours.

2. DNA and RNA extraction and amplification by polymerase chain reaction

2.1 DNA extraction

Extraction of genomic DNA was the first essential technique required in order to allow genotyping and other investigations. Seedlings or rosette leaves were placed in a 1.5ml tube together with approximately 50-100 glass beads, and immediately put into liquid nitrogen. Frozen tissues were grounded for 30 seconds using a Silamat grinding machine, in order to break cell walls. Immediately after that, 250µl of DNA extraction buffer was added in each tube, 20 minutes of incubation allowing dissolving cell membranes. After this period, 250µl of a mix of chloroform - isoamyl alcohol (24:1 proportion) was added, followed by 10 minutes of spinning in a centrifuge at 13 000 rotations per minute (rpm). The top clear interphase was then transferred to a fresh tube containing 0.7 transfer volume of isopropanol. After several minutes, the tubes were mixed and spinned for 7 minutes, liquid phase being aspired after that by using an aspiration system based on Venturi effect, leaving DNA pellet at the bottom. DNA pellets were washed with 70% ethanol, shaken and again spinned for a few minutes and ethanol was then aspirated. After that tubes were put into vacuum-based desiccator in order to evaporate residual ethanol, and after a day, the DNA pellet was dissolved into 30 µl of distilled water. Samples were placed in 50°C incubator for 10 minutes to allow proper resuspension of the DNA pellet. Extracted DNA was used as a template in all further PCR amplification reactions.

2.2 RNA extraction and reverse transcription

2.2.1 RNA extraction

Qiagen RNeasy plant mini kit was used in order to extract RNA from plant tissues. Commonly chosen tissues were inflorescence (including flowers and flower buds), this choice allowing sufficiently representative transcriptome sample.

Collected tissues were deep frozen in liquid nitrogen. Prior to extraction, frozen tissues were grounded with mortar and pestle into a complete powder. RLT buffer was added to the grinded tissues, obtained liquid was transferred to QIAshredder spin column and spun for 2 minutes. Note that all spinning procedures were done at 8,000-13,000 rpm. Supernatant was then transferred to a tube containing 0.5% transfer volume of pure 99.8% ethanol. The samples were

then transferred to RNeasy spin column and spun for 15 seconds. A 500 ul of RW1 buffer was added to the column and spun for 15 seconds, followed by a 15 seconds and a 2 minutes spinning after addition of RPE buffer. A supplementary spinning for 1 minute with a new collection tube followed to allow drying of the membrane. RNA sample was finally eluted from the membrane with 30-50µl of RNAse free water and centrifuging for 1 minute in order to collect RNA in a 1.5ml collection tube.

As RNA is a very fragile biopolymer, many cautions have been taken during whole procedure, with strictly cleaned environment and using of RNaseZAP™ cleaner from Sigma-Aldrich to prevent degradation by omnipresent RNAses. Obtained RNA was stored in deep freeze -80°C environment, and reverse transcription systematically followed RNA extraction as soon as possible to avoid unfortunate RNA degradation after long term storage.

2.2.2 DNA-free treatment

Contaminant DNA is present in a non-negligible amount during RNA extraction, and that is why DNA-free treatment was systematically used after RNA extraction. Ambion® DNA-free™ kit was used for this purpose, being preferred to alternative methods for the absence of final heat treatment to inactivate DNAse, which was experienced as a source of RNA degradation prior to cDNA synthesis.

Standard reaction volume was 50µl, consisting of nuclease-free water, 10x DNase I Buffer, rDNaseI and RNA samples, these having been previously measured by spectroscopy (nanodrop spectrometer) and diluted in order to obtain identical concentration for each sample. Treatment was achieved at 37°C, DNase being added in two steps during one hour treatment, in order to obtain more rigorous treatment, as recommended by protocol. DNase Inactivation Reagent was then used to deactivate DNase at room temperature, and then separated by spinning for 1 minute at 8000 rpm. The supernatant containing treated RNA is then transferred into a fresh tube ready for reverse transcription reaction.

2.2.3 Reverse transcription

In order to obtain complementary cDNA from RNA samples, reverse transcription were done using ImProm-II™ Reverse Transcription System from Promega. As ribosomal RNA and tRNA, as well as small interfering RNAs are not the subject of this work, used technique features did not take care of those molecules, focusing on polyA tailed mRNA: oligo dT's (18 mers) primers consisting of a chain of thymine and binding to PolyA tail of mRNA were used for reverse transcription, giving a representative cDNA library of samples based on the isolated mRNA pool.

Technically, after DNase treatment, RNA was first mixed with random primers and denaturated for 5 minutes at 70°C and immediately chilled, to remove RNA secondary structures and facilitate reverse transcriptase amplification. 5µl of the treated samples were then added to 15µl of reaction mix, containing nuclease-free water, ImProm-II™ 5x reaction buffer, $MgCl_2$ solution for reaction enhancement, dNTP mix as a source of oligonucleotides for cDNA synthesis and ImProm-II™ Reverse Transcriptase for reaction catalysis. Using a thermocycler, primers annealing was achieved at 25°C during 5 minutes, followed by elongation (cDNA synthesis) at 42°C for one hour. Reverse Transcriptase was then inactivated by incubation at 70°C for 15 minutes. Obtained cDNA samples were stored at -20°C, ready to be used as PCR templates.

2.3 Polymerase chain reaction

The PCR technique has been used with several variations depending on the purpose of the experiment. Polymerase used for amplification requiring subsequent product isolation and its usage for cloning in order to transform plants was Phusion™ high fidelity polymerase, with proof-reading activity, minimizing the risk of product mutations, while all other PCR tasks of our project which does not require a future use of PCR product were done with a non-proof reading Merciáza™ Taq polymerase. Each polymerase uses specific reaction buffer and has different elongation speed. Optimal annealing temperature also appears to be higher with Phusion™ because of its thermal stability.

3. Mutant lines characterization

Arabidopsis thaliana has a wealth collection of mutant lines available in repositories donated by institutions such as SALK. The available mutant lines are an alternative to specific self-made induced mutations. For this work, only mutant lines from public repository were used, which unfortunately implicated some inherent problems, as will be explained in the results section.

3.1 Features of T-DNA insertion and point mutation lines used

Investigations of knock-out mutant alleles have been done for *eif3b1*, *eif3b2* and *eif3e* genes, and also for CSN7 (*fus 5*) and CSN1 (*fus 6*) subunits of COP9 complex. Note that the denominations Fus 5 and Fus 6 will be used to name COP9 subunits, as those denominations are most commonly used.

Most of the investigated mutant lines were T-DNA insertion lines, consisting of a section of T-DNA intercalated in part of the gene coding region or a promoter (Figure 12). A single point

mutation line *fus 5-1*, was also used (Figure 12). All lines, except *eif3b2*, were of heterozygous genotype. Antibiotical resistance gene is included in T-DNA insertions, allowing antibiotical selection of seedlings. However, for the massively used SALK T-DNA insertion lines, frequent silencing of the antibiotic resistant gene inducing kanamycin resistance tends to make this method of genotyping unreliable (tested in practice). Only Feldmann's line used for *fus 6-1* presented reliable antibiotical selection. Five mutant lines were used in practice. A review table showing all lines is available at Appendix 2.

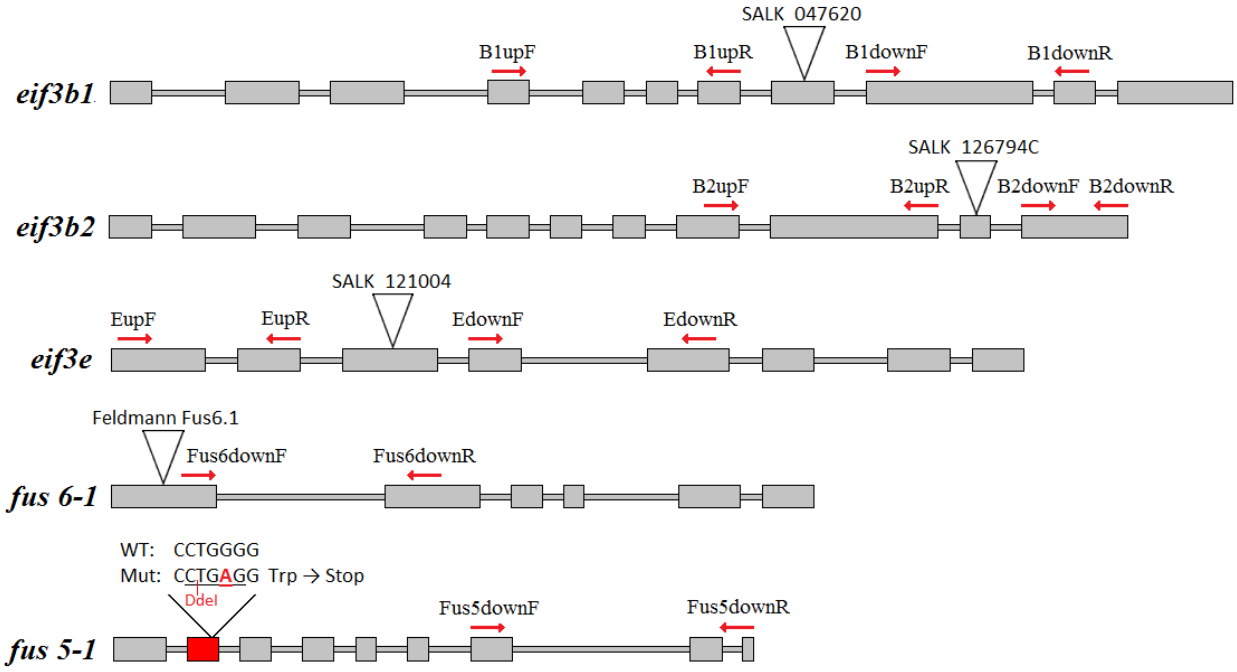

Figure 12. Schematic representation of studied genes showing exons (boxes), introns (lines) and the approximate position of T-DNA insertions or point mutation. Red arrows represent primers for semi-quantitative reverse transcription PCR (see section 3.3).

3.2 Genotyping methods

For T-DNA insertion lines, genotyping was achieved by designing a pair of primers, one located upstream of supposed T-DNA insertion site, the second one downstream. A third primer, named LB (left border) binds a specific region near the upstream end of the T-DNA insertion (SALK primers LB2 and LB1.3 were used, except for *fus 6-1* – see Appendix 3). This classical technique produce an amplicon between left and right gene-specific primers when T-DNA insertion is absent and amplicon between left gene-specific primer (or right primer, if reversed orientation) and the T-DNA specific LB primer in the presence of T-DNA insertion, this product being shorter. Wild type individuals show a longer fragment only, heterozygous mutants show two bands, longer and shorter fragments corresponding to amplification from

wild type and mutant alleles (biallelic), while a homozygous mutants show shorter fragment only corresponding to mutant amplicon.

For *fus 5.1* point mutation, genotyping was performed using dCAPS technique which involves amplification and digestion using an appropriate restriction enzyme (in the case of *fus 5.1* being DdeI restriction enzyme), that allows cleavage of mutant or wild type fragment as a result of gained/loss of restriction site brought about by the point mutation. Note that a similar technique was also used to genotype Male sterile *ms1*plants that are used for transmission and *in vivo* pollen growing.

3.3 *Semi*-quantitative reverse-transcription PCR

As mutations concerning our lines of interest are knockout mutations, there is no guarantee that the mutation completely impairs the function of coded protein, even though it is highly probable. Therefore *semi*-quantitative reverse transcription PCR (semi qRT PCR) technique was used to quantify amount of mRNA obtained from wild type and heterozygous lines using inflorescences as a tissue of choice.

For each gene, primers pairs were designed upstream and downstream to known T-DNA insertion / point mutation region of the gene (Figure 12). Amplification level obtained by PCR, visible through the band intensity on agarose gel, allowed evaluation of transcripts abundance for heterozygous/homozygous mutant compared to wild type plant. Note that used primer pairs were designed in order to amplify a region containing an intron: the intron being absent in cDNA, which eliminates the risk of biasing in case of presence of residual genomic DNA contamination.

Another caution consisted to add cDNA template already in master mix of the PCR reaction, before making aliquots for individual reactions, preventing results biasing through pipetting imprecision (potentially important for small volumes); note that cDNA template volume/concentration in PCR had to be adjusted for each gene in order to obtain clearly interpretable results.

To ensure unbiased interpretation, a constitutively expressed reference gene, in my case ubiquitin 10 (UBQ10, AT4G05320), as well as a reaction with genomic DNA template were always performed alongside genes of interest using a common master mix without primers.

4. Phenotypic screen of mutant lines

Multiple objectives were included in reverse genetics investigations, in order to observe effects of mutation on male and female gametophyte, as well as post fertilization. The objectives include notably the study of male gametophyte maturation defects, in-vivo growth of pollen tube fitness, fertilization and general transmission ratio statistics, all this being a measure of gene function on plant fitness with the focus on gametophyte.

4.1 Screen of sporophytic phenotype

Sporophytic phenotype was mainly evaluated by direct observation of in soil cultivated plants compared to wild type individuals of same ecotype grown in similar conditions. Vertically *in vitro* growth on MS medium was occasionally done in order to achieve a more accurate comparison on young seedlings.

4.2 Pollen phenotype observations

4.2.1 Mature pollen grains phenotype observation by DAPI staining

The first systematical experiment consisted of observation of mature pollen grains, using GUS buffer and DAPI staining (4µl of DAPI in 15ml of GUS), DAPI being a fluorescent molecule which binds to Adenine and Thymine bases of DNA. This solution has to be conserved in refrigerator and in darkness and samples can be conserved up to 3 weeks. Mature flowers were put in this solution and shaken, in order to release pollen, spun down to allow pollen sedimentation and sampling by pipetting. Observations were done in bright field to observe general pollen grains morphology, and under ultraviolet with appropriate filter to see vegetative and the generative cells of the male germ unit with the help of DAPI fluorescence, and to characterize and count germ cell division defects. Generally, 200 pollen grains were counted per plant in order to obtain relevant statistics, and a minimum of 7 plants were screened per line for reproducibility.

4.2.2 *In vivo* pollen tube phenotype observation with aniline blue

Another commonly used technique for pollen grain fitness investigation is the study of pollen tube growth inside the pistil of a manually pollinated *ms1* plant. After 20-22 hours of pollen tube growth, flowers were collected and submerged into fixative solution for 2-3 hours. Samples were then rehydrated by replacing fixative with 70% ethanol, followed by 50%, 30% ethanol and finally in distilled water. Alkaline treatment with 1M NaOH solution was then performed over night. Tissues were rinsed with distilled water for 15 minutes followed by

application of decolorized aniline blue solution (DABS) for 2-3 hours in the dark allowing coloration of callose, which is a major component of pollen tube cell wall (Mccormick, 2004). Obtained samples were either visualized immediately or stored at +4°C in the dark for later observations.

Microscopical observation under UV irradiation allows visualization of the proportion of pollen tubes growing through the pistil and a comparison between wild type pollen tubes and pollen tubes coming from mutant plant pollen. Note that it is important to take into consideration pollen loading on stigma, as well as photographical exposure time. Wild type pollen was systematically used for comparison in each experiment and pollen loading was photographed in bright field in order to assess pollen grain loading and to choose comparable samples. Such an observation remains semi-quantitative, but useful in the frame of our investigations.

4.3 Siliques phenotype observation

Siliques phenotyping naturally follows ongoing investigations of possible post-fertilization defects caused by mutated genes. *Arabidopsis thaliana* silique usually contains 40 to more than 60 seeds, which are the result of the same number of fecundated female gametophytes. As fecundation can be impaired by several male/female gametophyte mutations as well as a compromise in embryo development, I decided to proceed to a global screening of siliques phenotype in plants carrying mutations of the gene of interest.

We usually observe two classical examples of impaired seed development, one case of unfertilized gametophyte/very early developmental abortion after fertilization (we will call this phenotype as “unfertilized seed” in a general way), and one case of a seed resulting from proper fertilization, but having experienced a deficiency later in embryo/endosperm development, leading to the death of the seed (we will call this phenomenon as “collapsed seed”).

Obtained results have to be taken with caution, mainly because each female gametophyte has two chances of being fecundated, the two synergid cells contained in embryo sac offering two fertilization attempts (Dresselhaus and Franklin-Tong, 2013); proper comparison with other data (transmission, male gametophyte phenotype) is necessary for clear conclusions. Some siliques can also be accidentally affected by a high rate of failed seeds developments, that is why 5-6 siliques have been screened per plant from a minimum of 7 plants per line.

5. Generation of constructs for promoter and protein localization

A routine investigation in cellular and molecular biology for gene function consists in studying promoter expression patterns and protein localization and distribution in different tissues at the cellular and subcellular levels. Several techniques using for example fluorescent microscopy have been developed. For instance promoter fusion with a fluorescent coding protein as a reporter of promoter activities throughout plant development. Obtained results give much useful information allowing deducting numerous important facts on a putative gene function.
In this work, eIF3B1, eIF3B2 and eIF3E have been tracked by association with Green Fluorescent Protein (GFP). Promoter activity was also investigated in a *semi*-quantitative way, mostly as verification at the tissue level. Similarly, full-length proteins of interest driven by their native promoters were tagged with GFP to report protein subcellular localization. Colocalization between individual subunits and other cellular structures were also performed. This experiment is also the first step for further investigations on COP9 mutation effects in relation to eIF3E regulation.

5.1 Gene cloning

For all the constructs, a Gateway® gene cloning technique was used to create promoter-reporter destination vectors as well as protein fusion-reporter destination vectors. All vectors were then transformed into *Agrobacterium tumefaciens* to facilitate plant transformation.

5.1.1 Creation of Gateway™ entry clones

The initial step in creating gateway destination vector is the integration of the sequence of interest into an entry clone that will be further used in a recombination reaction to create a destination vector. Sequence was first amplified from wild type genomic DNA template by PCR amplification. Primers used for amplification were designed to add specific attB sequence at 5' and 3' end that will serve as recombination sites for integration of the amplicon. First reaction consisted of gene-specific amplification with only half of attB sequences, followed by a second PCR with attB primers, using the product of first reaction as a template in order to obtain a product flanked with full length attB sequences at both ends. Note that one or two bases had to be intercalated in the primers between gene-specific and 3' attB sequence in order to follow open reading frame (ORF) in destination vector, to ensure proper marker translation

together with gene. Polymerase used for this amplification was Phusion™ high fidelity polymerase.

After running gel electrophoresis, products were isolated from gel by using Qiagen gel extraction kit. After cutting the products under UV, gel samples were put into Buffer QG for melting at 50°C, the sample being then mixed with isopropanol and centrifuged into a QIAquick spin column for 1 minute at 13,000 rpm. This step was followed by DNA washing with 750µl Buffer PE and 1 minute spinning. After that, 30µl of Elution buffer was added on the column membrane, incubated for few minutes at room temperature and spun for 1 minute to elute DNA into a 1.5ml tube. Obtained concentrations were usually low (approx. 10ng/µl), but sufficient for next step.

Obtained product was then integrated in pDONR221 donor vector in order to obtain entry clone in a reaction catalyzed by BP Clonase™. Obtained products were mixed with 1:3 molar ratio proportion of donor vector, with 2µl of BP Clonase™ and TE buffer, for a 10µl reaction and kept at 25°C for one hour (or more) before deactivation by Proteinase K (10min at 37°C).

5.1.2 Bacterial transformation and plasmid purification

Obtained plasmid was then transformed into TOP10α Escherichia Coli bacteria by heat shock: competent bacteria cells were taken out from -80°C deep freeze, mixed with 3µl of the BP reaction product and kept on ice for 30 minutes before heat shock at 42°C for 30 seconds in a water bath. Transformed cells were quickly re-chilled, and then put into 250µl of SOC medium for one hour of incubation at 37°C, allowing plasmid replication and expression of antibiotic resistance gene.

Transformant bacteria were put on petri dish with LB-agar culture medium containing kanamycin antibiotical selection (medium preparation and bacterial culture being done in flowbox under sterile conditions). After 24 hours of cultivation at 37°C, several colonies were obtained on the medium. In order to check the presence of correct entry clone in the colonies, colony PCR was performed with gene specific primers, using directly bacteria as PCR reaction template. Note that previous reapplication and re-culture of obtained colonies into stripes on a fresh Petri dish is a common rule, not only for practical reasons, but also in order to prevent false positives in colony PCR, as BP reaction product applied on LB medium together with transformed bacteria can be sufficient to act as a template by itself.

Positively identified colonies were then cultivated in LB broth liquid culture at 37°C overnight with vigorous shaking, allowing amplification of entry clone quantity. Qiagen Miniprep kit was then used for plasmid isolation as follow: After pelleting 3 ml of the bacteria cells, the pellet

was resuspended with 250µl of resuspension buffer. The same volume of lysis solution was then added, followed by the addition of 350µl of neutralization solution. The tube was centrifuged for 5 minutes at 13,000 rpm, then the supernatant was transferred to GeneJET spin column and centrifuged for 15 seconds. Two centrifugations with 500µl of wash solution then followed. After a last dry centrifugation in order to remove excess ethanol from the column membrane, DNA was eluted into a 1.5ml tube with 50µl of elution buffer by spinning at full speed for 1 minute.

5.1.3 Verification of vectors by restriction digest and sequencing

Obtained isolated plasmids were first checked by restriction, a digestion with available enzymes being first simulated in silico using SnapGene software. Cut sites were chosen whenever possible within cloned gene sequence. Vector digestion was achieved by using the chosen restriction enzymes combination together with associated buffer. Products of restriction digest where assessed by gel electrophoresis. Beyond this first check, confirmation by sequencing was systematically done. Sequencing primers were designed approximately 700 base pair intervals on cloned sequence and mixed with the plasmid solution, before sending for sequencing to GATC Biotech, Germany.

5.1.4 Creation of destination clones and agrobacterium transformation

Once proper entry clone were confirmed, LR reaction catalyzed by LR Clonase™ was used to integrate sequence contained in entry clone into a binary destination vector, which includes sequences for genomic integration, antibiotical selection genes for selection of transformed seeds, potential other markers and fluorescent protein coding sequence, immediately following cloned gene. The procedure used to create, amplify, isolate and check destination vector was similar to the procedure used for entry clone, and LR reaction is similar to BP reaction, cloned gene being replaced by entry clone and donor vector being replaced by destination vector. Spectinomycin was the antibiotic used for bacterial selection. Two destination vectors were used to successfully clone fragments of interest: pB7FWG for promoter cloning (after a failed attempt with a mutated pKGWFS7 vector allowing no selection) and pFASTR07 for whole gene cloning (Figure 13).

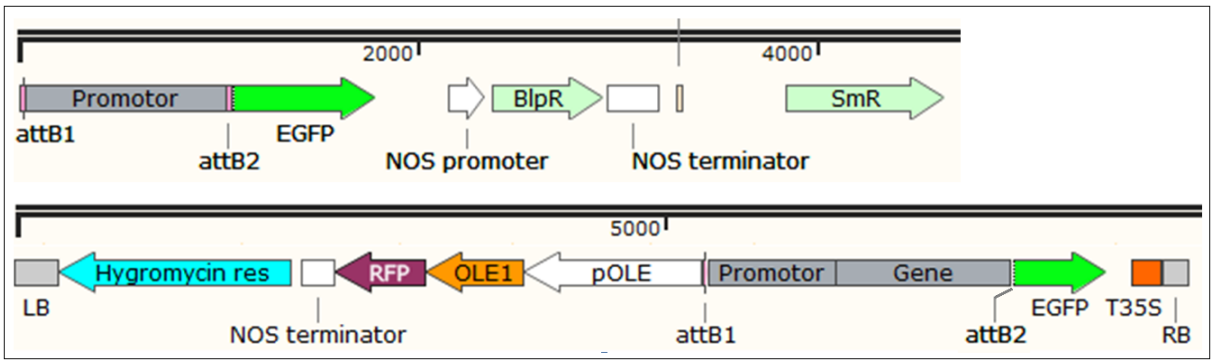

Figure 13. Top: T-DNA section from pB7FWG vector in a linearized overview map used for reporter genes. SmR confers resistance to spectinomycin in E. Coli and agrobacterium, BlpR confers resistance to phosphinotrycin (commercial name BASTA) in plants. Bottom: T-DNA section from pFASTR07 vector used for protein localization. We can see OLE1 oleosine coding gene with RFP marker for seed selection.

Next step consisted of *Agrobacterium tumefaciens* GV3101 transformation by using electroporation. This was achieved by an electroporating machine (Eporator from Eppendorf). YEB liquid culture specific for culturing Agrobacterium was prepared, 2µl of destination vector being then transferred to 30µl of Agrobacterium competent cells. This mix was transferred to electroporating cuvette, and subjected to 2000V under 5.8ms. Electroporated cells were recovered with 950µl of chilled YEB medium and transferred into 1.5ml Eppendorf tube. This was followed by a culture on YEB medium with agar on Petri dishes, with triple selection of antibiotics (gentamycin, rifampicin and vector-specific antibiotic – spectinomycin for this case). Note that optimal growing temperature is 28°C for Agrobacteria and growing speed is twice slower compared to E.Coli.

Another colony PCR followed, positive colonies being subsequently used for plant transformation. Sequencing was not repeated again at this step. For long term storage of transformed bacteria, glycerol-bacterial culture were systematically produced from liquid cultures, 300µl of 80% glycerol being added to 700µl of bacterial culture with antibiotical selection before freezing and conservation at -80°C. The same measure was taken for previously described E.Coli bacterial cultures. This allows years-long conservation for a quick re-use for further experiments without the need of new bacterial transformation.

5.2 Plant transformation by floral dipping technique

5.2.1 Plant dipping procedure

Transformed *Agrobacterium tumefaciens* GV3101 were cultivated in liquid YEB medium, with triple selection of antibiotics, in order to apply Clough and Bent, 1998 plant transformation protocol (Clough and Bent, 1998). After removal of siliques, plants in early flowering stage

were dipped for 45 seconds into infiltration media containing resuspended pellet of previously spinned agrobacteria, MS salts (2,165g/l), Gamborg vitamins (3.16g.l), 2-[N-Morpholino] ethanesulfonic acid (0,5g/l), sucrose (50g/l), benzylaminopurine (1g/l) and Silwet L-77 commercial product (300µl/l). Plants were kept in darkness for 24 hours and later returned in a normal plant growth circle of 16 hours light.

5.2.2 Selection of first and second generation of transformants

Transformed seeds ratio does not exceed 1-2% in the first generation. For pB7FWG transformants, transformed plants were selected on ½ MS medium plates containing 10µg/ml of phosphinotrycin, whereas for pFASTR07 transformants, oleosine:RFP (Red Fluorescent Protein) marker expressed in seeds was used to select first generation of transformants. The antibiotic resistance gene failed to function fully and hence was not used for plant selection.
Fluorescent expression is variable between transformants, so the selection was mainly based on expression level screening in sporophyte and male gametophyte; effort was done in order to produce a homozygous second generation, but this was not possible in every construct. For eIF3B2 promoter-reporter transformants, expression in male gametophyte was very weak in the first generation, but fortunately, second generation offered better results. For protein-GFP transformants, we were able to obtain homozygous lines for eIF3E and eIF3B1. Even though obtaining homozygous transformants is not a capital objective, it constitutes an objective by principle, making further investigations easier by the existence of homogenius lines.

6. Promoter activities and protein localization

6.1 Samples preparation

6.1.1 Used tissues and preparation specificities

Analyzed tissues were 5-days old seedlings cultivated on ½ MS medium, as well as rosette leaves fragments and mature pollen from in soil cultivated plants. *In-vitro* grown pollen tubes were also used. Distillated water and specific buffers for reference tissue staining were used for the preparation.

6.1.2 Tissue-specific reference stainings

In order to obtain a reference for proper orientation into observed tissues, propidium iodide and DAPI nucleotide-intercaling agents were used. Endoplasmatic reticulum tracker was also tried once, but without satisfactory results. Obtained pictures are systematically given as a reference together with pictures showing protein:GFP or reporter gene-coded GFP expression itself.

Transformants allowing protein localization were also subsequently transformed with another vector, PolyA binding protein 3 (PABP3) and PABP5 bound with RFP. For transformants selection, induced resistance to Hygromycin B was performed implicating short light exposure immediately after seeds plating, followed by two days of darkness and one day in light, allowing detection of transformants by increased hypocotyl elongation. In the case of doubtful results, which happened for some cases, 10 days of waiting were necessary in order to achieve a proper selection.

6.2 Detection of fluorescence signal

6.2.1 First screen by epifluorescent microscope

Nikon TE2000E inverted microscope was used for the first expression screening in order to obtain a first representation and to select best candidates for second generation screen. Moreover, ordinary microscope screening is not time-consuming and allows gathering of preliminary data; these are definitely poorer than high definition images from confocal microscope, but allow screening quickly high amounts of samples in order to observe results reproducibility and to select best candidates, which appears necessary even when a proper homozygous transformants line is available. For those reasons, this first step was systematically done with sporophyte and matures pollen grains.

6.1.2 Promoter activity and protein subcellular localization by confocal microscopy

Zeiss LSM 800 laser scanning confocal microscope (CLSM) equipped with Argon laser and Zeiss C-Apochromat x40 9 /1.2 water-corrected objective was used to obtain the final images presented in this thesis. For co-localization, dual fluorescence channels and DIC were used simultaneously for live cell imaging.

7. Used software

For sequencing, cloning and other experiments planification, SnapGene™ software was used for this work. It was also used for sequence alignment, together with web-based T-Coffee alignment tool - www.tcoffee.org. GeneSnap was used for electrophoresis gel capturing, Zeiss Zen 2.3 for microscopy imaging. Images were analysed and assembled with ImageJ (http://imagej.net), Adobe Photoshop CS6 (www.adobe.com) and Ink-scape (www.inkscape.org) software. Microsoft Excel was used for data processing and graphical presentation. Photos brightness and contrast were sometimes retouched, directly in Microsoft

Word or occasionally in Adobe Photoshop, however only for clearer presentation, the guideline being an absence of artificial biasing on comparative images, especially for *semi* quantitative PCR gels, in vivo growing pollen tubes imaging being unretouched.

III. RESULTS

1. Characterization of *eif3b1, eif3b2 and eif3e* mutants

1.1 Verification of knockout by semi-quantitative reverse transcription PCR

1.1.1 *eif3b1*

For *eif3b1* heterozygous mutant, semi qRT PCR presented some difficulties in consistency of the results, but finally showed quite clear results. Results showed only slightly reduced transcripts levels in heterozygous plants inflorescence (two reactions for line 1 as well as two reactions for line 2) compared to wild-type control (Figure 14). In such a heterozygous context, this experiment is not sufficient to prove functional impairment of mutant gene, but potential impairment caused by T-DNA insertion associated with a reduction of transcripts abundance remains a very probable source of severe functional impairment.

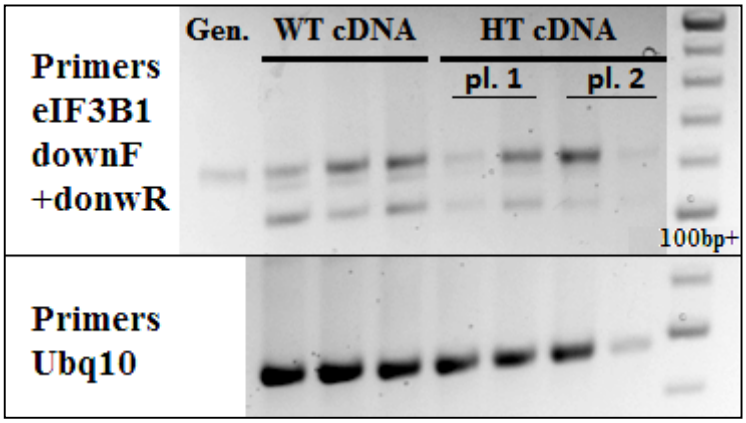

Figure 14. *Semi* qRT PCR for heterozygous *eif3b1*. Genomic reference is present at left, followed by wild type (WT) cDNA and heterozygous (HT) cDNA, lower band corresponding to cDNA without introns (upper band presence is likely caused by genomic DNA contamination). At bottom, reference reactions with Ubiquitin 10 primers with same cDNA templates.

1.1.2 *eif3b2*

eif3b2 homozygous mutant line was confirmed by genotyping, allowed us to obtain a relevant idea of the reduction of gene expression following eIF3B2 knockout by *semi* qRT PCR. Gene-specific primers were located upstream, as well as downstream to the T-DNA insertion location (Figure 15). Results clearly showed a significant reduction of transcripts abundance in mutant plants.

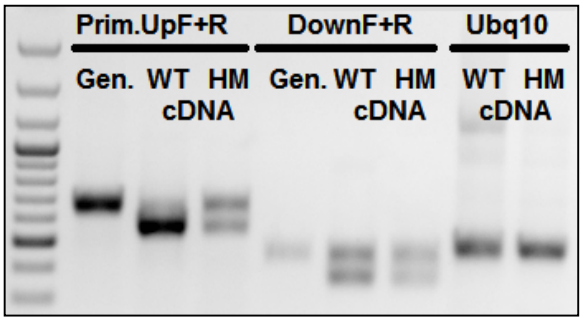

Figure 15. *Semi* qRT PCR results, comparing presence of eIF3B2 transcripts on WT and HM *eif3b2* mutant individual. Two sets of primers, upstream (UpF+R) and downstream (DownF+R) of insertion region, were used. Ubiquitin 10 primers serve as reference: transcripts level is similar, showing the results are unbiased.

1.1.3 *eif3e*

In *eif3e* heterozygous mutant, the presence of the T-DNA insertion did not really affect mRNA transcript presence and turnover, as we can see for upstream primers pair, where no real reduction can be observed (or only a slight decrease, which can be explained by reactions efficiency alias, as comparable Ubiquitin 10 reference shows) (Figure 16). For reactions using downstream located primers, the transcript reduction was much more significant (Figure 16).

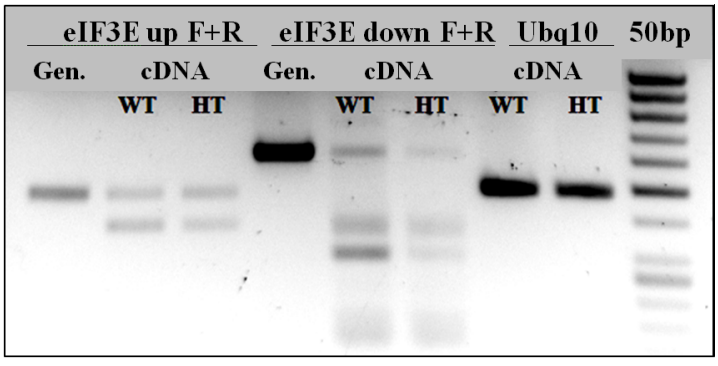

Figure 16. *Semi* qRT PCR gel of *eif3e* heterozygous mutant compared to WT, using primers located upstream (UP F+R) and downstream (DOWN F+R) of T-DNA insertion location. Genomic DNA reference is used, as well as Ubq 10 primers for both cDNA's from WT and mutant templates.

1.2 A screen for sporophytic phenotype

1.2.1 *eif3b1*

As we will see later, two of the four *eif3b1* studied lines (line 10 and line 11) appeared to be impaired by a supplementary insertions problem, leading to severe pollen defects. Line 11 was particularly affected and also showed global developmental defects and delay in its life cycle. Lines 1 and 2 did not show such impairment and sporophytical phenotype appeared identical to wild-type plants of same Columbia ecotype with similar rate of life cycle.

1.2.2 *eif3b2*

For *eif3b2*, homozygous mutant plants showed a delayed development, with approximately 10 days delayed flowering compared to WT plants grown in similar conditions. Heterozygous plants, obtained by crossing HM mutant with WT plant of same Columbia-0 ecotype, did not show such a delay. Homozygous plants also generally recover a normal developmental speed when complemented through transformation (dipping) of parent plant to reintroduce a functional copy of eIF3B2 gene in the genome (see part 1.7 of this chapter). Creation of background-free *eif3b2* homozygous mutants and a repeat of vertical *in vitro* seedling growth for proper unbiased measuring would be necessary to clarify *eif3b2* sporophytic phenotype.

1.2.3 *eif3e*

For *eif3e* heterozygous mutants, general plant development showed no impairment compared to wild type individuals of same Columbia-0 ecotype and compared to wild type segregants of the mutant line, suggesting, as for *eif3b1*, a recessive nature of *eif3e* mutant allele.

1.3 Screening of mature pollen phenotype

1.3.1 *eif3b1*

Pollen grains were stained with DAPI and observed under bright field and fluorescence microscope. No significant phenotypical defects were apparent in the 1st generation, except in plant number 11. To investigate the authenticity of line 11 further, two heterozygous lines, heterozygous plant 10 and 11 from the first generation were grown again. Investigations of sibling plants showed a first strange thing: a mild frequency of abnormal pollen grains in bright field for about 1/3 of line 10 heterozygous plants, and a moderate frequency of abnormal pollen grains in bright field for about 2/3 of line 11 heterozygous plants, the remaining plants having pollen with “normal” phenotype in bright field (Figure 17).

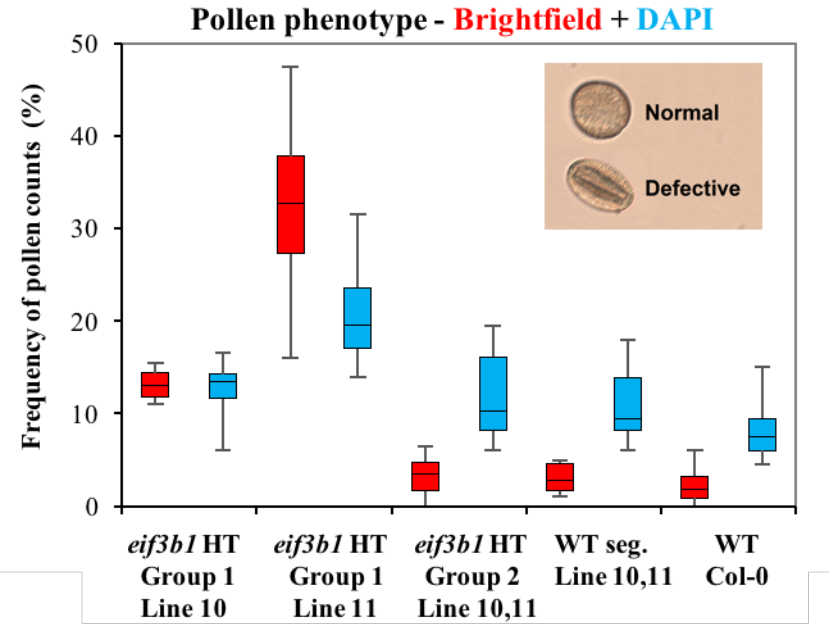

Figure 17. Frequency of pollen defects for two *eif3b2* heterozygous mutant lines, with wild type segregants and "clean" wild type reference. The picture in top right corner represents an example of defective pollen grain.

The segregation and phenotypic features appeared not to be correlated, with descendants from line 10 segregating almost only into wild type, while descendants from line 11 were now splitted into wild type segregants with high amount of collapsed pollen, and heterozygous segregants with slower sporophytical development and delayed flowering, but producing pollen without noticeable defects. One fact is clear about line 10 and line 11; a segregating background insertion is likely present (probably heterozygous), which lead to inconsistent but severe pollen grains collapsing phenotype in lines 10 and 11, intolerable to achieve proper investigations. An investigation was attempted by running a PCR reaction with HT and WT segregants according to *eif3b1* genotyping from line 11 by using primers which are specific to the kanamycin resistance gene of used T-DNA insertion, but despite many efforts, results were highly variable and non-reproducible.

Since the likely presence of multiple insertions was probably biasing the results for lines 10 and line 11 with inconsistency to *eif3b1* segregation, two more lines from first generation, line 1 and line 2, were grown to obtain additional evidence. Results appeared to be much more consistent with *eif3b1* segregation following analysis of 10 heterozygous mutant plants and 6 wild type segregants. For these two newly grown line 1 and line 2, we observed a constantly normal phenotype in bright field and a slightly increased level of aborted mitotic division of the generative cell in DAPI nuclear staining (Figure 18). The phenotype is also present in a milder frequency in wild type segregants, compared to proper wild type plants (Figure 18). The result

is in fact similar to the result obtained with plants from line 10 and line 11 which were falling in the category without severe collapsed pollen grains phenotype (Figure 17). Global variance remains low and does not allow a clear conclusion, but a second discrete background mutation presence is still likely. However, such a small difference can also be simply explained by natural aliases between lines. Transmission and segregation analysis is necessary in order to clarify more of this inconsistency. To conclude, line 1 and line 2 of *eif3b1* heterozygous parents appear much more useful in the frame of this thesis and only those lines will be used in next described experiments.

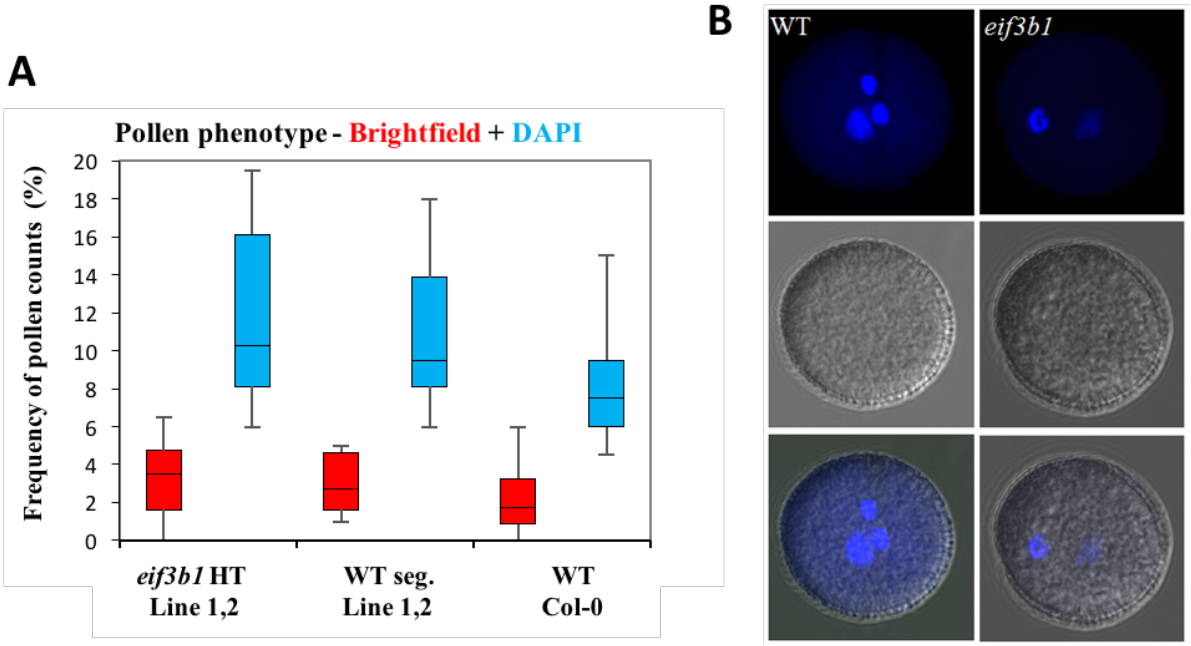

Figure 18. (A) Results of pollen grains defects frequency on *eif3b1* line 1 and line 2. Heterozygous mutants are compared to wild type segregants of the line and to Col-0 wild type as reference. (B) Micrographs of pollen grains showing vegetative and generative nucleus with DAPI staining and in bright field and a merge of the two micrographs. We clearly see the mitosis impairment leading to a block in generative cell division to produce two sperm cells.

1.3.2 *eif3b2*

Phenotype screening of mature pollen grains was first done on available homozygous mutant plants (as ordered from the seed stock center) to obtain the preliminary data. The presence of abnormal "collapsed" pollen grains in bright field was observed, at significant frequency, in all mutant plants, although with slightly variable proportion (Figure 19). Presence of cell division defects (as observed with DAPI staining) was also noted in an increased occurrence, relative to wild type reference. Two second generation lines from parents with moderate phenotype (with approximately 13% of abnormal pollen grains) were grown for phenotypic screening (Figure 19).

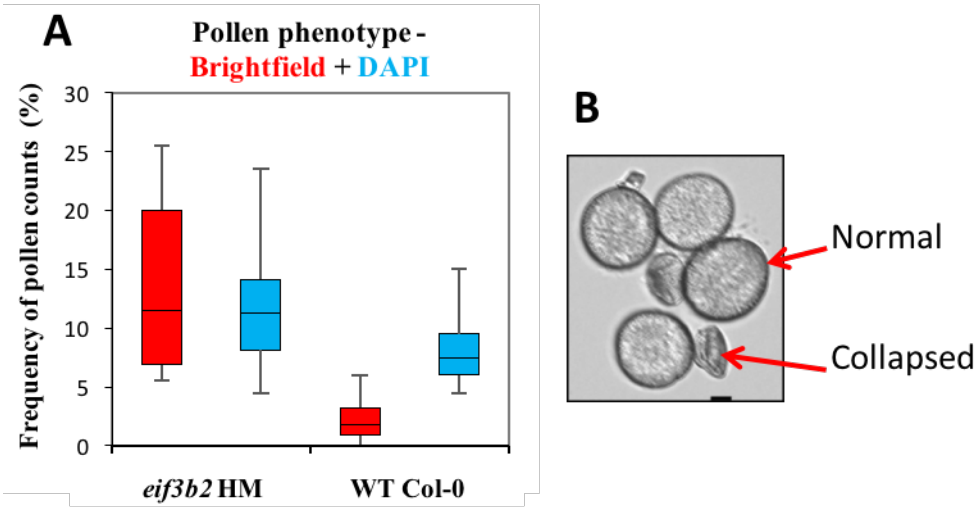

Figure 19. (A) Results of pollen grains frequency of defects for *eif3b2* homozygous mutants, with WT reference. (B) Example of defective collapsed pollen grains in *eif3b2* homozygous mutant line.

The direct link between pollen collapsing and *eif3b2* mutation was placed in doubt by the absence of phenotypical recovery in complemented homozygous individuals having received at least one insertion of full length eIF3B2 under its native promoter. Further investigations were undertaken to investigate yet this another inconsistency further.

First, homozygous *eif3b2* were crossed to *ms1* female to separate *eif3b2* T-DNA insertion. When F1 heterozygous *eif3b2* lines were obtained (in Col-0/Landsberg hybrid background, then Col-0 pure background)), instead of a constant half-reduced collapsed pollen grain frequency compared to homozygous, only 7 plants in a total of 28 showed a similar phenotype to original homozygous parents, the others showing no phenotype at all (Figure 20). This splitting, together with the complementation experiment that failed to restore a clean phenotype (see part 1.7), makes evident the presence of extra insertion sites biasing the results. Insertion seems having been outcrossed and separated from the large majority of obtained *eif3b2* heterozygous plants. However, phenotype occasionally reappeared on F2 generation, selections being now done in order to try complete outcross of the putative additional insertion/s. Figure 20 shown the pollen phenotype screening results for F1 heterozygous generation. Plants have been separated in two groups: The "background" group counts the 7 *eif3b2* heterozygous plants with severe pollen phenotype. The "Clean" group contains the 28 *eif3b2* heterozygous plants having normal pollen phenotype.

We can see that pollen morphology in bright field is in fact not affected by the potential extra insertion, and no cellular division impairment is notable beyond normal variability as observed in wild type reference (Figure 20). Even background-affected individuals showed no significant

impairment in mitotic division (Figure 20). We can conclude that absence of eIF3B2 subunit does not affect microgametogenesis and production of sperm cells.

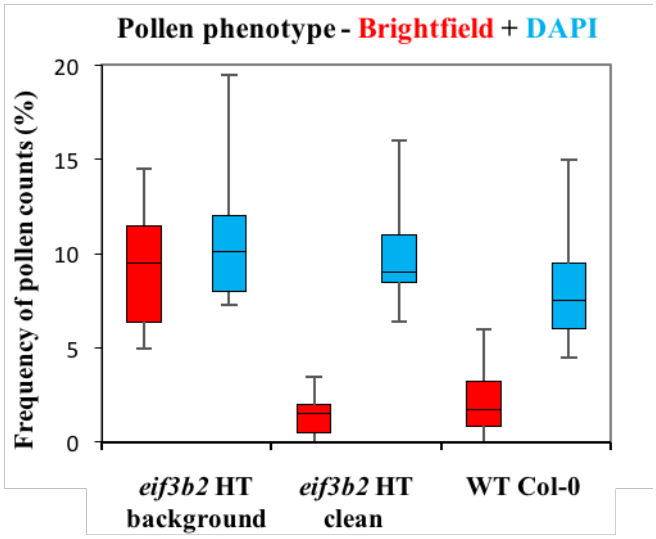

Figure 20. Results of pollen grains defects frequency on *eif3b2* F1 HT lines, split in "background" (background-affected) and "clean" (background-free) groups. Col-0 WT reference statistics are at right.

1.3.3 *eif3e*

Pollen grains phenotype was investigated using seven heterozygous mutant plants obtained from initial 25 individuals. As we can clearly see, there is no impairment in bright field, and only a slightly increased percentage of abnormal pollen grains in terms of nuclei division defects observed with DAPI staining (Figure 21). However, the difference is not significant. As we will see later, early abortion of mutant grains during microsporogenesis is unlikely; we can say that *eif3e* mutation does not affect mature pollen development.

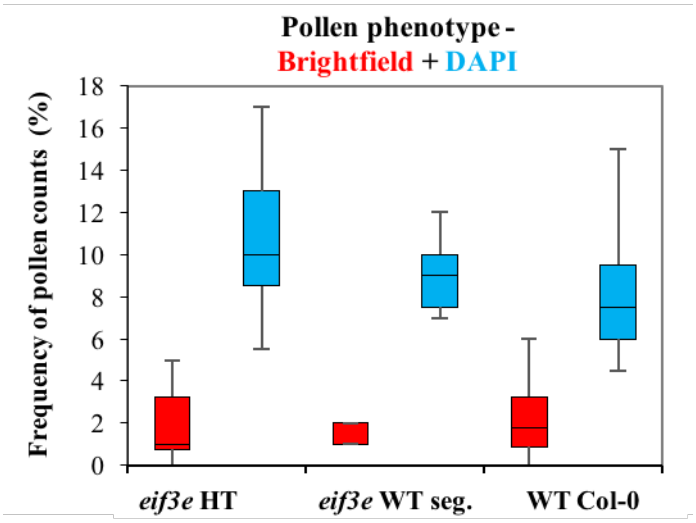

Figure 21. Results of pollen grains frequency in *eif3e* HT mutants, compared with WT reference.

1.4 Analysis of *in vivo* pollen tube growth

1.4.1 *eif3b1*

Next we investigated pollen tube growth fitness of *eif3b1* in planta by pollinating pistils of *ms1* plants. For heterozygous *eif3b1* line, a maximum of 50% of (haploid) pollen grains are expected to be mutant, and therefore in a case of severe phenotype a reduction of 50% maximum pollen tube density (germination rate and pollen tube length) compared to wild type pollen. Pistils were observed after callose staining with aniline blue stain allowing visualization of pollen tubes under the UV light. For comparison, pollen of WT Col-0 and pollen of WT segregant were also used to pollinate *ms1* pistils.

Similar pollen tube viability in WT and WT segregant was clearly observed suggesting absence of severe impairing background mutation (Figure 22). Observations then clearly showed a reduced pollen tube growth with pollen from heterozygous *eif3b1* mutant plants compared to WT segregant and WT Col-0 pollen (Figure 22). However, these results from heterozygous mutant pollen were taken with skepticism, as later segregation test by genotyping revealed a contradictory results (see section 1.6 Transmission and segregation analysis of the mutant T-DNA lines). A possible explanation for these conflicting results is that when the aniline blue staining was done, available HT mutant plants were old producing their last flowers, which could have decreased global pollen viability. For this reason, the aniline blue experiment was repeated using pollen from HT mutants at early flowering stage. As we can see, the second experiment with pollen from "fresh" flowers with similar stigma loading, 22 hours after pollination, showed a fully normal *in vivo* pollen tubes growth for heterozygous *eif3b1* mutant pollen compared to WT reference. This suggests a normal fitness of male gametophytes carrying the *eif3B1* mutant allele.

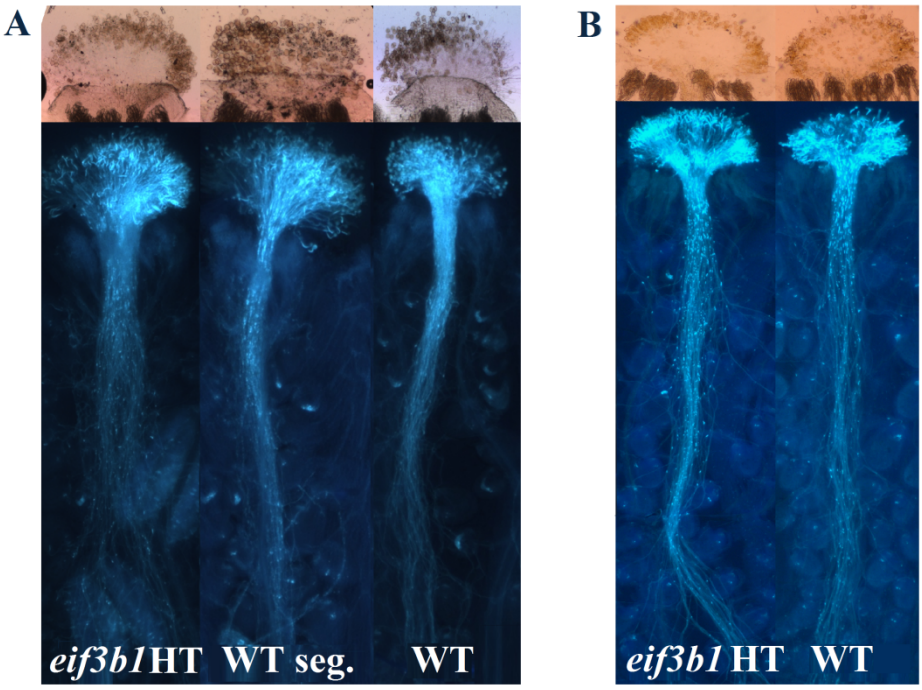

Figure 22. (A) *In vivo* growing pollen tubes from *eif3b1* HT mutants, stained by aniline blue, compared to WT segregant and WT Col-0 reference. (B) Second more relevant experiment with fresh material. Stigma loading in bright field is shown on the top of each micrograph for reference.

1.4.2 *eif3b2*

Aniline blue staining technique was first done with the original homozygous mutant descendants. The results showed constant reduction of pollen tube growth fitness compared to wild type Columbia, but these results should be taken with skepticism, as additional insertion can notably affect them and wild type segregants being absent at this stage for direct comparison. Even though we could observe a clear difference, it remained minor, suggesting that if pollen tube growth was really affected by the absence of eIF3B2 functional allele, the fitness decrease was mild. Further investigations was done on F2 homozygous descendants with no pollen phenotype from original *eif3b2* homozygous plant crossed with wild type plant, as the background phenotype on mature dry pollen could have biased the results.

Results of the new aniline blue experiment showed that *eif3b2* mutant having apparently been cleaned from background impairment showed no lack of pollen tube fitness (Figure 23). As pollen donor is homozygous mutant, every male gametophyte is carrying the knockout mutation, which would have caused a more apparent difference in case of decreased fitness contrarily to heterozygous pollen donors. Further investigation on mutant *eif3b2* segregation will clarify the aniline blue staining results.

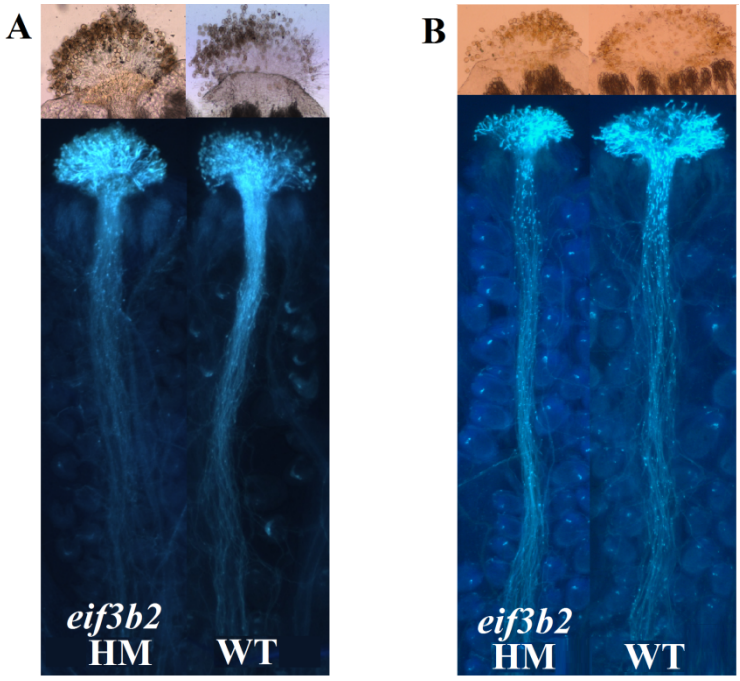

Figure 23. (A) In vivo growing pollen tubes from *eif3b2* HM mutants compared to WT segregant and WT Col-0 reference. (B) second more relevant experiment with HM "clean" line.

1.4.3 *eif3e*

In vivo pollen tube growth observation after 22 hours post pollination with heterozygous *eif3e* mutants as pollen donor showed a potential difference between *eif3e* HT and Col-0 WT pollen tube fitness (Figure 24), however the difference is reduced to constitute an analytically relevant fact, especially with this kind of *semi*-quantitative technique. Comparison with transmission data will allow a concrete conclusion in global experimental approach on *eif3e* pollen tube fitness and *in vitro* pollen growth is planned.

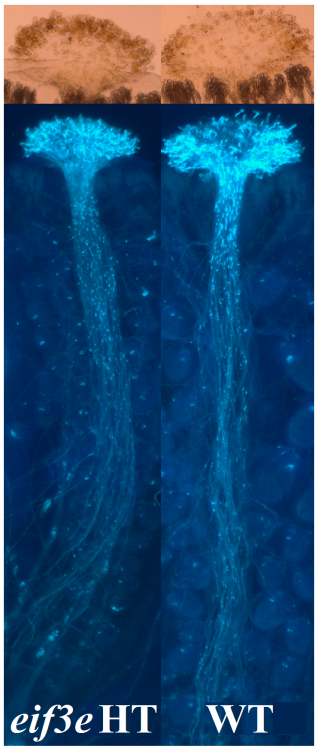

Figure 24. *In vivo* growing pollen tubes from *eif3e* HT mutants compared to WT Col-0 reference.

1.5 Dissection of siliques phenotype

1.5.1 *eif3b1*

To test post-fertilization defects, mature siliques were dissected from self fertilized *eif3b1* heterozygous mutant lines line 1, line 2, line 10 and line 11. Seeds from four to six siliques checked per plant with a total number of 6-7 plants per mutant line, 5 plants for WT segregant and 6 plants for WT Col-0 reference. Line 11 being different from the others lines, showed an average of 12.25% of unfertilized ovules, however, due to its potential background mutation. For the remaining lines, we can clearly see that seeds collapsing, corresponding to a problem during embryo development after fertilization is present in a similarly negligible level for wild type segregants as for wild type reference (Figure 25). Frequency of unfertilized gametophyte/very early aborted seeds is slightly increased in mutant plants, but nothing really drastic to allow deductions, let alone that increased frequency was observed only time to time in some individual siliques, and not as a global consistency, with the average value showing no real difference (Figure 25).

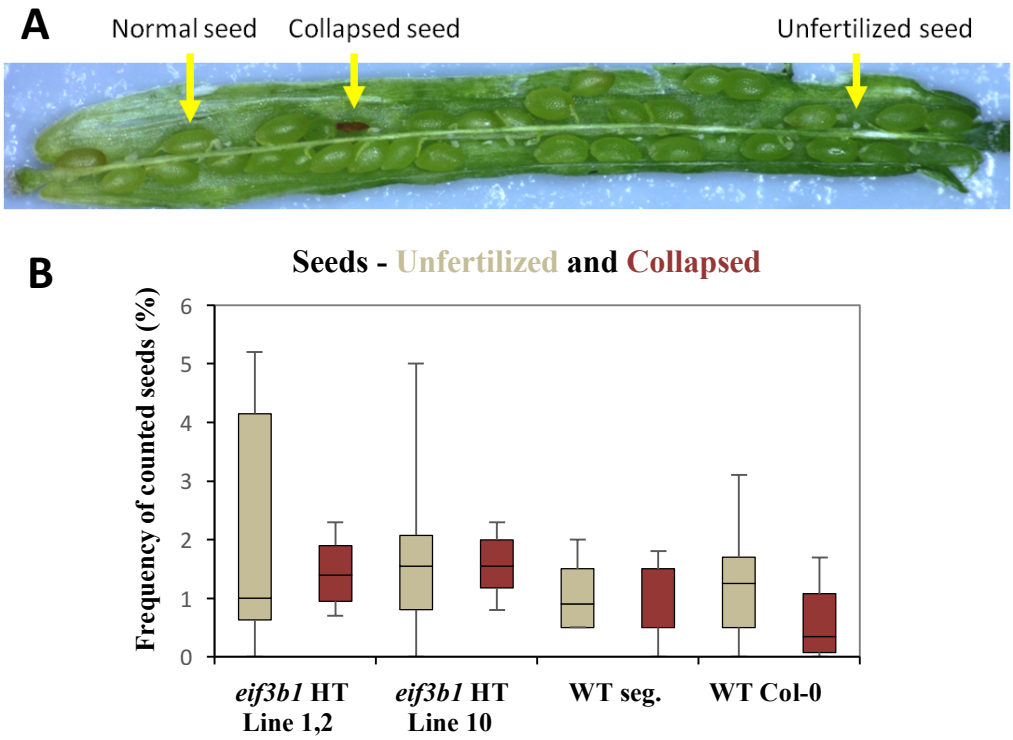

Figure 25. (A) Representative silique. (B) Percentage of unfertilized female gametophytes and collapsed seeds on *eif3b1* mutant lines 1, 2 and 10, compared to WT segregant and Col-0 WT references.

1.5.2 *eif3b2*

Similar to *eif3b1*, collapsed seeds were rare in *eif3b2* homozygous mutants siliques as they are in wild type reference, but we observed a significantly increased proportion of unfertilized seeds in descendants of original homozygous population. Six heterozygous individuals without pollen background from F1 Col-0 generation were also phenotyped. F1 heterozygous generation shows no difference in siliques phenotype compared to wild type, while the original homozygous affected by background showed a difference, unfertilized/early aborted embryo sac being a phenomenon of increased frequency (Figure 26). As siliques of heterozygous mutant coming from self-pollination show no impairment, we can conclude to an absence of effect on female gametophyte. *eif3b2* mutation appears without effect on pollen tube growth, subsequent fertilization and early embryo development.

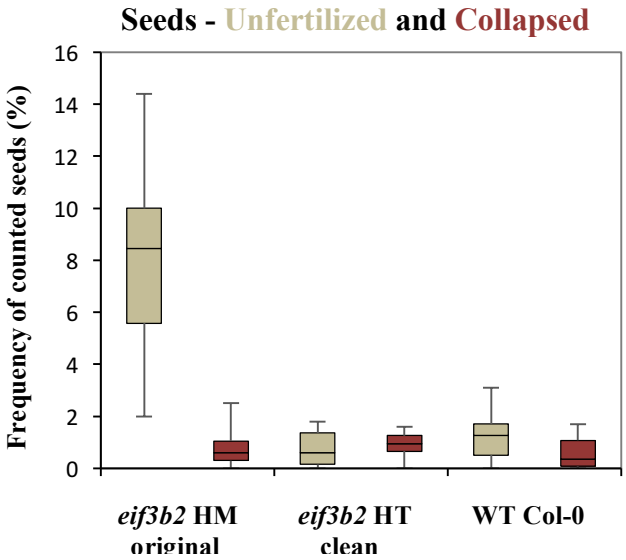

Figure 26. Results of seeds frequency of defects for *eif3b2* original HM mutants and F1 HT mutants, with WT reference.

1.5.3 *eif3e*

For our group of mutants, siliques screening gave practically nominal data, with only occasional presence of siliques with abnormal unfertilized ovules. However, obtained results are sufficient to show a very low (almost negligible) frequency of unfertiled/early aborted embryo sacs, collapsed seeds ratio being also non-significant (Figure 27).

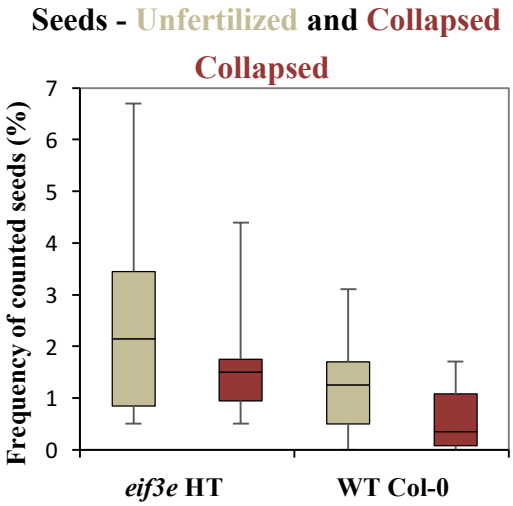

Figure 27. Results of seeds frequency of defects for eif3e HT mutants, with WT reference.

1.6 Transmission and segregation analysis of the mutant T-DNA lines

1.6.1 *eif3b1*

Seeds from first generation of heterozygous line 1 were used to test transmission efficiency of the *eif3b1* mutation after self-pollination. The entire population for genotyping and statistical test was derived from seedlings grown on ½ MS medium as well as plants grown in soil for phenotyping. In total, about 170 plants were genotyped. Agarose gels are presented here as illustration and obtained statistics are given below (Figure 28). Following genotyping, no homozygous mutants could be recovered, while heterozygous mutant were present at twice more the frequency than wild type segregants resulting in a ratio of 1:2:0 wild type:heterozygous:homozygous (Figure 28). The transmission diverged from the mendelian ratio and clearly pointed on homozygous *eif3b1* lethality. The 2:1 HT/WT relevance was verified by Chi-square value, which is calculated by the sum of following values: [(Obtained-Expected)^2/Expected] of each category. We obtained $\chi^2 = 0.145$, deeply under 5% significance level for 2-values situation (3.84), allowing us to conclude to the absence of decreased fitness caused by the mutation in male or in female gametophyte, supporting the *in vivo* pollen tube growth experiment.

A

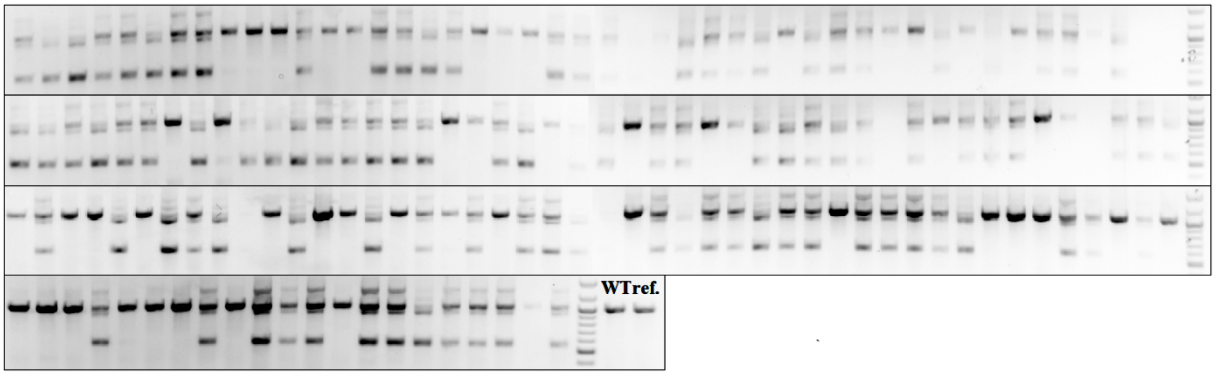

B

eIF3b1 segregation, seedlings from HT parent						
Data	WT	HT	HM	% WT	% HT	% HM
Expected Mendelian	42,25	84,50	42,25	25,0	50,0	25,0
Expected with HM lethal	56,33	112,67	0,00	33,3	66,7	0,0
Obtained with Line 1	54	115	0	32,0	68,0	0,0
Chi-square value (HM leth.)	0,097	0,048	N/A	χ2 = 0,145		

Figure 28. (A) Agarose gels showing results of genotyping seedlings obtained from self-pollination of *eif3b1* HT mutant. (B) Statistics table showing segregation of *eif3b1* mutation.

1.6.2 *eif3b2*

Segregation analysis (as well as other investigations described in previous sections) naturally necessitate the need to create heterozygous lines from the original homozygous plant obtained by crossing *eif3b2* HM mutants with *ms1* and with Col-0. Fully heterozygous nature of F1 generation was verified by genotyping. When these plants were matures, seeds of three individuals that where background free were chosen to perform segregation analysis of seedlings grown on ½ MS medium. Results were conclusive for two of the lines, but ambiguous for a third line. This problematic line was excluded for further segregation analysis. Contrarily to *eif3b1* mutation, *eif3b2* mutant segregated in a normal mendelian ratios of 1:2:1, suggesting absence of homozygous lethality in *eif3b2* deficient seedlings or any gametophytic defects that impede mutant transmission (Figure 29). Note that Chi-square value was calculated again and is $\chi^2 = 0.955$, which is inferior to 5% significance level for 3-values situation (5.99%).

A

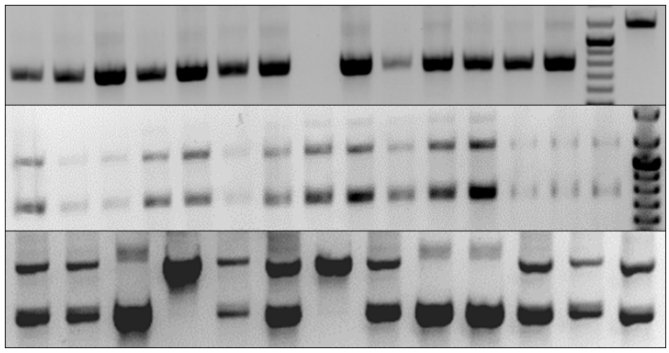

B

eIF3b2 segregation, seedlings from HT parent						
Data	WT	HT	HM	% WT	% HT	% HM
Line 1 Col x Ler	8	15	7	26,7	50,0	23,3
Line 3 Col x Ler	11	33	13	19,3	57,9	22,8
Expected Mendelian Total	21,75	43,5	21,75	25,0	50,0	25,0
Line 1+2 Obtained Total	19	48	20	21,8	55,2	23,0
Chi-square value	0,348	0,466	0,141	χ2 = 0,955		

Figure 29. (A) Original homozygous plants genotyping (with WT reference). Genotyping of descendants of the cross of a *eif3b2* homozygous mutant with *ms1* plant to obtain F1 heterozygous generation. F2 generation genotyping. (B) Statistics of segregation of *eIF3B2*.

1.6.3 *eif3e*

Mutant line *eif3e* caused more problems at the beginning, because genotyping was less efficient as with other mutant lines (reaction with left border LB primer together with gene-specific left primer - LP offering lower product abundance compared to LP-RP), this being superposed to the low transmission rate of this mutation, but the problem was finally solved, allowing to

complete main core investigations on a reduced group of plants. Large transmission statistics experiments are planned for the future, but our preliminary data show that transmission through male gametophyte (by cross with *ms1*) appears to be blocked or at least transmitted very rarely (Figure 30). For this reason, segregation by self-pollinating is likely similar to transmission through female gametophyte, and it seems also affected, female gametophyte being viable with reduced frequency (Figure 30). More consistence reciprocal crosses followed by genotyping will be formed to affirm exact transmission efficiency of mutant eif3e allele transmission through male and female gametophyte.

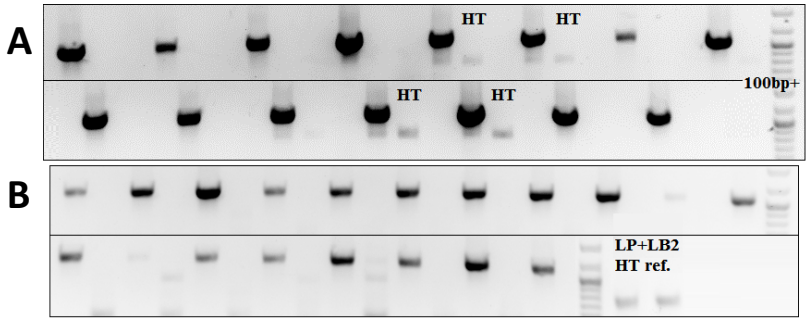

C

eIF3e male transmission and segregation, seedlings from HT parent							
Data		WT	HT	HM	% WT	% HT	% HM
Transmission through male gametophyte	Expected Mendelian	10,5	10,5	N/A	50,0	50,0	N/A
	Obtained by *MS-1* cross	21	0	N/A	100,0	0,0	N/A
Segregation (= transmission through female. gamet.)	Expected Mendelian	12,5	12,5	N/A	50,0	50,0	N/A
	Obtained by self pollination	18	7	N/A	72,0	28,0	N/A

Figure 30. (A) *eif3e* plants genotyping illustration, with for each plant LP + RP, and LP + left border primer. (B) Genotyping after pollinationg *ms1* with eIF3e HT pollen, with reference reaction of LP + LB with known mutant plant at right. C: Table of obtained results.

1.7 Complementation of the mutant *eif3* alleles

Complementation by transforming mutant plants with the same gene that had been knocked-out by the mutation was achieved in *eif3b2* homozygous mutants and about 20 transformants were obtained, confirmed by protein-associated GFP expression in sporophyte. Without surprise, phenotype observed in pollen was not rescued at all, proving its origin from a background mutation. However, reduced developmental speed observed on those mutants disappeared in complemented plants, which grew as wild type Col-0 did. This was observed on plants growing on jiffs, in same conditions (watering, light...) together with wild type plants on the same plate, the 10-days delay having disappeared; however, vertical growth experiments with precise quantification will be required in the future. This is showing a direct link of slowed down development with *eif3b2* mutation, however without allowing saying if this mutation was acting alone in this slowing down, or together with background mutation. Complementation is

planned in the future for *eif3b1* heterozygous in order to try to restore homozygous viability, and is planned for *eif3e* for further transmission statistics investigations.

2. Promoter activities of eIF3B1, eIF3B2 and eIF3E

2.1 Generalities about expression profiles

Gene expression dataset mined from public repository, Arabidopsis eFP browser (bar.utoronto.ca/efp/cgi-bin/efpWeb.cgi) showed that for eIF3 subunits, reasonable levels of transcription were detected in different sporophytical tissues and in pollen during microgametogenesis, and almost no transcription in dry pollen and following pollen imbibition and germination (Figure 32). This suggests that eIF3 core factor and transcripts coding its subunits must be present in sufficient quantity in mature-dry pollen, in order to be ready to ensure quick translational initiations after pollination. Note that eIF3E subunit (and, less prominently, also eIF3C1 and eIF3F) is globally more intensively transcribed in sporophyte and in male gametophyte, and remains transcribed in non-negligible levels in growing pollen tube (Figure 31A, B).

Sperm cell specific microarray data (Borges et al., 2008) show that contrarily to eIF3B (eIF3B1 and eIF3B2 being not distinguished in this specific experiment), which is transcribed more abundantly in sperm cells than in vegetative cell, eIF3E is transcribed more abundantly in vegetative cell, its expression being weaker in sperm cells (Figure 31C).

Data from eFP browser show that eIF3B1 and eIF3B2 have similar transcription level (Figure 31A), however, dry pollen RNA seq data (Loraine et al., 2013) show a notable difference in mature pollen, eIF3B2 being much less transcribed (Figure 31D). eIF3E follows similar variability between tissues of the sporophyte and during male gametophyte development despite overall higher abundance than eIF3B1 and eIF3B2 (Figure 31A, B). This pattern suggest a likely progressive slow-down of translation activities in later stages of pollen tube growth and that present proteins of each of the subunits being probably abundant enough and stable to complete the translation requirements to complete pollen tube growth.

In rehydrated seed, translation of stored transcripts plays a major role (Galland *et al.*, 2014) as for rehydrated pollen grains (Honys *et al.*, 2000). However, the situation is not completely similar; data from eFP browser show that translation initiation factors subunits coding genes (particularly for eIF3) are very intensively transcribed in seeds 24 hours after rehydration (and

even dry seeds), contrarily to rehydrated pollen (Figure 31), showing a divergence in protein synthesis rate for those two "specialized tissues".

A

eIF3 genes absolute transcription levels in *Arabidopsis thaliana*

Tissue	Sporophytic tissues								Pollen maturation				Pollen tube growing			
Gene	imbseed	root	vegros	genros	merist	stem	flower	silique	unicell	bicell	tricell	mature	dry	30min	4h	in style
eIF3A	559	397	377	222	441	166	284	245	505	462	87	81	17	19	19	42
eIF3B1	399	198	205	147	295	108	178	155	217	176	12	25	6	4	7	22
eIF3B2	399	198	205	147	295	108	178	155	217	176	12	25	6	4	7	22
eIF3C1	796	419	493	365	556	254	388	321	433	363	142	150	57	56	42	47
eIF3C2	4	9	4	12	8	10	7	10	195	115	77	79	6	7	8	14
eIF3E	1333	615	676	420	730	276	458	380	1004	790	263	299	98	94	86	45
eIF3F	996	590	440	301	584	268	358	316	781	705	154	244	33	35	29	49
eIF3H	769	473	403	261	522	258	285	283	546	391	81	61	18	20	19	30
eIF3D	388	237	301	195	425	148	221	224	191	183	25	7	1	3	1	6
eIF3G1	999	691	583	403	827	358	565	579	1049	912	143	127	4	3	2	22
eIF3G2	92	65	89	55	115	20	62	42	221	173	40	39	3	5	4	6
eIF3K	1184	935	808	683	953	656	615	666	1455	1346	356	226	17	12	11	20

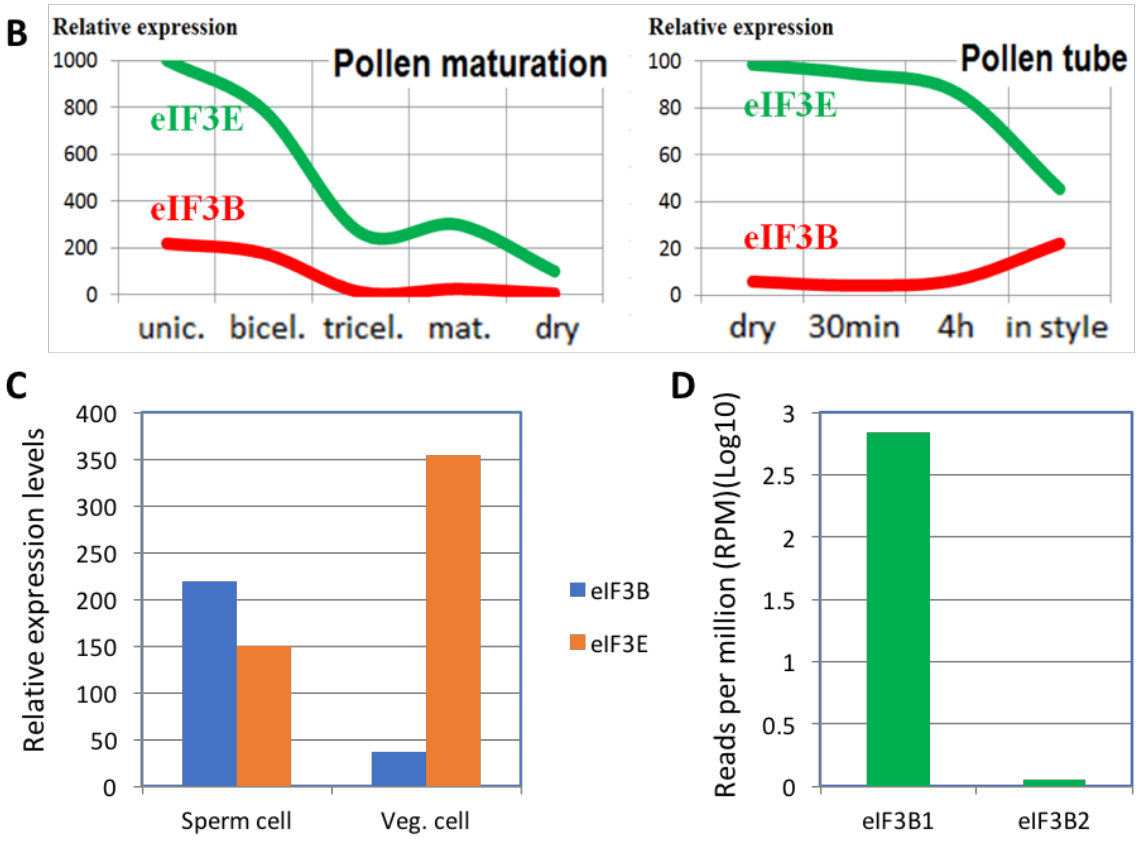

Figure 31. (A) Heat map of genes coding eIF3 complex and COP9 – CSN complex proteins (subunits) in *Arabidopsis thaliana*. Genes that are specifically subjected to our study are in red. (B) Absolute transcription levels of eIF3B1 and eIF3B2 (which are similar) compared to eIF3E during microgametogenesis stages and pollen tube growing. Data were gathered from eFP browser. Units are standardized fluorescent levels, allowing relative comparisons between genes. (C) Data from microarray comparing expression of eIF3B and eIF3E in sperm cells and vegetative cell (whole pollen)

(Borges et al., 2008). (D) Data from RNA seq technique distinguishing eIF3B1 and eIF3B2 expression in pollen (Loraine *et al.*, 2013).

2.2 Promoter activities in sporophyte

Promoter activities provide precise relative differences of gene activity in different tissues, by using reporter gene to observe gene expression profile and abundance. Unlike transcriptome data, promoter-reporter analysis gives precision on transcriptional active zones of the plant with a resolution at the tissue level. The data we obtained are very complementary to previously given absolute expression data from microarray. For each subunit, approximately 1000 bp fragment upstream of +1 ATG start codon were used as putative promoter region and fused to GFP reporter. For sporophyte, results are presented from 5 days-old seedlings and in vegetative rosette epidermis.

2.2.1 eIF3B1

eIF3B1 promoter is active in all sporophytic tissues, and is particularly active in tissues with intense cell division, which are root meristem, root elongation zone, apical meristem and leaf primodia (Figure 32A). In epidermal cells, there is a moderate constant expression. GFP is obviously diffusing in the nucleus (Figure 32B).

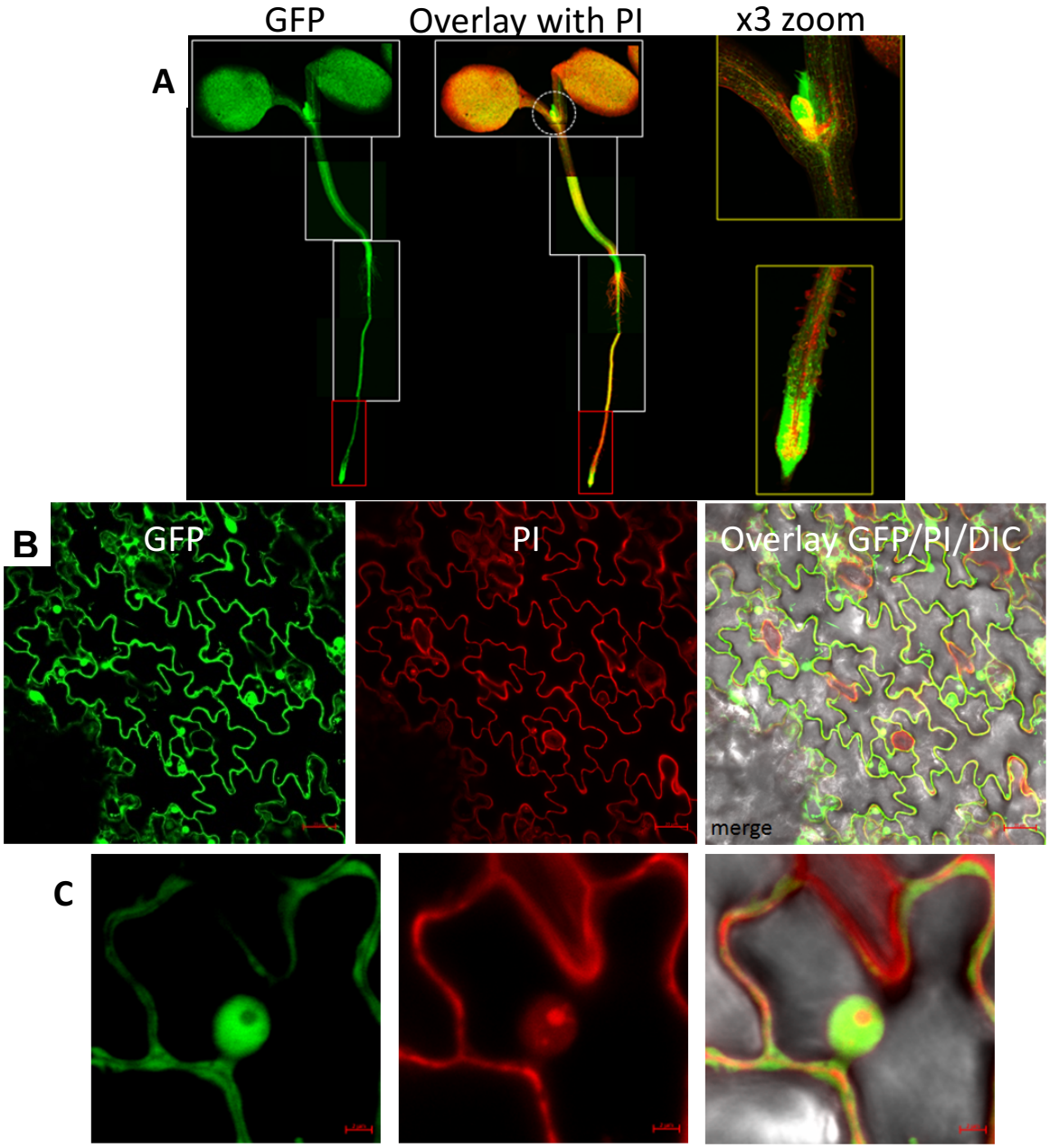

Figure 32. (A) eIF3B1 promotor activity in seedling, with propidium iodide-stained reference (PI), with emphasis on apical and root meristem (zoom) as most active sites of the eIFB1 promoter activity. (B) eIF3B1 promoter activity in leave epidermis showing broader expression in all cell types (C) visible GFP signal in the cytosol of the epidermal cells as well as nucleoplasm.

2.2.2 eIF3B2

Similar analysis with eIFB2 showed a much weaker signal in proeIF3B2:GFP transformants, and showed similar patterns of promoter activities to eIF3B1 (Figure 33). This weaker expression and the pattern of eIF3B2 promoter activity was observed in several lines suggesting a likely true weaker activity of eIF3B2 promoter compared to eIF3B1 expression. These results resolve the issue with microarray where precise eIF3B1 and eIF3B2 expression could not be

defined because of the common probe used for hybridization in the microarray chip (Figure 33).

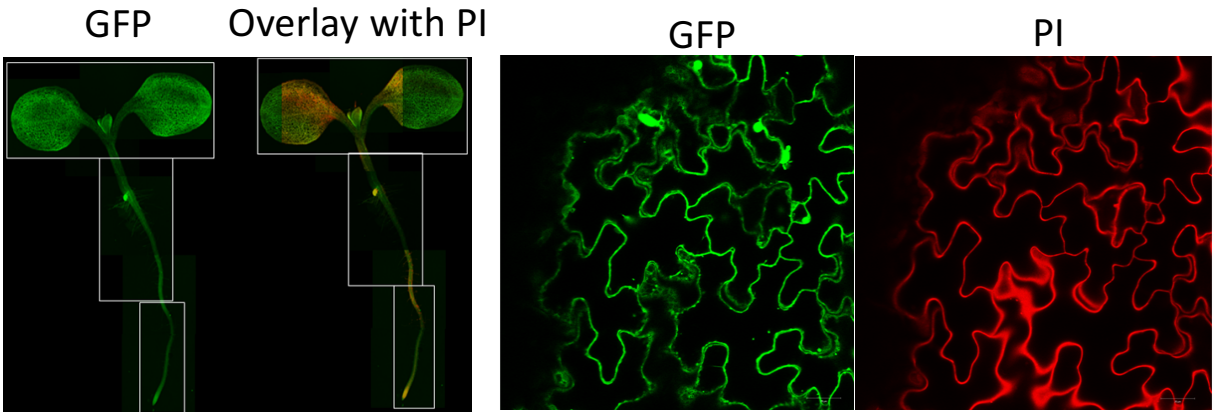

Figure 33. eIF3B2 promoter expression in sporophyte, with propidium iodide reference.

2.2.3 eIF3E

The situation is similar for eIF3E, with, once again, an increased promoter activity in meristems, root elongation zone and leaf primodium (Figure 34). Global level of expression is higher than for eIF3B1 and eIF3B2, which confirms the stronger activity of eIF3E promoter we already presented in Figure 31.

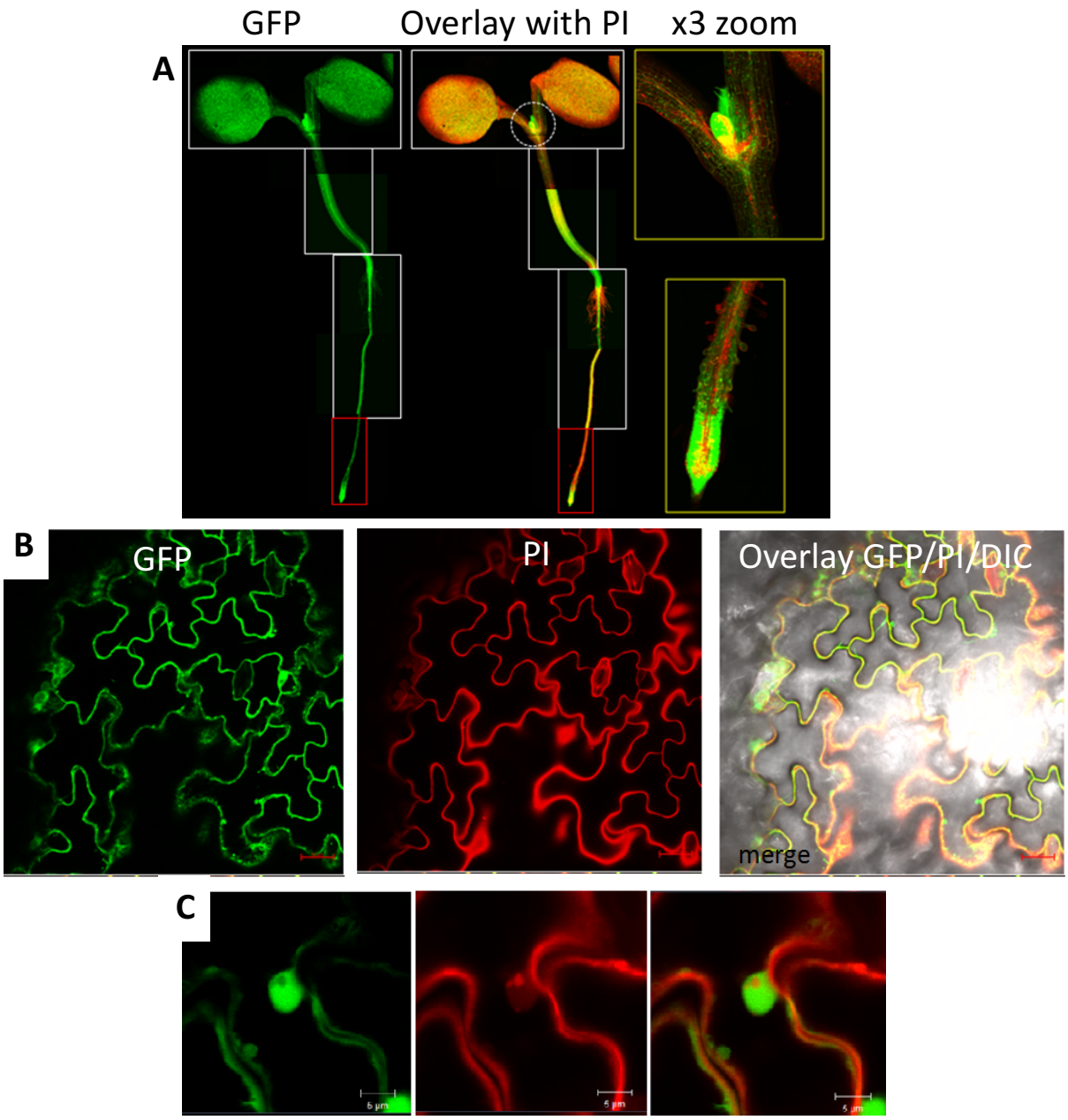

Figure 34. (A) eIF3E promotor activity in seedling showing elevated activities in apical and root meristem (zoom). (B and C) eIF3E promotor activity in epidermis cells of the cotyledon of 5 days old seedlings with signal in the cytosol and nucleoplasm.

2.2.4 Conclusion

Collectively, we can see that observed expression profiles are relatively similar for eIF3B1, eIF3B2 and eIF3E promoters. This strongly correlated with the expression profiles observed from transcriptome data (results section 2.1). In epidermal cells of the rosette leaves, GFP freely diffused in cytosol and in nucleoplasm, and the co-localization with propidium iodide orient the cell wall boundaries of individual cells and defined the cytosolic localization. In seedlings, eIF3B1 and eIF3E profiles overlapped in their peak expression in meristematic cells of the leaf

primordia and root meristematic and elongation zone, where high cell division and translation activities are expected.

2.3 Promoter activities in mature pollen and pollen tube

The same reporter genes were used to establish their pattern of activities in the male gametophyte, more precisely in mature pollen and in *in vitro* grown pollen tubes. DAPI staining was used to visualize DNA in vegetative and generative cell nuclei.

2.3.1 eIF3B1

In dry pollen, eIF3B1 promoter was active in the vegetative cell and the sperm cells (Figure 35A). There was a cumulative signal in the vegetative cell nucleus, however, this could be due to free GFP diffusion and concentrated inside the nucleus (Figure 35). Similarly, although unlikely, the sperm cell signal could also have arise because of the GFP diffusion from the vegetative cell and not from true promoter activities. eIF3B1 protein localization under its native promoter verified the promoter activities in both cell types of the male gametophyte (see below). Co-localization with propidium iodide and DAPI stain verified the promoter activities in respective cell types of the male gametophyte (Figure 35A). In pollen tubes, promoter activities could be observed predominantly in the extending vegetative cell (Figure 35B).

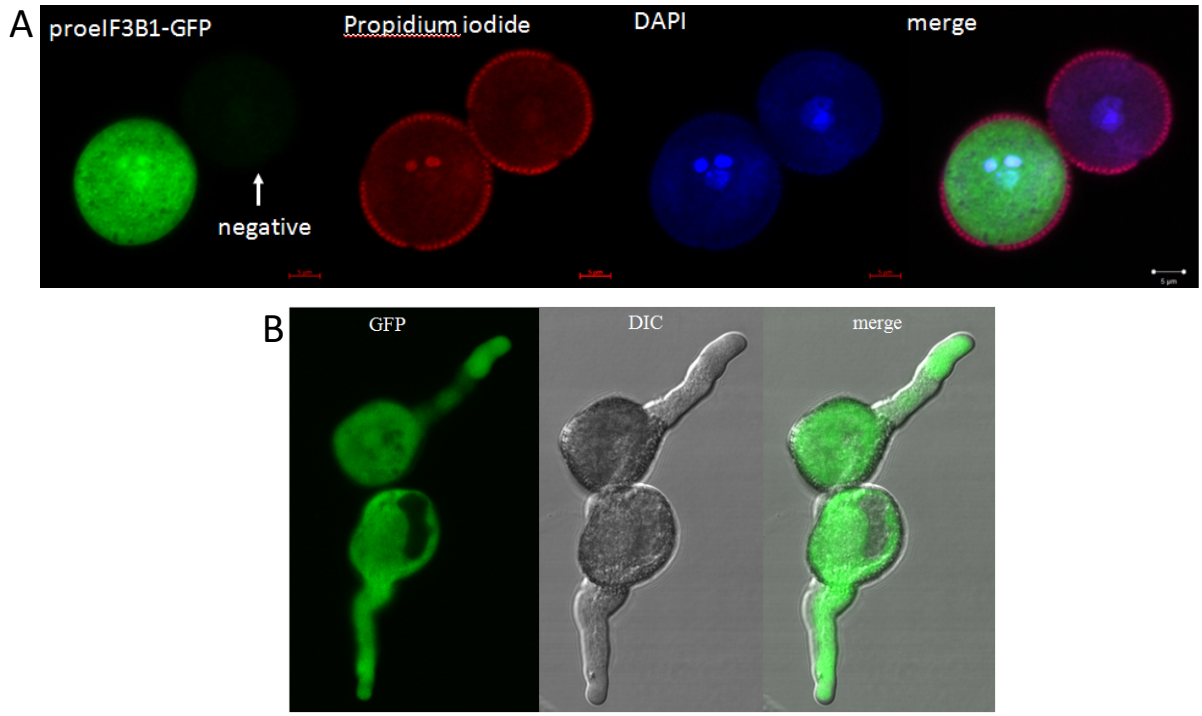

Figure 35. (A) eIF3B1 promoter activity in mature pollen with propidium iodide and DAPI staining references. (B) eIF3B1 promoter activity in 4 hrs *in vitro* grown pollen tubes.

2.3.2 eIF3B2

For eIF3B2, promoter activities in dry pollen could not be clearly detected in several analyzed T1 lines. This corresponded to the profile observed with the microarray data (Figure 36). Similarly, in growing pollen tubes, eIF3B2 promoter activities were slightly higher than in dry pollen predominantly in the vegetative cell (Figure 36). These results suggest that eIF3B1 might be more transcribed compared to eIF3B2, this was not distinguishable in microarray due to a common probe used, but was distinguished by RNA seq, with a particularly important difference in mature pollen (see Figure 31D). Analysis of eIF3B1 and eIF3B2 by quantitative RT-PCR will be necessary to clarify the abundance of these two close paralogs.

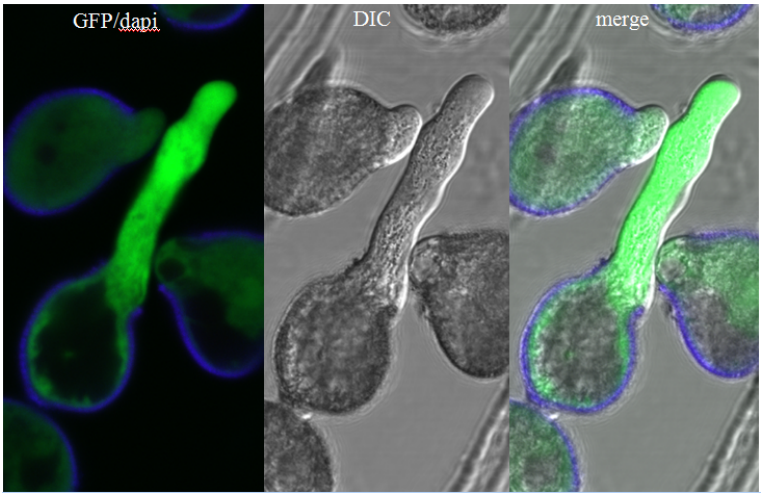

Figure 36. eIF3B2 promoter activity in 4 hrs *in vitro* grown pollen tubes.

2.3.3 eIF3E

Promoter activites of eIF3E were a lot more comparable to eIF3B1. GFP reporter expression could be seen in the vegetative cell as well as in sperm cells, although at reduced intensity for sperm cells (Figure 37), confirming data from RNA seq experiment (Figure 31). Co-localization with propidium iodide and DAPI further confirmed expression profile of eIF3E promoter activities (Figure 37). eIF3E promoter activities also correlated with eIF3B1 in pollen tubes with dominant activities in the extending vegetative cell (Figure 37).

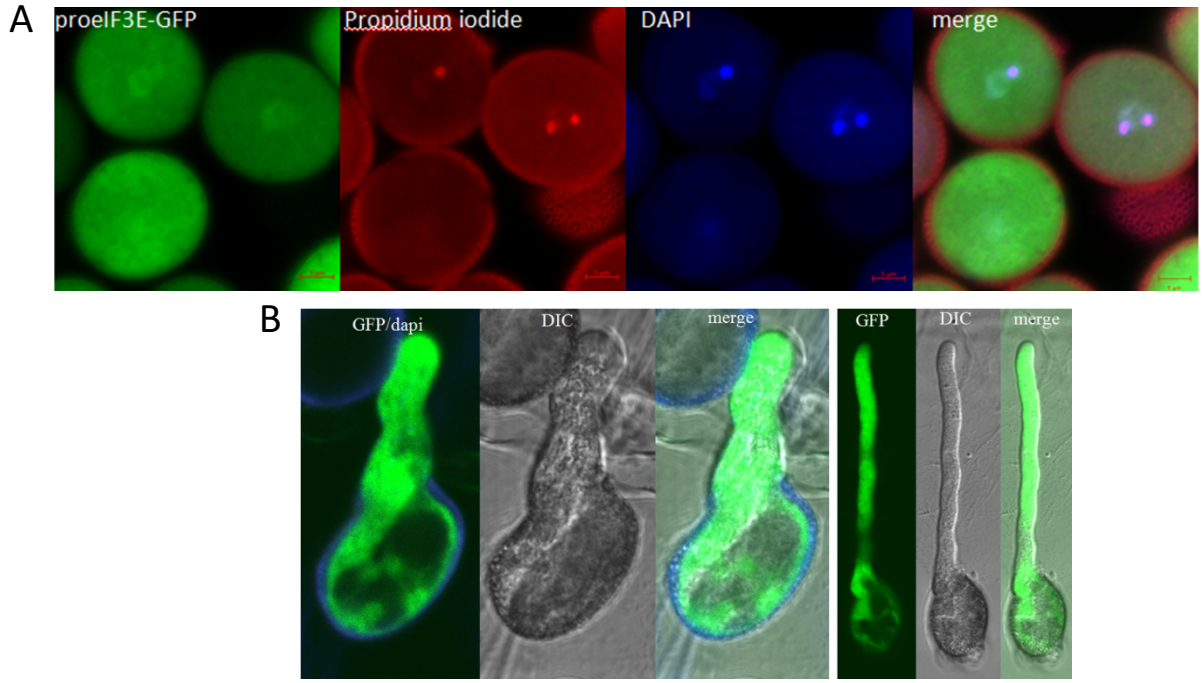

Figure 37. (A) eIF3E promoter activity in mature pollen with propidium iodide and DAPI staining references. (B) eIF3E promoter activity in 4 hrs *in vitro* grow pollen tubes.

2.3.4 Conclusion

For the putative 1.5 kb promoter fragment used for all the three subunits, eIF3B1, eIF3B2 and eIF3E, dominant promoter activity was observed in vegetative cell and at reduced level in the sperm cells of mature pollen. During pollen tube growth, no change in expression profiles was observed with predominant activities being in the vegetative cell. Collectively, all the subunits are likely to be transcribed in both cell types of the gametophyte, suggesting independent translational activities in vegetative cell and within the sperm cells.

3. Verification of eIF3B1 expressed isoforms

As previously mentioned (Chapter I, section 3.2.2), eIF3B1 is potentially present in two isoforms from alternatively spliced intron 2, the shorter one being more similar to eIF3B2 (Figure 9). One question is about true expression of those two isoforms, almost no data being available. Therefore, we designed two sets of reverse primers that would allow detection of both isoforms and performed RT-PCR experiment to detect them using influorescence (stem, flower buds and open flowers as well as siliques) derived cDNA where eIF3B1 is expected to be expressed (Figure 38). The infuorescence represent tissues of the gametophyte as well as the sporophyte, useful in a case where one of the expressed isoform is of tissue specific origin. A template of genomic DNA was used for reference. The potential result of the PCR on agarose

gel was simulated in SnapGene™ software, and then compared to the effective experimental result, as illustrated in Figure 38.

The results of the PCR revealed that only the short isoform is expressed and likely that intron 2 is spliced out correctly in all tissues (Figure 38). Therefore eIF3B1 gene annotation in TAIR database might be the source of error. However, further investigation can be done with various tissues and developmental stages to subsequently discover of potential representation pattern and functionality of eIF3B1 subunit longer isoform and the role of additional sequence in RNA recognition motif. It is important to note that even though the difference between eIF3B1 isoforms is without real importance in the frame of this work, further investigations may potentially take this fact into significant consideration; plants transformation with intronless eIF3B1 coding genes are already done in our laboratory and further investigations field may be opened with a wide perspective.

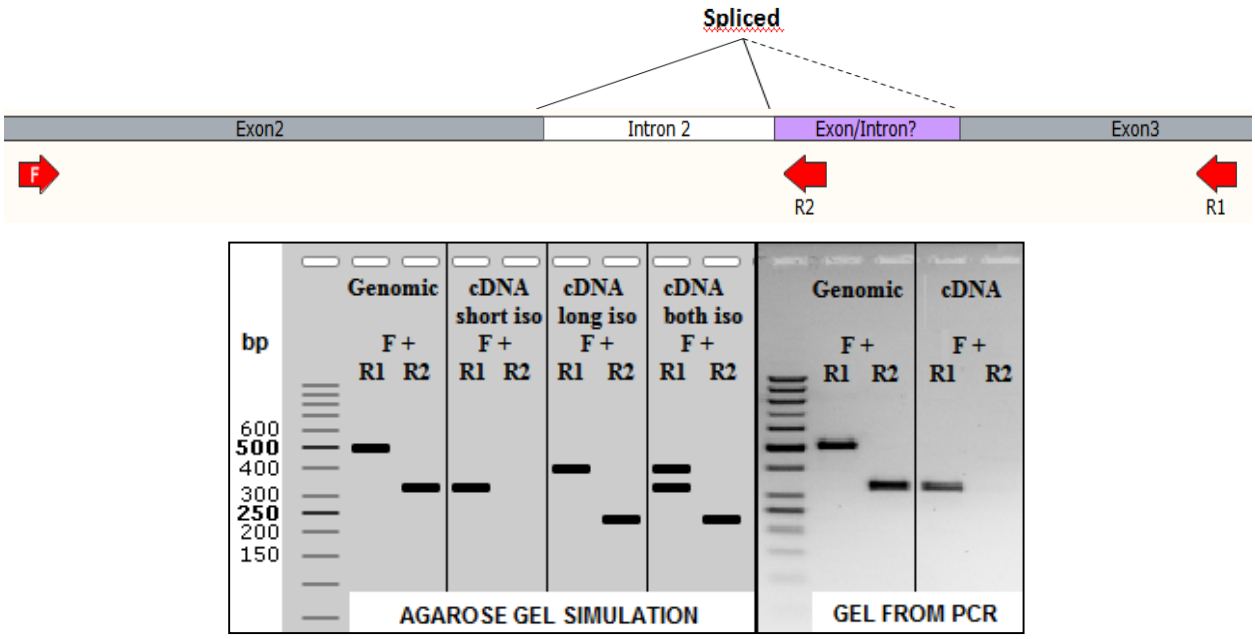

Figure 38. Detection of eIF3B1 alternative splicing. The scheme above shows alternative splicing localization on the gene and primers position (red arrows). Simulated agarose gel (left) shows potential PCR results if only short or only long isoform, or both, were present. Real PCR gel is on the right.

4. Subcellular localization of eIF3B1, eIF3B2 and eIF3E

To compare the pattern of eIF3B1, eIF3B2, and eIF3E subcellular localization in the two cell types of the male gametophyte, the vegetative cell and the sperm cells, with the sporophytic tissues localization, full length coding sequence together with their native promoters where

fused at the C-terminal with GFP. The two cell types of the male gametophyte follow two different cell fates with the sperm cells characterized to have condensed chromatin, reduced transcription activities and likely translation activities. Therefore, the two cell types could potentially show different patterns and activities of eIF3B1, eIF3B2, and eIF3E. Further, unlike sporophytic tissues, pollen is characterised with massive transcripts storage towards maturation, and therefore, understanding the association of eIF3B1, eIF3B2, and eIF3E with actively translated mRNAs or translationally repressed transcripts is essential towards establishing the mechanism of translational repression and de-repression in the male gametophyte. At least 15 T1 plants were generated for each subunit and screened for GFP localization by confocal microscopy.

4.1 Sporophyte

A screen of rosette leaves from 5 days old seedlings revealed that all the three subunits localized in the cytosol in a granular morphology (Figure 39). The cytosolic localization was emphasized in guard cells where the large vacuole constricts the cytosol and concentrates the GFP signal (Figure 39). As expected, co-localization with 10 μM propidium iodide revealed that none of the subunits localizes in the nucleus in a detectable quantity. Further, no preferential localization around cell membrane can be clearly noticed in sporophytic cells. As a global illustration, situation being similar for all three subunits, distribution pattern in sporophytic tissues from vegetative rosette leaf is presented for eIF3E.

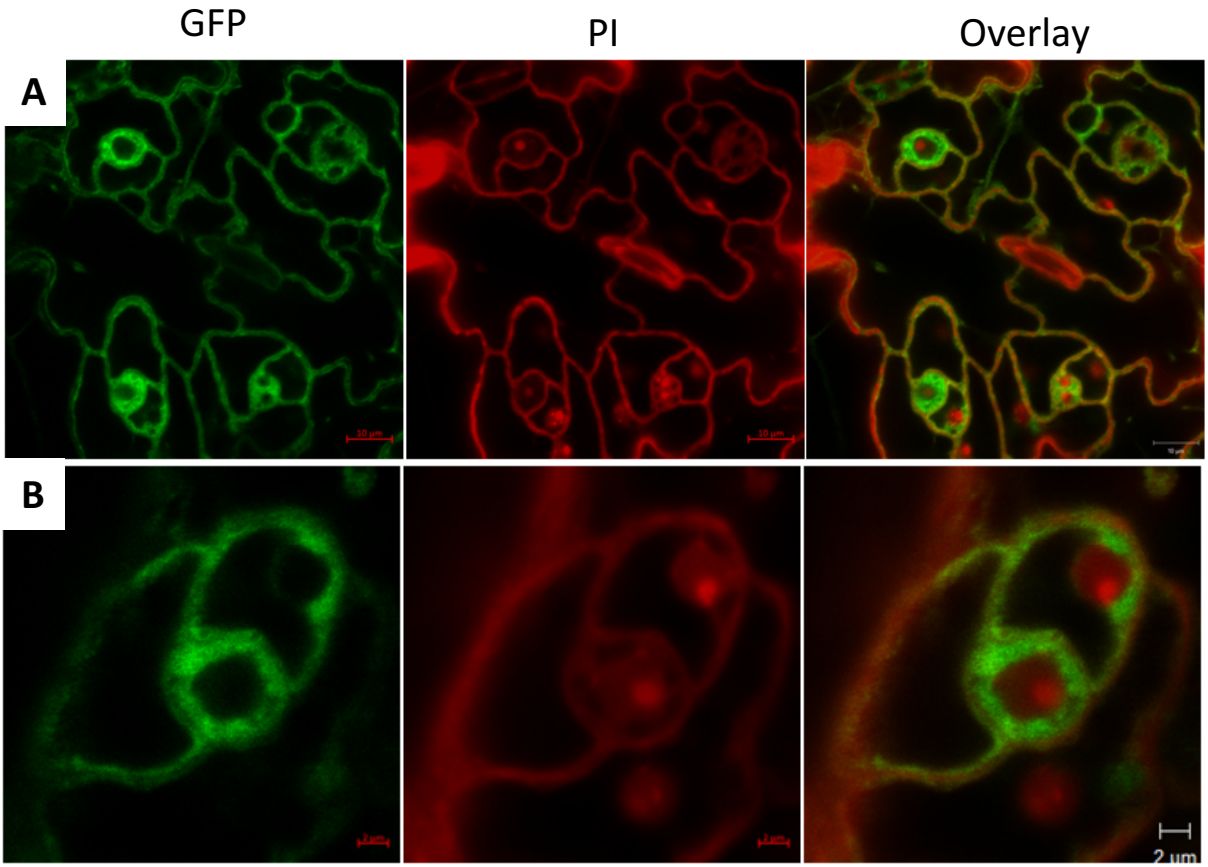

Figure 39. (A) eIF3E distribution in cotyledon leaf epidermal cells of 5 days old seedlings. (B) Granular localization emphasized in guard cells of stomata is particularily enhanced. PI: propidium iodide.

4.2 Mature pollen and pollen tube

4.2.1 eIF3B1

For localization in pollen, mature pollen grains were mounted first on 30 % glycerol and later on DAPI staining solution for nuclear co-localization. eIF3B1 showed granular localization in the cytosol of the vegetative cell suggesting potential translation hot spots and/or sites of stored RNA garnules (Figure 40). More interestingly, eIF3B1 signal increased around the vegetative cell and sperm cells membranes and not in vegetative or sperm cells nuclei (Figure 40A). The localization around the sperm cell nuclear need further emphasis to establish in which side of the membrane is eIF3B1 localized and/or whether the signal is also in sperm cell cytosol (see discussion).

During *in vitro* pollen tube growth, we observed two different patterns of localization in the vegetative cell. When pollen tubes were mounted with 10 µM ER-tracer solution (Thermofisher) for co-localization with the ER lumen as likely sites of translation hot spots, we observed granular localization of eIF3B1 in the vegetative cytosol that partially co-localized with the ER tracer (Figure 40B). However, when pollen tubes were observed directly on

germination slides, the granular localization in the vegetative cell was less prominent and more uniform localization was observed (Figure 40B, magnified). The disappearance of this granular pattern localization during pollen tube growth seems typical for RNA binding proteins (Hafidh et al., unpublished). The distinct sperm cell membrane localization was maintained even during pollen tube growth (Figure 40B, magnified).

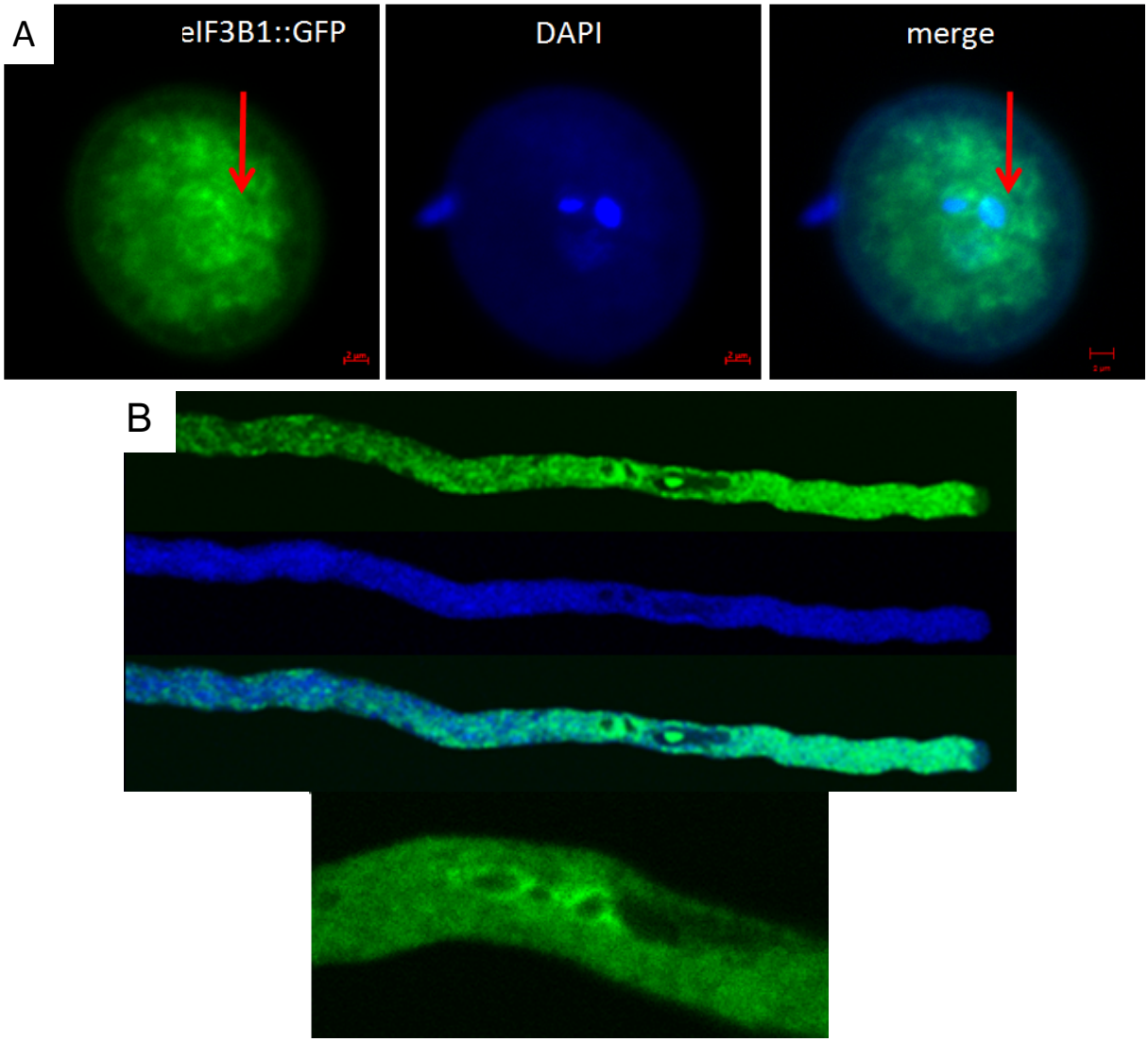

Figure 40. (A) eIF3B1 protein localization in mature pollen grain co-stained with DAPI showing vegetative nucleus and sperm cells nuclei, red arrow showing potential localization around sperm cells membrane. (B) eIF3B1 protein localization in growing pollen tube. Sperm cells are visible. ER tracer in blue, with merge.

4.2.2 eIF3B2

Similar to eIF3B1, we also observed granular localization in the vegetative cell of mature pollen and increased concentration around vegetative cell membrane (Figure 41A). The slight weaker expression of eIF3B2 made it challenging to observe reproducible localization around the sperm

cells membrane in mature pollen (Figure 41A). In pollen tubes, the vegetative cell granular localization also disappeared and a clear increased concentration around sperm cells membrane was observed (Figure 41B).

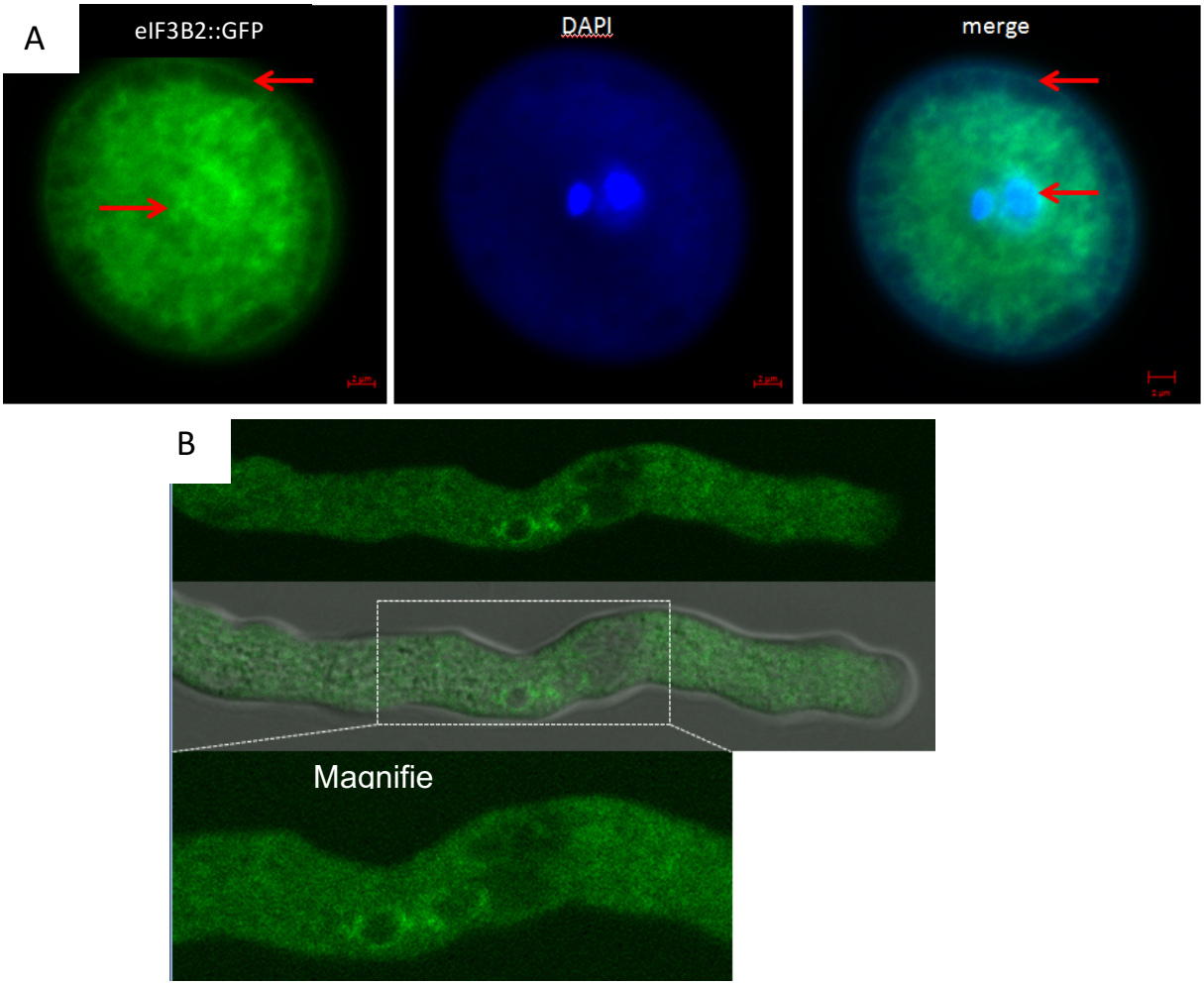

Figure 41. (A) eIF3B2 protein localization in mature pollen grain co-stained with DAPI. Red arrows showing potential localization around sperm cells and vegetative cell (grain perimeter) membrane. (B) eIF3B2 protein localization in pollen tube showing emphasis in sperm cells localization and diffuse localization in the vegetative cell cytosol.

4.2.3 eIF3E

Confocal analysis of eIF3E revealed protein localization around vegetative cell membrane with less prominent sperm cells membrane localization that could be identified (Figure 42A). However, the sperm cell membrane localization was observed in some pollen grains. During *in vitro* pollen tube growth, eIF3E showed ER-like pattern in the vegetative cell cytosol which was also slightly granular compared to eIF3B1 and eIF3B2 (Figure 42B). This suggests a clear overlap of the three subunits but also a likely distinct pattern for eIF3E localization. Localization around the sperm cells membrane was clearly visible in pollen tubes, but remains weaker compared to eIF3B1 and eIF3B2 (Figure 42B).

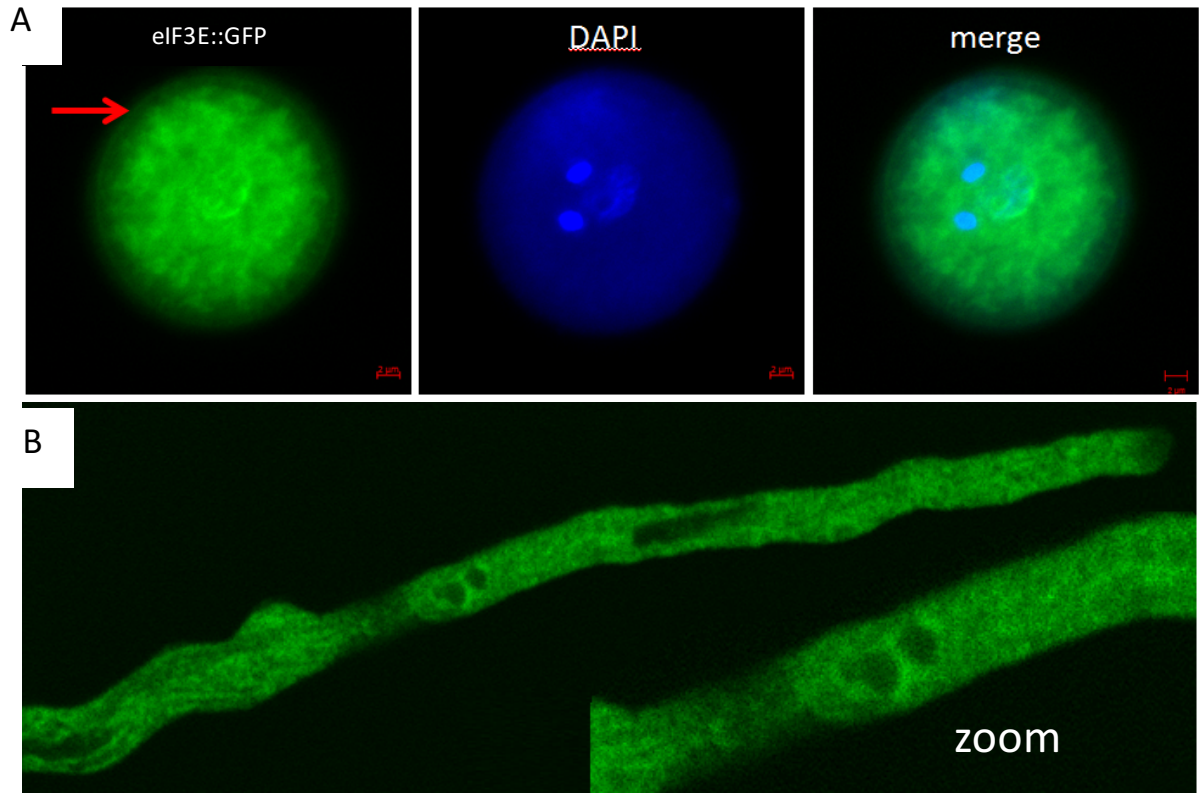

Figure 42. (A) eIF3E protein localization in mature pollen grain co-stained with DAPI. Red arrow shows potential localization around vegetative cell (grain perimeter) membrane. (B) eIF3B2 protein localization in pollen tube showing ER-like strands and a clear localization around the sperm cells membrane is visible.

4.2.4 Summary

Protein localization in the sporophyte and especially in the male gametophyte showed similar patterns for all the three subunits of interest, showing notably granular patterns in dry pollen grain and a diffuse cytosolic localization in pollen tube with the exception of eIF3E. We can conclude that there is no substantial difference between eIF3B1 and eIF3B2 isoforms spatial localization, however, eIF3E seems to show overlapping but also distinct pattern of localization to eIF3B1 and eIF3B2 in the vegetative cytosol. This might hint on potential extended role of eIF3E on top of its role and association with eIF3 translation initiation complex. Similar patterns of localization were also observed around the sperm cell membrane. It is not clear if the sperm cell membrane localization of the three subunits is on vegetative cell side or inside the sperm cells. The clarification is important to establish whether there is a translation initiation hot spots around the sperm cells where ER can also be found to facilitate protein import into the sperm cells or there is no inter-dependence on translation machinery between the two cell types. Co-localization with cytoskeleton is also difficult to establish for actual data. A summary

localization derived from eIF3B1, eIF3B2 and eIF3E together with illustrative pollen cartoon is presented (Figure 43).

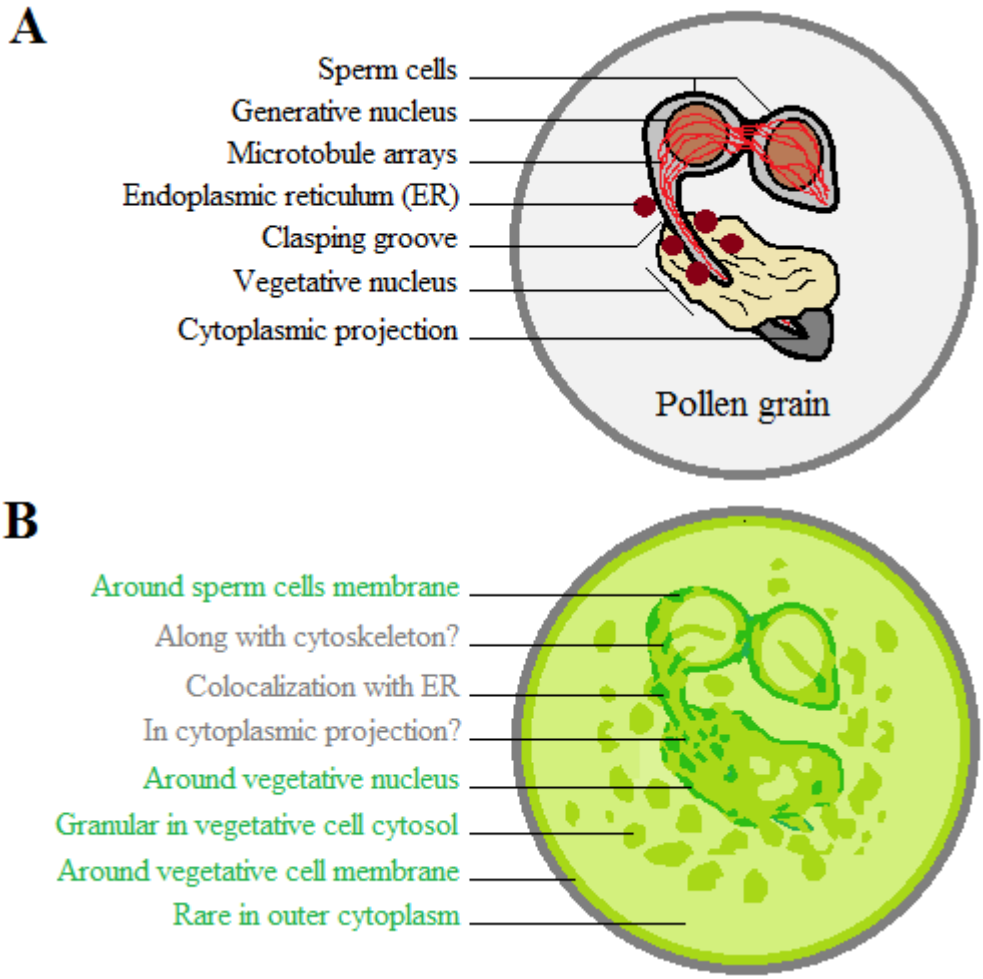

Figure 43: (A) Schematic representation of a pollen grain with sperm cells and main organelles. (B) Summary of subcellular localization pattern of eIF3 subunits eIF3B1, eIF3B2 and eIF3E based on our observations, showing clear (labels in green) and hypothetical (labels in grey) relations with structures shown in the scheme that have been observed at least for one of the studied subunits. Pale green: weak, often "area-wide" signal; medium green: moderate signal showing structures, typically the global "granular" distribution; dark green: intense signal showing structured patterns.

5. PolyA binding protein localization

Among other PolyA binding proteins (PABP's), PABP3 and PABP5 are almost specific for male gametophyte, as shown by transcription levels of these proteins from eFP browser data (Figure 44A). As translational complexes are mainly inactive in dry pollen, with ribonucleoprotein complexes containing transcripts and translation initiation factors, it is interesting to observe the distribution of those PABP, in order to establish if PABP is already associated with stored mRNA, allowing its storage in a circularized configuration as in

translational initiation, or if this initiation step occurs only after rehydration, when abundant mRNA translation quickly starts. As shown in Figure 44B, PABP (marked with red fluorescent protein – RFP) shows similar distribution pattern as eIF3B1, eIF3B2 and eIF3E in dry pollen, with granular localization in vegetative cytosol, around vegetative cell membrane and around sperm cells membranes, which plaids for the hypothesis of an association with mRNA transcripts. Colocalization with eIF3B1, eIF3B2 and eIF3E is planned in the near future to allow more precise investigations.

A

	PolyA binding proteins PABP3 and PABP5 expression level				
	Rosette	Root	Stem	Mature pollen	Pollen tube
PABP3	16	9	14	741	21
PABP5	16	14	17	2750	1111

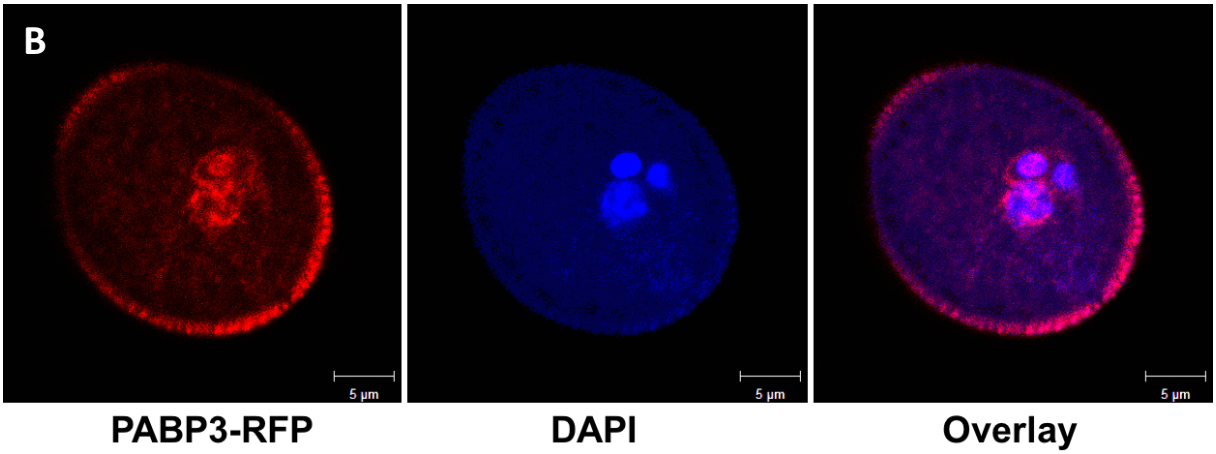

Figure 44. (A) Heat map showing expression of genes coding PABP3 and PABP5. (B) PABP3 localization in mature pollen grain, with DAPI staining as reference.

6. COP9 complex mutants in the male gametophyte and relation with eIF3E

6.1 Characterization of *fus 5 (csn-7)* and *fus 6 (csn-1)* mutants

COP9 subunits Fus 5 and Fus 6 (CSN-7 and CSN-1 respectively) were subjected to similar phenotypic investigations as eIF3 subunits. The objective was to study the link between COP9 signalosome imposed regulation with eIF3E turnover in the context of the male gametophyte where eIF3E is speculated to have a multifunctional role. The strategy of the experiment was to measure eIF3E-GFP expression levels in *fus5* and *fus6* mutant pollen by quantifying amount of GFP relative to eIF3E-GFP expression in wild type. The outcome of this investigation is expected to address whether the mechanisms of eIF3E regulation is maintained between the

sporophyte and the gametophyte despite the differential translational status of the two cell lineages.

6.1.1 Genotypic verification of *fus 5-1* and *fus 6-1* mutants

Extraction of genomic DNA to prove the homozygous status of slow-growing seedlings obtained from germinated "purple seeds" (see Chapter I, 4.2) was done for both lines, using two groups of 12 seedlings per line for a pool DNA extraction. For *Fus 6-1*, another goal was a proofread of kanamycin selection reliability. For *fus 6-1*, DNA extracted from parents of plants that showed a proportion of descendants resistant to kanamycin, and DNA of plants having produced only sensitive descendants, were genotyped using gene-specific and insertion-specific primers: only parents of partly resistant descendants showed heterozygous genotype (Figure 45). For *Fus 5-1* point mutation, a specific genotyping technique termed derived cleaved amplified polymorphic sequences (dCAPS) was used. The technique explores the polymorphism introduced by the point mutation to facilitate design of a primer with few mismatches that together with the point mutation creates or destroy a restriction endonuclease sensitive polymorphism. Amplification followed by restriction digestion with DdeI restriction enzyme, leading to clear distinct patterns on agarose gel. The *fus 5-1* mutation creates a DdeI restriction site in PCR product (as previously shown in Figure 12): the largest fragment obtained by digestion on wild type is cut in two fragments: the smallest one is barely visible at the bottom of the gel, but the larger fragment has reduced length, which is clearly visible (Figure 45). Both patterns are present on heterozygous plants.

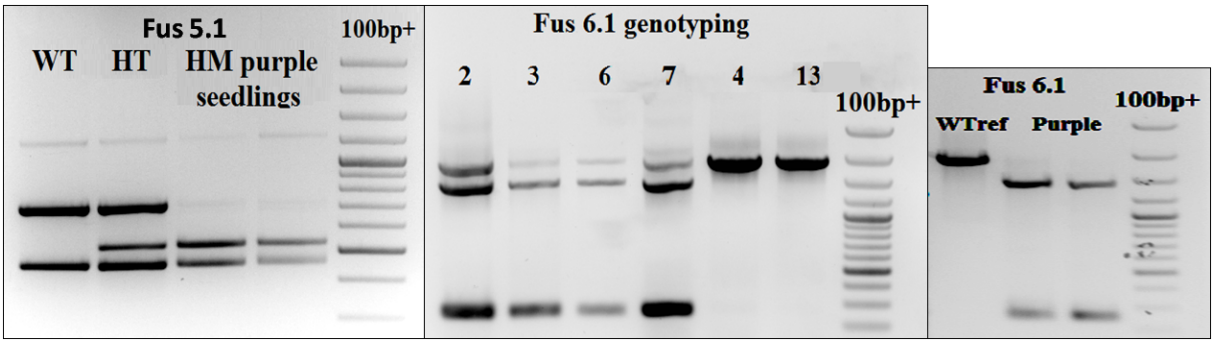

Figure 45. Left gel shows genotyping for *fus 5-1* mutation: WT reference, HT and two HM "purple seeds" groups. Middle gel shows genotyping for *fus 6-1* mutation of DNA extracted from four plants (2, 3, 6 and 7) having produced kanamycin resistant descendants (at 2/3 proportion), and of two plants (4 and 13) having produced only kanamycin sensitive descendants, clearly showing correlation between kanamycin resistance and *fus 6-1* (HT in this case) mutation presence. Right gel shows HM mutant status of seedlings derived from *fus 6-1* "purple seeds" (and also WT reference).

6.1.2 Verification of knockout by semi-quantitative RT-PCR

As expected for *fus5-1,* an allele with a point-mutation, *semi*-qRT PCR showed an almost identical amount of transcripts in heterozygous plants as in wild type (Figure 46). Only downstream pair of primers were used, which is largely enough to conclude to the result that quantity and integrity of transcript is maintained (Figure 46). The double band appearance for Ubq10 reference gene was constant and difficult to explain, but the results were clear. This semi-qRT PCR naturally does not give conclusions about mutant gene protein functionality, but it is probably very reduced because of the early occurrence of translation stop codon (Figure 46).

As we can see, *Fus 6* transcript appears to be present at similar level in inflorescence tissues in wild type plant as in heterozygous *fus 6-1* mutant plants. The PCR results even suggest a higher transcript presence in mutant lines (the experience having been reproduced three times, for optimization reasons, with similar differences each time); however, the difference is not significant and important enough for further investigations in the context of this work. In conclusion, we can say that both *fus 5-1* and *fus 6-1* heterozygous lines show no reduction of transcripts abundance in the sporophyte.

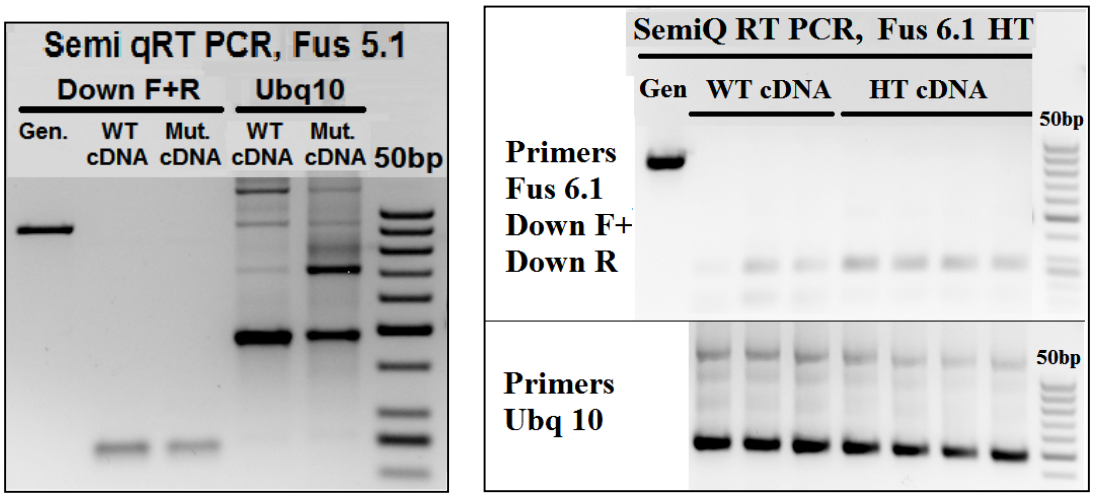

Figure 46. Semi-qRT-PCR results showing WT cDNA and heterozygous mutant cDNA of *fus 5-1* and *fus 6-1* T-DNA insertion mutants. Ubq10 amplification from same cDNA samples and genomic DNA.

6.1.3 Analysis of sporophytic phenotype

We did not observe any phenotypic alteration in the sporophyte life cycle of *fus 5-1* and *fus 6-1* heterozygous plants, but homozygous plants had severely affected phenotype, characteristic for COP9 mutations we already described in Chapter I, 4. Anthocyanin accumulation, reduced germination level, absence of elongation in the dark, extremely slowed down growth and

lethality at first true leaves stage were also observed by us on *in vitro* grown *fus 5-1* and *fus 6-1* homozygous mutant seedlings (Figure 47).

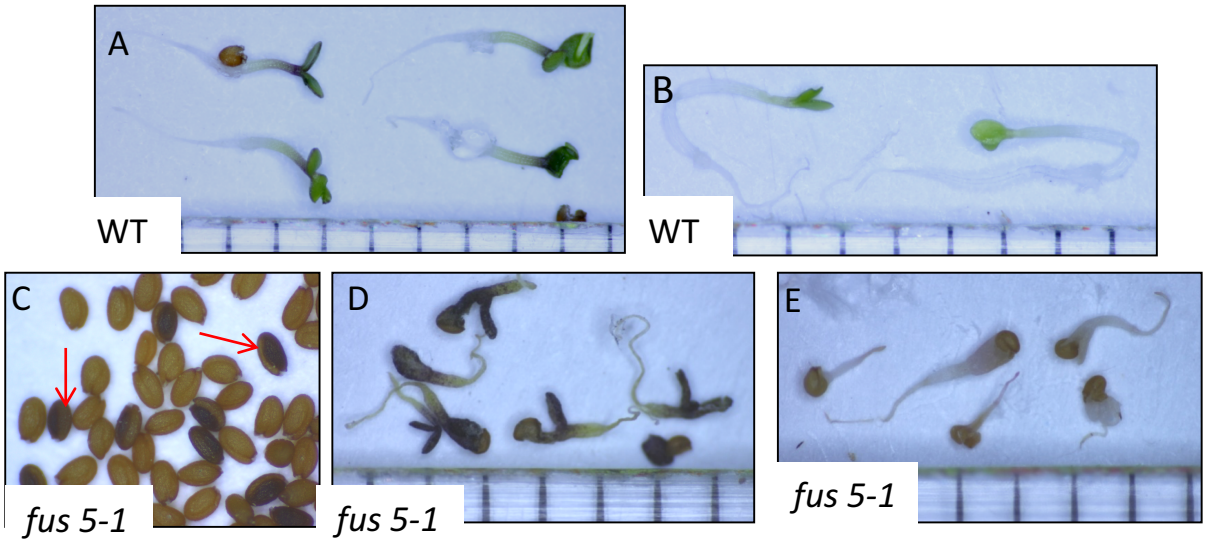

Figure 47. Seedlings grown vertically on ½ MS medium. (A) For reference, 2-days old wild type seedlings. (B) For reference, 3-days old wild type seedlings grown in dark. (C) Seeds from *fus 5-1* heterozygous plants, with purple homozygous seeds. (D) *fus 5-1* homozygous mutant seedlings after 3 weeks of growth in light. (E) *fus 5-1* homozygous mutant seedlings after 3 weeks of growth in darkness. The ruler at the bottom gives a scale in mm.

6.1.4 Screening of mature pollen phenotype

Severe pollen phenotypic defects were observed in *fus 5-1* mutant line with high frequency. These defects include collapsed pollen grains with notable deformities, and frequent presence of cytosolic inclusion bodies (Figure 48). At the cellular level, defects could be observed in various stages of pollen development, during mitosis I and mitosis II (Figure 48). Nuclear defects observed under UV with DAPI staining were partly overlapping with general morphological defects of pollen grains (including collapse pollen and cytosolic inclusions) observed in bright field.

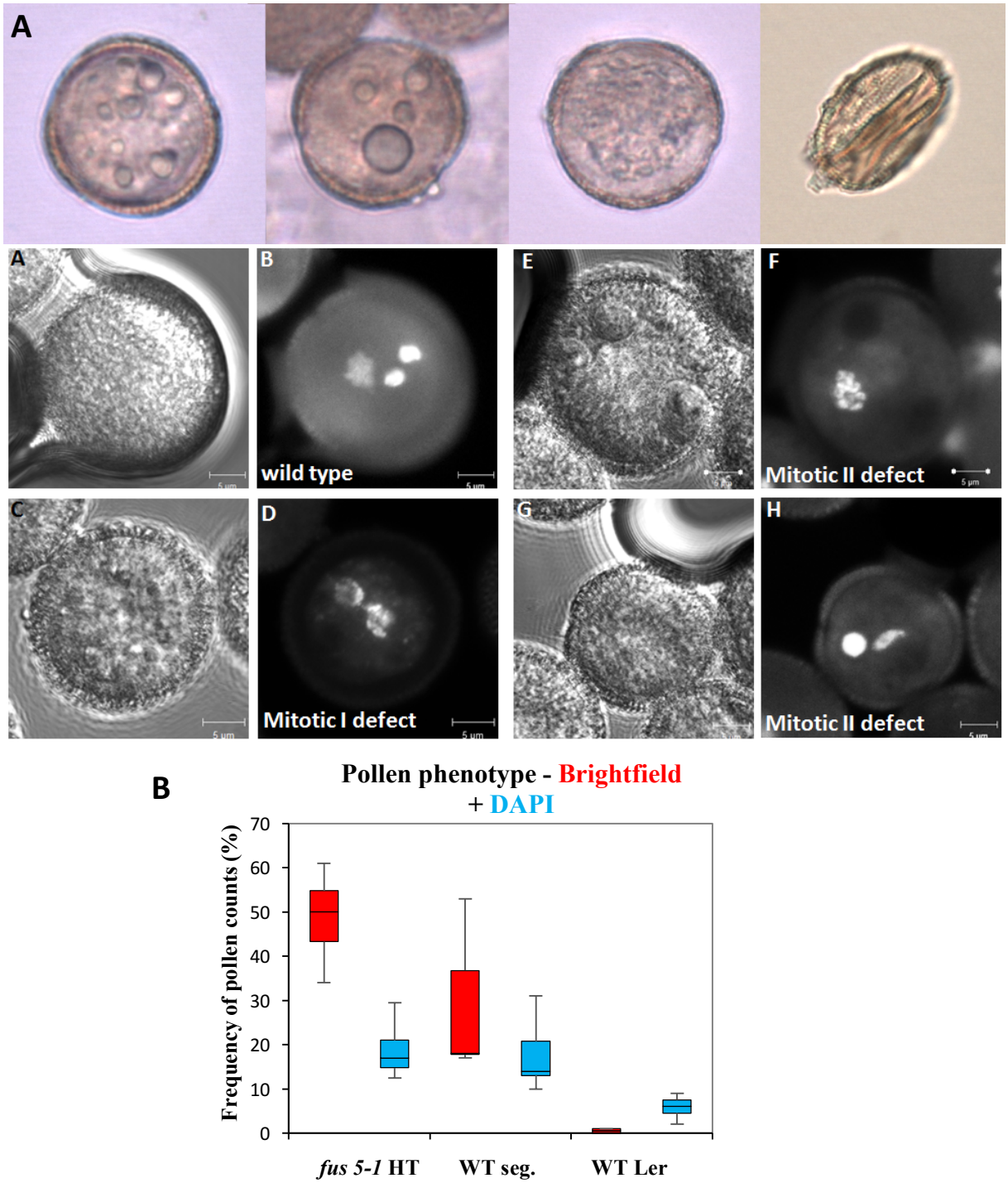

Figure 48. (A) Various anomalies of *fus 5-1* mature pollen grains in bright field. Nuclear staining with corresponding bright field micrographs showing various mitotic defects at the first division of the unicellular microspore (Mitotic I) or a second division of the generative nuclear (mitotic II) of *fus* 5.1 mutant pollen. (B) Frequency distribution of the phenotypic classes in heterozygous (HT), wild type segregants from HT *fus* 5-1 and a wild type of Landsberg (Ler) ecotype.

However, a huge problem was discovered in this line (unfortunately a recurrent problem with almost all mutant lines used in this work). As we can see, phenotype was also observed in wild

type segregants, with a significantly reduced frequency, but clearly present (Figure 48). This fact suggests a possible presence of other mutations in the genome of the *fus 5-1* line. Also, this background phenotype does not seem to segregate away from *fus 5-1* alelle, generation to generation, implying a likely close linkage with the *fus 5-1* mutation. Even if a clear correlation between *fus 5-1* mutation and pollen phenotype is observed, it is impossible to tell what is the exact origin of the phenotype without this issue. For this reason, a cross with *a male sterile 1* (*ms1*) plant was done in order to outcross the background phenotype. Obtained F1 generation showed almost no phenotype in wild type segregants from *fus 5-1* heterozygous plants, except rare plants (4 in almost 30, 2 WT and 2 HT) and no significant difference now appeared between heterozygous mutants and wild type segregants (Figure 49).

Contrarily to *fus 5-1* mutant line, *fus 6-1* line appeared to be much cleaner, probably without other background mutations or insertions. As we can see, no developmental abnormalities appears on pollen grains as seen in bright field (Figure 49). However, DAPI staining shows that there is a slight increase in pollen mitotic defects in *fus 6-1* heterozygous plants compared to pollen from wild type segregants or that of pure wild type pollen (Figure 49). This difference remains very minor. Figure 49 shows results of phenotyping for both *fus 5-1* crossed with *ms1* (Both Landsberg ecotype and excluding few individuals with huge phenotype) and *fus 6-1*. In both lines, final result shows the absence of real phenotype in mutant pollen.

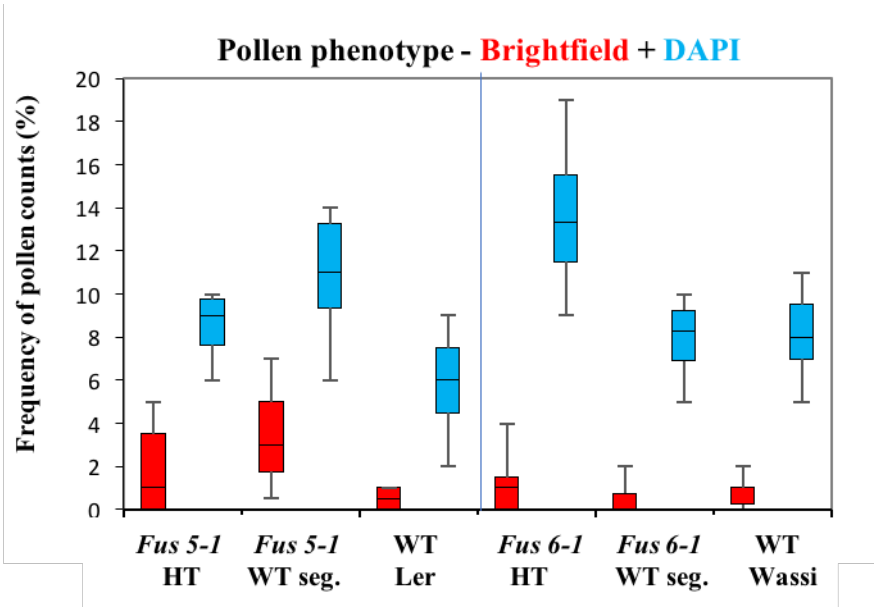

Figure 49. Results of pollen phenotypic screen of *fus 5-1 and fus 6-1* HT mutant, comparison with wild type segregants of this line and with Wassilievskia wild type reference.

6.1.5 Analysis of *in vivo* pollen tube growth

While *fus 5-1* mutant line, which was biased by background mutations, was not subjected to *in-vivo* pollen tube growth, such an experiment was done for *fus 6-1* mutant line in order to complete segregation transmission statistics results with a male gametophyte fitness test. The results clearly show that pollen tube fitness is absolutely not reduced in any way by the mutation (Figure 50), which was later confirmed by transmission statistics (Figure 50). Since the COP 9 subunits are known not to be functionally redundant, these results suggest that Fus 6 is likely not required for pollen tube growth.

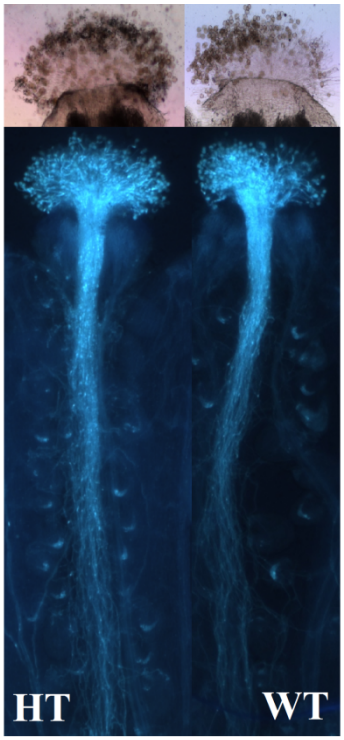

Figure 50. *In-vivo* pollen tube growth of HT *fus 6*-1 mutant compared to WT reference 20 hours after pollination and visualized by aniline blue staining.

6.1.6 Dissection of siliques phenotype

First visible sign observed on siliques for both lines is the presence of seeds containing anthocyanin, which indicate homozygous for the *fusca* mutation. These purple seeds are present in heterozygous mutant plants, in a proportion of about 15% in *fus 5-1* and 20% for *fus 6-1* heterozygous, after screening 8 plants with 5-6 siliques per plant for each line (Figure 51C). The reduced proportion of homozygous mutants compared to 25% expected from Mendelian laws is not surprising for such a homozygous early lethal condition.

These results have been obtained for healthy plants growing in good conditions. One group of *fus 5-1* plants which was grown as a backup was neglected and suffered a succession of under-watering and over-watering periods, giving a non-planned occasion to discover that abiotic stress had an effect on this average frequency, reducing the amount of purple seeds. The age of

the plant also plays a role; some siliques were once collected on almost senescent plant and appeared to contain much less purple seeds.

Heterozygous mutants together with wild type segregants and pure wild type lines of the same ecotype were also screened for general infertile and collapsed seed phenotype. *fus 5-1* HT mutants appeared not be affected by the background mutation at the seed level, and obtained results are similar with *fus 6-1* HT mutant (Figure 51D). These results suggest that the potential background mutation in *fus 5-1* mutant line is only impacting pollen development (a problem we solved for pollen screening by outcross) and not embryo development.

For both lines, obtained results (8 plants for HT, 5 for WT segregants and 5-7 for WT reference) shows a very slightly increased unfertile female gametophyte ratio in mutants (Figure 51D). This can be considered as a possible partial explanation to decreased proportion of HM mutant seeds according to Mendelian rules, this HM status leading to an increased risk of early embryo lethality.

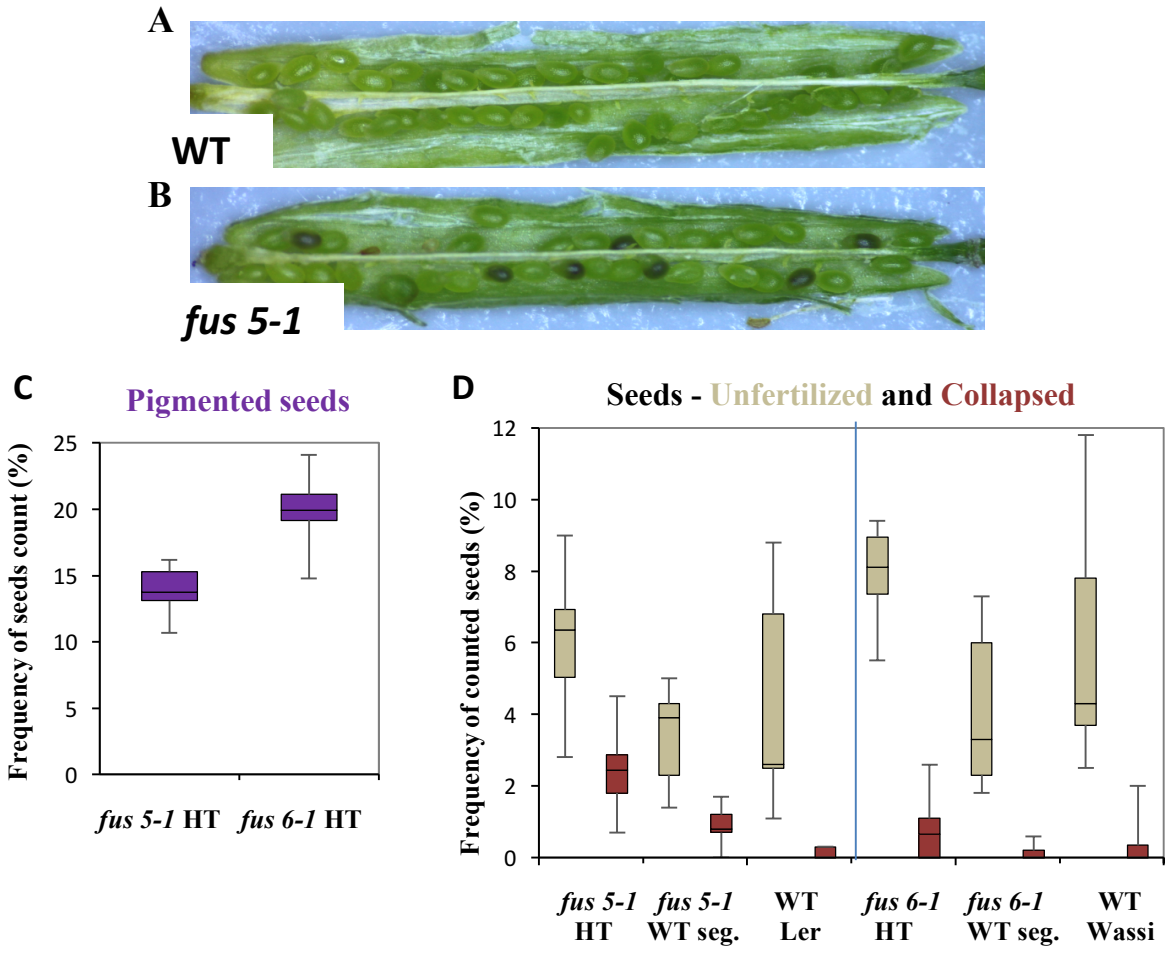

Figure 51. (A) Silique from *fus 5-1* WT segregant (B) Silique from *fus 5-1* HT mutant. (C) Graph showing frequency of the pigmented seeds observed in *fus* 5-1 and fus 6-1 heterozygous plants. (D) Results of siliques phenotyping in *fus 5.1* and *fus 6.1* HT

lines, compared to WT segregants of those lines and pure WT individuals of the same ecotype.

6.1.7 Transmission and segregation analysis of the mutant *fus 5-1* and *fus 6-1*

As homozygous mutant genotype results in early lethality, only heterozygous and wild type segregants were used for segregation statistics. Amounts of purple homozygous seeds are not a reliable indicator, as they are varying depending on development conditions, as we already pointed out. PCR coupled with dCAPS restriction digestion-based genotyping for segregation analysis was done for *fus 5-1* genotyping (Figure 51A), while kanamycin antibiotical selection was used to achieve similar results for *fus 6-1* segregation analysis. The antibiotical selection was a great help, allowing simple counting of thousands of resistant/sensitive individuals (Figure 52B). Five different parent lines were screened. As for previously described *fus 5-1*, no homozygous mutant had a chance to be counted, those seeds barely starting their badly delayed germination after a time (approximately 10 days) when normal plants were already at the late stage of seedling development baring cotyledons and at least two true leaves.

Although the background phenotype problem was susceptible to affect the results, it was decided to proceed to test for *fus 5-1* mutants transmission also as a test of the effect of the background mutation, by genotyping descendants of self-pollinated heterozygous parents (Figure 51). A main transmission test was done with approximately 50 seedlings using a parent with representative phenotype, other data were gathered from current genotyping which had previously been done when different generations and lines were grown for phenotypic investigations (Figure 51).

For *fus 5-1*, there was a substantial deviation between the amount of resistant and sensitive seedlings between lines (Figure 51). However, the much reduced population that was genotyped for most of the lines could have contributed to this variability. Despite, we can preliminarily conclude that in some lines there is a significant reduction in mutant allele transmission, however, this could be a result of an additive effect of *fus 5-1* mutation and the background mutation(s) adverse effects on pollen development and may be the female gametophyte development. Further investigations are needed in order to find out a real relation between phenotypical severity of pollen defects and transmission ratio, with a much higher amount of plants for each line. This was not performed for now but will be performed once we obtain a background-free line. Independent experiment to investigate male and female transmission efficiency of the mutant *fus 5-1* allele will also be very informative.

For *fus 6-1*, we can clearly see that transmission is unbiased through male and female gametophyte (Figure 51) and that heterozygous embryo is perfectly viable and seed germination

is unaffected. Divergence with Mendelian transmission segregation was found only at the side of homozygous mutants (not presented in the table, as not counted in this test), homozygous seeds being in reduced number and having reduced germination rate, see previous section. *Fus 6-1* results are clearly pleading for an unbiased transmission of a COP9 core subunit coding gene mutation, with 2/3 HT and 1/3 of WT plants observed.

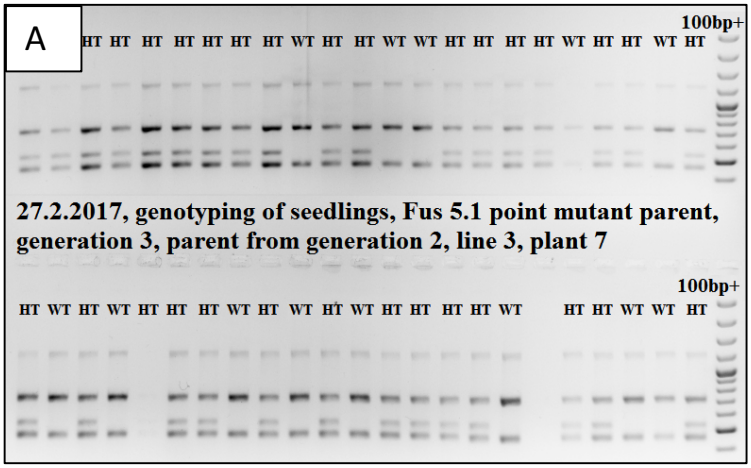

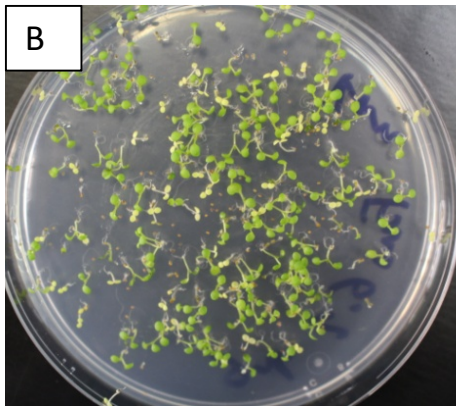

Fus 5.1 genotyping, seedlings from HT parents				
Line	HT	WT	HM	% HT
Gen.1	12	7	0	63,2
G2.2	8	6	0	57,1
G2.3	13	6	0	68,4
G3.3.2	7	3	0	70,0
G3.3.3	5	5	0	50,0
G3.3.7	32	13	0	71,1
Exp. tot.	65,3	32,7	0	66,6
Total	64	34	0	65,3
χ2	0,026	0,052	χ2 = 0,078	

Fus 6.1 kanamycin resistance, seedlings from HT parents			
Line	Resistant	Sensitive	% resistant
G2.1	239	132	64,4
G2.2	119	61	66,1
G2.3	282	130	68,4
G2.6	592	263	69,2
G2.7	871	498	63,6
Exp. tot.	2124,7	1062,3	66,6
Total	2103	1084	66,0
χ2	0,222	0,443	χ2 = 0,665

Figure 52. (A) *fus 5-1* seedlings genotyped using dCAPS coupled restriction analysis. (B) *fus 6-1* seedlings on kanamycin selection. Bottom tables corresponding statistics for both lines.

6.2 Regulation of eIF3E in *fus 5* and *fus 6* mutants

As we stated in Chapter I, 4.2, eIF3E is regulated by COP9 complex and a malfunction of this complex in sporophyte leads to eIF3E over-accumulation, with serious phenotypical impairment. However, male gametophyte doesn't seem affected. We wanted to see if the absence of abnormal pollen phenotype and the absence of reduced pollen viability when COP9 complex is not functional could be explained by an absence of negative consequence of eIF3E over accumulation in pollen, or by an absence of COP9 necessity in pollen to prevent eIF3E over accumulation. For this purpose, *fus 6-1* heterozygous mutants and wild type plants were

transformed with eIF3E:GFP in order to investigate possible differences in eIF3E distribution and concentration in *fus 6-1* mutant pollen. Three fus *6-1* heterozygous plants were selected, as well as three wild type plants as reference. Because of *fus 6-1* heterozygous status, half of GFP positive pollen grains carry *fus 6-1* mutation and if there is a difference in eIF3E:GFP expression pattern, we can expect two different populations in GFP positive pollen.

First observation showed no variations in GFP signal distribution pattern, which is similar in all pollen grains to the pattern observed in wild type plants: eIF3E global distribution pattern is not affected. However, an increased quantity of bound or free eIF3E present in excess may be not necessarily detectable by expression pattern observation, that's the reason why a quantification of fluorophore signal expression was done.

When a second generation of mutants coming from one parent transformed with eIF3E:GFP will be available, comparison of global GFP signal intensity will be possible because of similar eIF3E:GFP expression. For now, variations are observed between transformants, because of different insertion sites. However, each transformant is heterozygous in eIF3E:GFP, because approximately 50% of pollen grains are positive, preventing biasing by multiple insertions (Figure 52A). Mean signal intensity was measured in ImageJ software by selecting an identical area in multiple pollen grains. 40-120 pollen grains were quantified per line and values were proportionally re-scaled to have an average expression of 100 (arbitrary unit) for each line. Except for first heterozygous line, where values are considerably variable (probably because of variable silencing of eIF3E:GFP expression), dispersion of values shows no difference between *fus 6.1* and wild type background (Figure 52B), no effect on eIF3E abundance being visible in COP9 mutants.

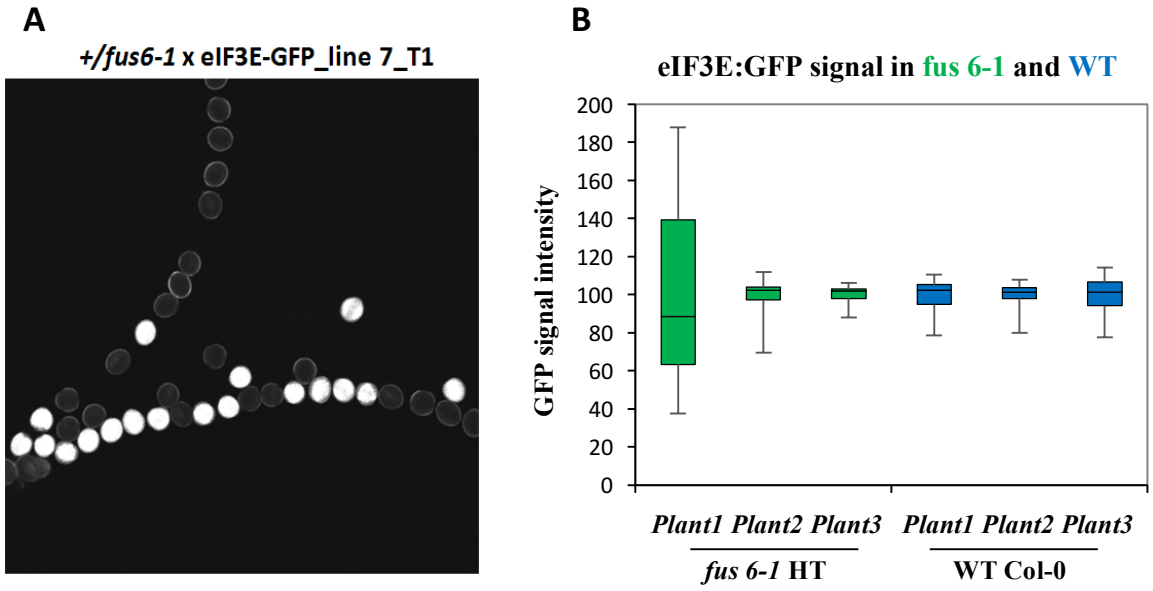

Figure 52. (A) Population of eIF3E:GFP negative and positive pollen grains from *fus 6-1* heterozygous mutant. (B) Graphic of eIF3E:GFP signal intensity variations between individual pollen grains in *fus 6-1* heterozygous and wild type background.

IV. DISCUSSION

1. Only *eif3e* mutation impacts the male gametophyte function but not *eif3b1* or *eif3b2*

1.1 Mutation of *eif3e* subunit has severe consequences in gametophyte

1.1.1 eIF3E is necessary for pollen functionality

In pollen, *eif3e* null mutation was previously reported as being lethal (Yahalom *et al.*, 2008), our investigations confirmed this finding and also corroborated that mutant transmission is blocked through male gametophyte. Therefore, absence of homozygous mutants is coming from the lack of transmission and not from sporophytical lethality caused by the absence of this core subunit. The hypothesis of an early lethality during microsporogenesis was informed by a previous study (Roy *et al.*, 2011), and observations concluded to an absence of abnormal phenotype in mature pollen, contrarily to the situation existing for example with *eif3f* mutants (Xia *et al.*, 2010). Pollen mitosis was shown not to be affected in *Arabidopsis* (Figure 24), as it already had been previously seen in rice pollen (Wang *et al.*, 2016). Interestingly, reduced germination of *eif3e* mutant pollen and pollen tube growth *in vitro* in Arabidopsis was also reported (Roy *et al.*, 2011), however, we could not observe this impairment *in vivo* (Figure 24). Nevertheless, our segregation data clearly indicated that even if *eif3e* mutant pollen is viable, it is not functional and unable to achieve a proper fecundation (Figure 30). There is probably no penetration in synergid, which is normally leading to immediate synergid death (Christensen *et al.*, 1997), as aborted fecundation attempts would have let to an increased frequency of early aborted embryo sacs, even with the two attempts offered by two synergids, and it is not the case (Figure 28). The exact mechanisms of such a malfunction need further investigation likely on events prior to gamete fusion during double fertilization.

1.1.2 Consequences of *eif3e* mutation are not limited to male gametophyte

Male gametophyte functional impairment being established, we can add that actors allowing partial viability in the absence of *eif3e* in the female gametophyte are unknown and present unique opportunity to investigate the differential activities of eIF3E in different tissues. Reduced abundance of mutant female gametophytes cannot be (or very little) explained by its developmental failure, again because of negligible abortion level in siliques (Figure 28), which is contrary to expected reduced seed set accompanying reduced mutant segregation.

Programmed cellular death of 3 from 4 cells after meiosis, which normally occurs during megasporogenesis (Christensen *et al.*, 1997), may possibly affect preferentially mutant cells. It is also possible that heterozygous seeds have reduced germination, even though heterozygous plants seem to have no phenotype, but it would be difficult to estimate because of natural variations in germination rate, no substantial reduction having been observed anyway.

1.2 Functional compensation may exist between eIF3B1 and eIF3B2 subunits

1.2.1 eIF3B1 is required in sporophyte

As we stated in Chapter I, 3.2, eIF3B is a core subunit and the presence of a second isoform is not documented in other organisms than plants. In *Arabidopsis*, we observe sporophytic lethality of *eif3b1* homozygous, no homozygous seedling being observed (Figure 28). To explain *eif3b1* homozygous lethality in sporophyte, several hypotheses are plausible: It is possible that eIF3B1 is the only isoform recruited to ensure proper translation of specific transcripts translated in specific localizations and the impairment of the target genes having consequences in sporophyte. Beyond translational initiation, an alternative vital function of eIF3B1 in sporophyte that cannot be complemented by eIF3B2 also cannot be excluded.

We also have to point out that *eif3b1* homozygous sporophytical lethality during embryo development which had been previously observed (Roy, 2010), was observed only in a minor level in this study (Figure 26). Other factors, as fertilization problems or proper homozygous seed development followed by non-germination, may be evoked to explain absence of homozygous descendants. The importance of such factors may be variable.

As eIF3B2 appears to play a complementary role for eIF3B1 in eIF3 subunit integrity and unaffected function only in the gametophyte, as we will see in next section, it may appear as a subunit with minor functional importance in plants. It is possible that following the duplication of original eIF3B coding gene, evolutionary process lead to a reduction of eIF3B2 functional capacity as eIF3 subunit, redundancy with eIF3B1 being not essential. However, this can be associated with functional divergence having given selective and adaptive advantages (specific implication of eIF3B2 in translating specific transcripts, or gain of alternative functions). This is supported by the potentially reduced growth rate of *eifb2* homozygous mutants. We can speculate that the duplication of eIF3B and its functions can in fact be multiple, eIF3B2 isoform having reduced specific roles also in the sporophyte.

1.2.2 Functional compensation of eIF3B1 by eIF3B2 in gametophyte

Contrarily to sporophyte, eIF3B1 malfunction is viable in male gametophyte. There is practically no impairment in pollen development (Figure 19, 20) and pollen tube growth (Figure 22, 23) in *eif3b1* and *eif3b2* mutants. This observation, associated with obtained transmission ratios (Figures 28, 29), allows almost certain conclusion that a functional complementarity between these two isoforms is efficient in male (and also female) gametophyte. This complementation is even total, at least in normal conditions, pollen tube fitness being normal in *eif3b1*. To verify this functional redundancy and demonstrate the role of eIF3B1 and eIF3B2 in the gametophyte, we will generate *eif3b1;eif3b2* double mutant plants and investigate phenotypic deviation. Note that this scenario is comparable with *eif3c1* and *eif3c2* subunits, where similar transmission results were observed (Roy, 2010). However, if further investigation show that *eif3b1* viability is in fact not linked to a complementation by eIF3B2 (if double mutant pollen is viable), we will be facing two hypothesis: The existence of another protein playing the role of eIF3B1 in male gametophyte, or a difference in translational mechanism in male gametophyte, eIF3B becoming an accessory subunit here.

2. eIF3B1, eIF3B2 and eIF3E subunits showed overlapping but also distinct localization

2.1 Comparison between individual subunits localization

2.1.1 Comparable localization pattern for eIF3B and eIF3E

All three studied subunits are transcribed with similar tissue-specific level variations in the sporophyte, transcription being more intense in tissues with abundant cell divisions, which are the meristems, elongation zone and leaf primodium (Figures 32-37) and they have similar subcellular distribution pattern in sporophyte as well as in male gametophyte (Figures 40-43). This clearly suggests that the main function of these subunits is being a part of eIF3 factor and that eIF3 factor itself is likely assembled in dry pollen. However, eIF3E is only mildly over-represented in sperm cells compared to vegetative cytosol, while the difference is more important for eIF3B1 and eIF3B2 (compare figure 35, 37 and 40, 41, 42). This cannot be explained at this stage (we will speculate about eIF3E in 2.1.3); however, it is clear that alternative functionalities of separate subunits which would potentially have involved differences in distribution are apparently marginal (in quantitative point of view, not necessarily in functional importance) compared to their main function as part of eIF3 complex.

2.1.2 eIF3B1 and eIF3B2 isoforms localization doesn't show temporal and tissue-specific functional specificities

Transcription of eIF3B isoforms eIF3B1 and eIF3B2 does not seem to show important spatial and temporal preferences in sporophyte (Figures 32, 33) and male gametophyte (Figures 35, 36): first deduction is that the main function of both isoforms is being part of eIF3 complex.
eIF3B2 has lower transcription rate, as shown by RNA seq (Figure 31) and confirmed by our observations of GFP signal, which its concordant with its "accessory" nature compared to eIF3B1, but its potential role for specific translational initiations is not visible from expression pattern at tissue level: eIF3B2 doesn't seem to be specifically transcribed in particular tissues in the context of a specific replacing of eIF3B1 in some tissues or development steps, as it is for example the case for PABP3 and PABP5, specific PABP's in pollen, almost untranslated in sporophyte (source: eFP browser). This doesn't mean that its importance for translation in different tissues doesn't vary (it may include the translation of specific transcripts, and/or maybe translational functionality and regulation in general), but this importance appears low, seemingly limited in male gametophyte to a function of redundancy in the case of eIF3B1 mutation, as we already stated in previous section.
We cannot exclude the existence of a linked mechanism of transcriptional regulation ensuring a convenient abundance of eIF3B, a reduced concentration of one isoform leading to an increased level of the second one. We also cannot exclude a potential role of eIF3B2 in pollen (and sporophyte) for example in a situation of hardened conditions, leading to the translation of specific transcripts. Many speculations can be emitted; however, we shouldn't forget that gene transcription is far away from being regulated in a perfectly pragmatic and economic way, genes being not necessarily silenced when not needed.
For protein localization, even though we plan to perform co-localization of individual subunits and with other factors associated with translation initiation, we can already say that at subcellular level, eIF3B1 and eIF3B2 localize similarly in mature pollen and growing pollen tube. As for transcriptional distribution, subcellular localization proves the main function of both subunits as a part of eIF3 and our speculations from section 1.2 of this chapter about functional divergence having lead to alternative functions are not supported (but not infirmed at all) by this experiment. However, one difference exists: eIF3B2 is more represented around vegetative cell membrane in dry pollen (Figure 41), which may suggest a preferential use of this isoform for some specific subset of transcripts, but this remains highly speculative. Other specificities cannot be clearly observed.

2.1.3 eIF3E turnover and specificities

For eIF3E, a higher transcription level is clearly present in sporophyte and male gametophyte (Figure 31) compared to eIF3B1 and eIF3B2. An increased quantity of synthesized protein would have been reflected in the observed pattern, not only by higher fluorophore brightness, but also probably by a different distribution because of proteins in excess, having not found their place in eIF3 complexes. However, nothing significant can be seen compared to eIF3B1 (Figure 40, 42). There is obviously an increased post-translational turnover, imposing a shorter life-time to eIF3E protein. This intensity of transcription/turnover may be explained by the fact that a precise regulation of this specific subunit may be necessary, which may be explained by adverse effects of eIF3E overexpression (see Chapter I, 4.2) and by the existence of alternative interactions and functions of this protein (see Chapter I, 3.3). At subcellular level, protein localization is similar to eIF3B1 and eIF3B2, except the less prominent abundance in sperm cells in mature pollen and in pollen tube: eIF3E transcription is lower in sperm cells (Figure 31) and protein abundance is lower accordingly (Figure 42), showing that lower expression in sperm cells is not compensated by lower protein turnover or by transcript/protein import. A lower abundance is visibly without consequence in sperm cells, which remain metabolically less active.

2.2 Functions of eIF3 in mature pollen are reflected in localization pattern

2.2.1 Transcripts storage in ribonucleoprotein complex and subsequent translation

The question goes further about the storage of mRNA together with proteins and potential involvement of eIF3 in translation repression in mature pollen grain. It is known that large ribonucleoprotein complexes serve for translationally silent mRNA storage together with assembled translational initiation factors (Honys *et al.*, 2009). A granular distribution of eIF3 subunits (Figures 40, 41, 42) and of PABP in dry pollen (Figure 44) shows that eIF3 factor is likely not freely present in the cytoplasm, but is integrated in assembled initiation complexes, themselves likely bound with cellular structures such as membranes (ER and others) and cytoskeleton (Klyachko *et al.*, 2000). Notably, even though it is not unanimously visible, our fluorescent localization experiments are suggesting a colocalization with ER (Figure 43), suggesting a general rule of localization at the place of future translation.

In growing pollen tube, localization pattern is comparable to sporophytic tissue (Figures 39-42), suggesting similar associations of translation complexes and polysomes with cellular structures, however with an enhanced granular localization and localization around the vegetative and sperm cell membranes, which may be associated with transcripts that are more likely translated in a context of membrane interaction.

2.2.2 Sperm cells and possible interaction with vegetative cytosol

Also, transcription of eIF3B1 and eIF3B2 subunits is slightly higher in sperm cells compared to vegetative cytosol (Figures 35, 36, 37) and protein abundance appears higher in sperm cells cytosol than in vegetative cytosol during pollen tube growing (Figures 40, 41, 42), even though more precise localization of eIF3 distribution around sperm cells membranes will be required. In this phase, sperm cells are known to possess a unique transcriptome, coding proteins involved in specific metabolic and regulatory mechanisms (Borges *et al.*, 2008). In this frame of investigations, a new phenomenon of transcripts (and may be protein) transport from the vegetative cell to the sperm cells likely via the connective membrane channel of the male germ unit (Figure 43) has been reported (Mccue *et al.*, 2011) and we cannot rule out this close association of the eIF3 with the male germ unit membrane network to participate by promoting "local" translation close to the import sites.

3. COP9 is not essential in the male gametophyte and does not seems to regulate eIF3E

3.1 *COP9* mutation does not impair male gametogenesis

A mutation in one of the core constitutive subunits of COP9 complex, *fus 5-1* and *fus 6-1*, did not lead to impairment in male gametogenesis (Figure 49) and pollen tube fitness (Figure 50), while the effect is extremely severe in the sporophyte homozygous mutants (Figure 47). The mutant alleles transmission was not reduced (at least for subunits CSN1 and CSN7, see Figure 52), so we can conclude that COP9 complex does not have any major non-redundant function in the male (and also female) gametophyte, even though genes coding for essential COP9 subunits are transcribed at a nominal level during early stages of microgametogenesis as shown by data from eFP browser. This does not exclude the possibility of an important alternative function of some of COP9 subunits when not associated with the COP9 complex. It is improbable that some core subunits of the complex are not essential subunits in male gametophyte, allowing a residual functionality in the mutant background.

One important thing to observe is that beyond eIF3E regulation, *cop9* mutant developmental impairment, which becomes more and more severe as sporophytical development continues, is mostly caused by associated accumulation of DNA damage leading to an arrest in the G2 phase of the cell cycle (Dohmann *et al.*, 2008) and this complication is probably not yet present in the male gametophyte, after only two cell divisions. But eIF3E overexpression in *cop9* mutants (Chapter I, 4.2) is also a severe adverse factor for organism development.

3.2 Absence of link of *COP9* mutation with eIF3E turnover in pollen

In fact, eIF3E subunit does not seem to over accumulate because of the absence of a functional COP9 complex in the male gametophyte, as such an accumulation would have been visible in fluorescent localization of eIF3E and would have had potential impact on pollen development, as it is the case when overexpression is induced (Yahalom *et al.*, 2008); none of that was observed (Figure 52). The absence of eIF3E over accumulation in the male gametophyte, when transcription levels of the gene coding this subunit are much superior to most of other eIF3 subunits in male gametophyte as in sporophyte, may be explained by other regulatory mechanisms. An explanation may potentially be found in the fact that eIF3E is encoded by 5'-terminal oligopyrimidine (TOP) mRNAs, a feature also found in eIF3F and eIF3H (Iadevaia *et al.*, 2008). All these three subunits have the highest transcriptional level of all eIF3E subunits in sporophyte and the male gametophyte. In vertebrates, the presence of TOP sequence is linked to growth-associated translational regulation (Iadevaia *et al.*, 2008), so there is a possibility of a similar regulation pattern in the male gametophyte of Arabidopsis thaliana. Other potential explanations may eventually be found in alternative specific degradation mechanisms at protein level other than the COP9 mediated protein turnover of eIF3E.

CONCLUSIONS AND FUTURE PERSPECTIVES

Inadvertently, the "messy" T-DNA insertion lines of *eif3b1*, *fus 5.1* and the difficulty in genotyping *eif3e* allele, hampered the progress of the project. Despite, most of the aims of this thesis were fullfiled and based on the obtained data, I can conclude that:

- *eif3b1* and *eif3b2* knock-out mutant lines showed that eIF3B1 subunit, which is vitally required for viability in the sporophyte, it is not dominant in the gametophyte probably due to functional redundancy with eIF3B2 isoform. Similarly, eIF3B2 is redundant in the gametophyte but not in the sporophyte, suggesting that eIF3B2 has a supporting role to eIF3B1 function in the gametophyte but not the sporophyte. Our results imply a partial redundancy of eIF3B subunits with a clear functional compensation in the gametophyte. It will be critical to generate *eif3b1*;*eif3b2* double mutants to establish the exact role of the eIF3B subunits in the male and female gametophytes and to investigate more deeply on their functional complementation.
- Interestingly, *eif3b1* is embryo lethal, implying that the supporting role of eIF3B2 is restricted to the gametophyte and not during embryogenesis
- *eif3e* knock-out is male gametophytic lethal. Interestingly, the female gametophyte is unaffected and remains viable with just decreased fitness. This observation was unexpected considering unknown redundancy of eIF3E being the only subunit. The point of *eif3e* male gametophytic lethality is still unclear, and immediate future characterization on pollen tube growth and fertilization events will be necessary to establish exact point of failure. Similarly, cell fate specific markers will be used to monitor the female gametophyte fitness.
- Promoter activity of eIF3B1, eIF3B2 and eIF3E is low in growing pollen tube, confirming the readiness of translational initiation machinery in order to ensure quick metabolism after imbibition. It is the case in vegetative cell and in sperm cells, where subunits had been massively synthesized during pollen maturation.
- Subcellular localization of eIF3B1, eIF3B2 and eIF3E is mostly overlapping and show organized distribution of ribonucleoprotein complexes in mature pollen, opening new horizons of investigation on transcripts storage modality and importance and variability of subcellular localization for proper protein targeting in the male gametophyte. Translational process might be inter-dependent between the vegetative cell and sperm cells due to the close proximity of the eIF3 subunits localization between the connective structures (the

male germ unit) of the male gametophyte. Future experiments will involve investigating a relationship between eIF3 factors dynamics with polyA binding proteins (PABP) to understand translation initiation and transcripts fate, particularly transcripts storage. A co-localization with ER-markers as well as cytoskeleton markers and membrane markers for sperm cells in particular, will help to clarify translation hot spots in dry pollen as well as during the initiation of pollen tube growth.

- Regulation of eIF3E by COP9 signalosome appears not to be conserved or redundant with another regulation mechanism in the male gametophyte, because of the absence of adverse phenotypical effects and of eIF3E overexpression when COP9 is non-functional. This is an intriguing fact, suggesting several differences in regulatory pathways between sporophyte and the gametophyte.

We believe that our future investigations will continue to clarify those established facts and contribute to impacted publications.

Appendix 1: List of cited genes identification references

This list is a repertory of eIF3 subunits and COP9 subunits coding genes, clarifying multiple appellations for research simplification. Even though all *Arabidopsis* genes references can be found in TAIR database, research based on protein name can be laborious when gene ID is unknown – that is what motivated the creation of the below table. Ubiquitin 10, used for main reference as a constitutive gene, is also presented. Genes used in the frame of practical investigations in this thesis are in **blue.**

Gene ID	Common names	Protein
AT4G11420	ATEIF3A-1, ATTIF3A1, EIF3A, EIF3A-1, TIF3A1	eukaryotic translation initiation factor 3A, eIF3A
AT5G27640	**ATEIF3B-1, ATTIF3B1, EIF3B, EIF3B-1, TIF3B1**	**eukaryotic translation initiation factor 3B1, eIF3B1**
AT5G25780	**ATEIF3B-2, EIF3B, EIF3B-2**	**eukaryotic translation initiation factor 3B2, eIF3B2**
AT3G56150	ATEIF3C-1, ATTIF3C1, EIF3C, EIF3C-1, TIF3C1	eukaryotic translation initiation factor 3C1, eIF3C1
AT3G22860	ATEIF3C-2, ATTIF3C2, EIF3C-2, TIF3C2	eukaryotic translation initiation factor 3C2, eIF3C2
AT3G57290	**ATEIF3E-1, ATINT6, EIF3E, INT-6, INT6, TIF3E1**	**eukaryotic translation initiation factor 3E, eIF3E**
AT2G39990	ATEIF3F, EIF2, EIF3F	eukaryotic translation initiation factor 3F, eIF3F
AT1G10840	TIF3H1, EIF3H	eukaryotic translation initiation factor 3H1, eIF3H1
AT4G20980	EIF3D (poorly referenced)	eukaryotic translation initiation factor 3D, eIF3D
AT3G11400	ATEIF3G1, EIF3G1	eukaryotic translation initiation factor 3G1, eIF3G1
AT5G06000	ATEIF3G2, EIF3G2	eukaryotic translation initiation factor 3G2, eIF3G2
AT4G33250	ATTIF3K1, EIF3K, TIF3K1	eukaryotic translation initiation factor 3K, eIF3K
AT3G61140	**ATCSN1, ATFUS6, ATSK31, COP11, CSN1, EMB78, FUS6, FUSCA 6, SK31**	**constitutive photomorphogenesis subunit 1, CSN1**
AT2G26990	ATCSN2, COP12, CSN2, FUS12, FUSCA 12	constitutive photomorphogenesis subunit 2, CSN2
AT5G14250	COP13, CSN3, FUS11, FUSCA 11	constitutive photomorphogenesis subunit 3, CSN3
AT5G42970	ATS4, COP14, COP8,CSN4, EMB134, FUS4, FUS8, FUSCA 4, FUSCA 8	constitutive photomorphogenesis subunit 4, CSN4
AT1G22920	AJH1, CSN5A	constitutive photomorphogenesis subunit 5A, CSN5A
AT1G71230	AJH2, CSN5, CSN5B	constitutive photomorphogenesis subunit 5B, CSN5B
AT5G56280	CSN6A	constitutive photomorphogenesis subunit 6A, CSN6A
AT4G26430	CSN6B	constitutive photomorphogenesis subunit 6B, CSN6B
AT1G02090	**ATCSN7, COP15, CSN7, FUS5, FUSCA 5**	**constitutive photomorphogenesis subunit 7, CSN7**
AT4G14110	COP9, CSN8, EMB143, FUS7, FUSCA 7	constitutive photomorphogenesis subunit 8, CSN8
AT1G22760	**PABP3, PAB3, POLY(A) BINDING PROTEIN 3**	**polyA binding protein 3**
AT1G71770	**PABP5, PAB5, POLY(A)-BINDING PROTEIN 5**	**polyA binding protein 5**
AT4G05320	**POLYUBIQUITIN 10, UBI10, UBIQUITIN 10, UBQ10**	**one of five polyubiquitin genes in *A. thaliana***

Appendix 2: List of used mutant lines

This list presents acquired mutant lines, which are T-DNA insertions except for *fus 5.1*. For genes ID, see Appendix 1. Main features are given, as well as practical experience (right table part, dark blue titles) we got with those lines, especially genotyping and phenotypical background (consequence of multiple mutations) mainly observed in pollen, and its severity. Gene inducing resistance to kanamycin is normally included in all those insertions, but its expression is frequently silenced. For used genotyping primers, see Appendix 3. In this work, we had to deplore the poor quality of those lines; this appears as a recurrent fact for such lines. In their original state, *eif3b* and *fus5.1* lines have at least one advantage: they can serve as pedagogical material in order to show how pollen grain development can be affected, or what is not recommended to purchase, or, in a more optimistic way, how to deal with such impaired lines in order to obtain proper results, which was successfully done in this work. Note that crosses in order to obtain background-free lines are being done by us, which will lead to clean lines in near future.

Gene	Insertion coll. ID	NASC ID	Location	Gen.	Ecotype	Germ.	Antibio. sel.	Genot.	Background
eIF3B1	SALK_047620	N547620	Exon 8/11	HT	Col-0	Correct	Rarely works, unreliable	Worked	Occasional-severe (+ constant-mild?)
eIF3B2	SALK_126794C	N686765	Exon 10/11	HM	Col-0	Correct	Dysfunctional	Worked	Constant-severe
eIF3E	SALK_113234	N613234	3' UTR	HT	Col-0	Failed	?	?	?
	SALK_121004	N621004	Exon 3/8	HT	Col-0	Correct	Dysfunctional	Worked	Seems clean
CSN7/ FUS5	fus5.1, EMS	N5223	?	?	Col-0	Failed	?	?	?
	fus5.1, cop15-1, EMS	N3833	Exon 2/9	HT	Ler	Correct	None	Worked	Constant-severe
CSN1/ FUS6	fus6.1, Feldmann	N6260	Exon 1/6	HT	Wass.	Correct	Reliable (kanamycin)	Worked	Clean (good pheno and kan. segreg.)
	fus6.2, Feldmann (finally maybe not)	N6261	5' UTR (or different?)	HT	Wass.	Correct	? (kan. and Basta failed)	Failed	Seems clean

Appendix 3: List of used primers

This list is a commented repertory of all primers used for this work, specifically designed or available from stock. Melting temperatures (Tm) are those given by the furnisher most of time. Given annealing temperatures (Ta) having been used in practice and leading to (whenever possible) proper results, with Taq-based polymerase, and also Phusion™ for cloning, mentioned. For Gateway® cloning primers, gene-specific section Ta is given (this section is in capital letters). Also for cloning, the "1ib" and "2ib" refer to the number of additional bases following last codon before STOP codon for gene cloning into Entry clone in Gateway protocol, to ensure in-frame translation of following marker coding sequence. The "one inserted base" pattern is compatible with almost all Destination vectors, with exception of pFASTR07 which requires 2 bases insertion.

Purpose	Primer	Sequence (5'-3')	Tm	Used Ta	Practical comments
p:eIF3-B1 (promoter) cloning	p:eIF3B1 LP	aaaaagcaggctTAATCTCATCTTCC	66,2°C	50°C (spec), Phus 63 (spec) - 67°C	Operational
	p:eIF3B1 RP	agaaagctgggtGATTTCAACC	66,2°C		
p:eIF3-B2 (promoter) cloning	p:eIF3B2 LP	aaaaagcaggctACATATCATGCC	65,9°C	50°C (spec), Phus 62 (spec) - 66°C	Operational
	p:eIF3B2 RP	agaaagctgggtGATTTCGAATC	66,3°C		
p:eIF3-E (promoter) cloning	p:eIF3E LP	aaaaagcaggctCACTACCCC	65,3°C	52°C (spec), Phus 52 (spec) - 63°C	Operational
	p:eIF3E RP	agaaagctgggtCGTCGCTAATC	68,4°C		
eIF3-B1 cloning (for expression and complementation [+stop = ends with STOP codon])	eIF3B1 LP	aaaaagcaggctCTCATCTTCCTCCTC ACTCCCTACG	79,5°C	61°C (spec), Phus 65 (spec) - 72°C	Operational
	eIF3B1 RP 1ib	agaaagctgggtaCGACTCTTGAACG ATTTCCTCAGTC	78,7°C		
	eIF3B1 RP 2ib	agaaagctgggtaaCGACTCTTGAAC GATTTCCTCAGTG	78,9°C		
	eIF3B1 RP +stop	agaaagctgggtttaCGACTCTTGAAC GATTTCCTCAGTG	79,1°C		
eIF3-B1 cloning (for expression and complementation [+stop = ends with STOP codon])	eIF3B2 LP	aaaaagcaggctCATCATACGGTGTC CAATACCAG	77,6°C	59°C (spec), Phus 64 (spec) - 72°C	Operational
	eIF3B2 RP 1ib	agaaagctgggtaCATCAACTCTTGA ACAATTTCCTCAGTAAC	76,6°C		
	eIF3B2 RP 2ib	agaaagctgggtaaCATCAACTCTTGA ACAATTTCCTCAGTAAC	76,8°C		
	eIF3B2 RP +stop	agaaagctgggtttaCATCAACTCTTG AACAATTTCCTCAG	77,0°C		
eIF3-B1 cloning (for expression and complementation [+stop = ends with STOP codon])	eIF3E LP	aaaaagcaggctGGATTCCCTTGAGT CTCCTTGGAC	80,1°C	64°C (spec), Phus 71 (spec) - 72°C	Operational
	eIF3E RP 1ib	agaaagctgggtaGCGAGTTGCTTGC GCCTG	83,2°C		
	eIF3E RP 2ib	agaaagctgggtaaGCGAGTTCGTTG CGCCTG	83,3°C		
	eIF3E RP +stop	agaaagctgggtctaGCGAGTTGCTTG CGC	79,0°C		
eIF3-B1 sequencing	B1SP-F1	CTCTCGGCTGATCTCTG	56,9°C	Never used as PCR primers, used for Sanger sequencing by	Operational, very rare unsuccessful results that were always solved after 2nd sample
	B1SP-F2	CCTTGATGGTGCAAAGC	60,4°C		
	B1SP-F3	CCCTGGGGTATGTGTAG	56,0°C		
	B1SP-F4	GTCTCATGCGTTATCAGC	56,7°C		

	B1SP-F5	CAACCTGCGAAGGTATG	57,6°C	GATC Biotech (Germany)	sending in those rare cases
	B1SP-F6	CGACTGGAAGGTCCTAC	55,3°C		
eIF3-B2 sequencing	B2SP-F1	AAGCCTATATCTCCCGC	56,7°C		Operational
	B2SP-F2	CCTAGGCACACACTCTC	53,6°C		
	B2SP-F3	CAAGTTGGACAAGTCTCAC	55,5°C		
	B2SP-F4	GCGTCTCATGCGTTATC	57,7°C		
	B2SP-F5	AGGTGGTGGAAACCAAC	58,2°C		
	B2SP-F6	TCACCAATTGCTGATGTTG	60,8°C		
eIF3-E sequencing	ESP-F1	GAGACCTAACAGACCTCG	54,5°C		Operational
	ESP-F2	CCTTCAAGAGCGTCAGC	59,8°C		
	ESP-F3	CTTGAAGAGCTTAACCGTC	56,6°C		
	ESP-F4	AGCAAGAGCACTACTCC	52,4°C		
eIF3B1 isoforms investigation	F iso B1 (F)	CCAGGATGACCAGTCTG	57,3°C	54°C	Operational
	R iso B1 (R1)	TCCCACTCCTCCTTCAC	58,6°C		
	R intron B1 (R2)	ACAACCTAGTTTGGGCTC	56,6°C		
Genotyping, T-DNA insertion specific primers	Salk LBb1	GCGTGGACCGCTTGCTGCAACT	71,4°C	52-55°C	Both used with Salk lines, with similar good results
	Salk LB1.3	ATTTTGCCGATTTCGGAAC	58,5°C	52-55°C	
	Feldmann LB	GATGCACTCGAAATCAGCCAATTTTAGAC	71,2°C	55°C	Used for Fus 6.1 line, operational
eIF3-B1 genotyping gene-specific	eIF3B1 T-DNA LP	ACAGTAGGACCTTCCAGTCGG	64,3°C	52-55°C	Successfully used in 3 primers mix
	eIF3B1 T-DNA RP	GTTTTCAATTGGAGGACCTGG	64,4°C		
eIF3-B2 genotyping gene-specific	eIF3B2 T-DNA LP	GGTACTGCTATCCAACAACGC	63,3°C	55°C	Acceptable results in 3 primers mix
	eIF3B2 T-DNA RP	GTTTCAAAGCTCGCAACTTTG	63,7°C		
eIF3-E genotyping gene-specific	eIF3E T-DNA LP	AACCTGGACAGACACTTGGTG	64,1°C	55°C	Have to separate primers, not to mix LP + RP + LB
	eIF3E T-DNA RP	AACGCAAGGAAATAGATGGTG	62,7°C		
Fus 5.1 genotyping gene-specific	Fus 5.1-Dde1-F	AGGCCTTGGCCCAGAAACTACG	71,0°C	52-54°C	Operational, restriction with DdeI for genotyping
	Fus 5.1-Dde1-R1	CACTGACCATTTGCTCTCTCTTG	68,2°C		
Fus 6.1/2 genotyping gene-specific	Fus 6 LP	AATGTTCTGTTGTTCCCATTCC	63,7°C	55°C	Successfully used in 3 primers mix
	Fus 6 RP	AGCATCTCCGAGCATACCAC	64,2°C		
eIF3-B1 semiQ RT PCR	eIF3-B1 Up-F	AGTCATTCGTTCTGGCCCTG	66,4°C	51-54°C	Variable results
	eIF3-B1 Up-R	AACAGGCCAAGAGGCACCA	68,2°C		
	eIF3-B1 Down-F	TGCCCTAGTCCAAATCCCGA	68,7°C	51-55°C	Operational
	eIF3-B1 Down-R	TGTCACTGCGGTTGCAACG	69,8°C		
eIF3-B2 semiQ RT PCR	eIF3-B2 Up-F	GTTCCTGAACAAGGTGGTGG	64,4°C	51-55°C	Operational
	eIF3-B2 Up-R	TCCAGTTGGGTCCCATTCGA	69,9°C		
	eIF3-B2 Down-F	TGGTTTACCGGATATCGAAGG	62,6°C	51-54°C	Operational
	eIF3-B2 Down-R	ATCAACTCTTGAACAATTTCCTC	60,1°C		
eIF3-E semiQ RT PCR	eIF3-E Up-F	ACAGAACTATGACCTGACG	54,9°C	52°C	Operational
	eIF3-E Up-R	TGGTAGCGTTCCTTGAGCAT	64,6°C		
	eIF3-E Down-F	TCGCCGTTAAACCAGGTGCA	70,7°C	57°C	Operational
	eIF3-E Down-R	CAAACACACATGCCAGGAAC	64,1°C		
Fus-5.1 semiQ RT PCR	Fus-5.1 Up-F	CATCGAAGCCACATCGCATC	69,0°C	55°C	Not really used, doubt subsists on results
	Fus-5.1 Up-R	GTGAGGACAGTGAGCTGCT	60,9°C		
	Fus-5.1 Down-F	CACGTCAGAGAATCTGCTCAT	62,1°C	55°C	Operational
	Fus-5.1 Down-R	CCTTGTTACAGGATGCCTCCTC	65,8°C		
Fus-6.1/2 semiQ RT PCR	Fus-6 Down-F	AAGCTGGAGAATGAGCTCAG	61,3°C	55°C	Operational
	Fus-6 Down-R	AGCATCTCCGAGCATACCAC	64,2°C		

References

Used internet resources:

The Arabidopsis Information Resource (TAIR) - https://www.arabidopsis.org (large database)

Arabidopsis eFP Browser - www.bar.utoronto.ca (gene expression in tissues)

Web of Science - https://www.webofknowledge.com (literature database)

Used literature:

AITKEN, C. E. et al. Eukaryotic translation initiation factor 3 plays distinct roles at the mRNA entry and exit channels of the ribosomal preinitiation complex. **Elife,** v. 5, p. 37, Oct 2016. ISSN 2050-084X. Available at: < <Go to ISI>://WOS:000390805100001 >.

AITKEN, C. E.; LORSCH, J. R. A mechanistic overview of translation initiation in eukaryotes. **Nature Structural & Molecular Biology,** v. 19, n. 6, p. 568-576, Jun 2012. ISSN 1545-9993. Available at: < <Go to ISI>://WOS:000304958200003 >.

BEDINGER, P. THE REMARKABLE BIOLOGY OF POLLEN. **Plant Cell,** v. 4, n. 8, p. 879-887, Aug 1992. ISSN 1040-4651.

BOAVIDA, L. C.; MCCORMICK, S. Temperature as a determinant factor for increased and reproducible in vitro pollen germination in Arabidopsis thaliana. **Plant Journal,** v. 52, n. 3, p. 570-582, Nov 2007. ISSN 0960-7412. Available at: < <Go to ISI>://WOS:000250298600015 >.

BORGES, F. et al. Comparative transcriptomics of Arabidopsis sperm cells. **Plant Physiology,** v. 148, n. 2, p. 1168-1181, Oct 2008. ISSN 0032-0889. Available at: < <Go to ISI>://WOS:000259810400041 >.

BURKS, E. A. et al. Plant initiation factor 3 subunit composition resembles mammalian initiation factor 3 and has a novel subunit. **Journal of Biological Chemistry,** v. 276, n. 3, p. 2122-2131, Jan 2001. ISSN 0021-9258. Available at: < <Go to ISI>://WOS:000166528000065 >.

CHRISTENSEN, C. A. et al. Megagametogenesis in Arabidopsis wild type and the Gf mutant. **Sexual Plant Reproduction,** v. 10, n. 1, p. 49-64, Feb 1997. ISSN 0934-0882. Available at: < <Go to ISI>://WOS:A1997WN66500008 >.

CHUNG, D.; DELLAIRE, G. The Role of the COP9 Signalosome and Neddylation in DNA Damage Signaling and Repair. **Biomolecules,** v. 5, n. 4, p. 2388-2416, Dec 2015. ISSN 2218-273X.

CLOUGH, S. J.; BENT, A. F. Floral dip: a simplified method for Agrobacterium-mediated transformation of Arabidopsis thaliana. **Plant Journal,** v. 16, n. 6, p. 735-743, Dec 1998. ISSN 0960-7412. Available at: < <Go to ISI>://WOS:000078001900010 >.

DOHMANN, E. M. N. et al. The Arabidopsis COP9 signalosome is essential for G2 phase progression and genomic stability. **Development,** v. 135, n. 11, p. 2013-2022, Jun 2008. ISSN 0950-1991. Available at: < <Go to ISI>://WOS:000255747700012 >.

DRESSELHAUS, T.; FRANKLIN-TONG, N. MaleFemale Crosstalk during Pollen Germination, Tube Growth and Guidance, and Double Fertilization. **Molecular Plant,** v. 6, n. 4, p. 1018-1036, Jul 2013. ISSN 1674-2052. Available at: < <Go to ISI>://WOS:000322410700003 >.

ELANTAK, L. et al. Structure of eIF3b RNA recognition motif and its interaction with eIF3j - Structural insights into the recruitment of eIF3b to the 40 S ribosomal subunit. **Journal of Biological Chemistry,** v. 282, n. 11, p. 8165-8174, Mar 2007. ISSN 0021-9258. Available at: < <Go to ISI>://WOS:000245081000049 >.

FRANCIOSINI, A. et al. The COP9 SIGNALOSOME Is Required for Postembryonic Meristem Maintenance in Arabidopsis thaliana. **Molecular Plant,** v. 8, n. 11, p. 1623-1634, Nov 2015. ISSN 1674-2052. Available at: < <Go to ISI>://WOS:000365049200005 >.

GALLAND, M. et al. Dynamic Proteomics Emphasizes the Importance of Selective mRNA Translation and Protein Turnover during Arabidopsis Seed Germination. **Molecular & Cellular Proteomics,** v. 13, n. 1, p. 252-268, Jan 2014. ISSN 1535-9476.

HAMAMURA, Y.; NAGAHARA, S.; HIGASHIYAMA, T. Double fertilization on the move. **Current Opinion in Plant Biology,** v. 15, n. 1, p. 70-77, Feb 2012. ISSN 1369-5266. Available at: < <Go to ISI>://WOS:000300813000012 >.

HINNEBUSCH, A. G. eIF3: a versatile scaffold for translation initiation complexes. **Trends in Biochemical Sciences,** v. 31, n. 10, p. 553-562, Oct 2006. ISSN 0968-0004. Available at: < <Go to ISI>://WOS:000241841500004 >.

HONYS, D. et al. The translationally repressed pollen-specific ntp303 mRNA is stored in non-polysomal mRNPs during pollen maturation. **Sexual Plant Reproduction,** v. 13, n. 3, p. 135-144, Nov 2000. ISSN 0934-0882. Available at: < <Go to ISI>://WOS:000165478800003 >.

_____. Cytoskeleton-Associated Large RNP Complexes in Tobacco Male Gametophyte (EPPs) Are Associated with Ribosomes and Are Involved in Protein Synthesis, Processing, and Localization. **Journal of Proteome Research,** v. 8, n. 4, p. 2015-2031, Apr 2009. ISSN 1535-3893. Available at: < <Go to ISI>://WOS:000264928200040 >.

HULZINK, R. J. M. et al. The 5 '-untranslated region of the ntp303 gene strongly enhances translation during pollen tube growth, but not during pollen maturation. **Plant Physiology,** v. 129, n. 1, p. 342-353, May 2002. ISSN 0032-0889.

IADEVAIA, V. et al. All translation elongation factors and the e, f, and h subunits of translation initiation factor 3 are encoded by 5 '-terminal oligopyrimidine (TOP) mRNAs. **Rna,** v. 14, n. 9, p. 1730-1736, Sep 2008. ISSN 1355-8382. Available at: < <Go to ISI>://WOS:000258996100005 >.

KANG, D. M. et al. A gain-of-function phenotype conferred by over-expression of functional subunits of the COP9 signalosome in Arabidopsis. **Plant Journal,** v. 23, n. 5, p. 597-608, Sep 2000. ISSN 0960-7412.

KARNIOL, B.; CHAMOVITZ, D. A. The COP9 signalosome: from light signaling to general developmental regulation and back. **Current Opinion in Plant Biology,** v. 3, n. 5, p. 387-393, Oct 2000. ISSN 1369-5266.

KLYACHKO, N. et al. Interaction of plant polysomes with the actin cytoskeleton. **Cell Biology International,** v. 24, n. 6, p. 351-358, 2000. ISSN 1065-6995. Available at: < <Go to ISI>://WOS:000087596200004 >.

KOLUPAEVA, V. G. et al. Binding of eukaryotic initiation factor 3 to ribosomal 40S subunits and its role in ribosomal dissociation and anti-association. **Rna-a Publication of the Rna Society,** v. 11, n. 4, p. 470-486, Apr 2005. ISSN 1355-8382. Available at: < <Go to ISI>://WOS:000227860500012 >.

KOSOWSKA, M. et al. Water-deficit-induced changes in cytoskeleton-bound and other polysomal populations in embryonic tissue during triticale caryopsis germination. **Acta Physiologiae Plantarum,** v. 26, n. 1, p. 67-74, 2004. ISSN 0137-5881. Available at: < <Go to ISI>://WOS:000220843600007 >.

LEFEBVRE, A. K. et al. Translation initiation factor eIF4G-1 binds to eIF3 through the eIF3e subunit. **Journal of Biological Chemistry,** v. 281, n. 32, p. 22917-22932, Aug 2006. ISSN 0021-9258. Available at: < <Go to ISI>://WOS:000239542600054 >.

LIN, S. Y. et al. Profiling of Translatomes of in Vivo-Grown Pollen Tubes Reveals Genes with Roles in Micropylar Guidance during Pollination in Arabidopsis. **Plant Cell,** v. 26, n. 2, p. 602-618, Feb 2014. ISSN 1040-4651. Available at: < <Go to ISI>://WOS:000333688300009 >.

LIU, Y. et al. Translation Initiation Factor eIF3b Contains a Nine-Bladed beta-Propeller and Interacts with the 40S Ribosomal Subunit. **Structure,** v. 22, n. 6, p. 923-930, Jun 2014. ISSN 0969-2126. Available at: < <Go to ISI>://WOS:000338206200014 >.

LORAINE, A. E. et al. RNA-Seq of Arabidopsis Pollen Uncovers Novel Transcription and Alternative Splicing. **Plant Physiology,** v. 162, n. 2, p. 1092-1109, Jun 2013. ISSN 0032-0889. Available at: < <Go to ISI>://WOS:000319819900043 >.

M.W.KING. **Translation of Proteins**. http://themedicalbiochemistrypage.org 2015.

MASUTANI, M. et al. Reconstitution reveals the functional core of mammalian eIF3. **Embo Journal,** v. 26, n. 14, p. 3373-3383, Jul 2007. ISSN 0261-4189. Available at: < <Go to ISI>://WOS:000248675600009 >.

MCCORMICK, S. Control of male gametophyte development. **Plant Cell,** v. 16, p. S142-S153, 2004. ISSN 1040-4651. Available at: < <Go to ISI>://WOS:000222210600013 >.

MCCUE, A. D. et al. Cytoplasmic connection of sperm cells to the pollen vegetative cell nucleus: potential roles of the male germ unit revisited. **Journal of Experimental Botany,** v. 62, n. 5, p. 1621-1631, Mar 2011. ISSN 0022-0957. Available at: < <Go to ISI>://WOS:000288029700009 >.

MOHAMMAD, M. P. et al. In vivo evidence that eIF3 stays bound to ribosomes elongating and terminating on short upstream ORFs to promote reinitiation. **Nucleic Acids Research,** v. 45, n. 5, p. 2658-2674, Mar 2017. ISSN 0305-1048. Available at: < <Go to ISI>://WOS:000397286600041 >.

MORRIS, C.; JALINOT, P. Silencing of human Int-6 impairs mitosis progression and inhibits cyclin B-Cdk1 activation. **Oncogene,** v. 24, n. 7, p. 1203-1211, Feb 2005. ISSN 0950-9232. Available at: < <Go to ISI>://WOS:000226898700007 >.

MUENCH, D. G.; ZHANG, C.; DAHODWALA, M. Control of cytoplasmic translation in plants. **Wiley Interdisciplinary Reviews-Rna,** v. 3, n. 2, p. 178-194, Mar-Apr 2012. ISSN 1757-7004. Available at: < <Go to ISI>://WOS:000301865800003 >.

PAIN, V. M. Initiation of protein synthesis in eukaryotic cells. **European Journal of Biochemistry,** v. 236, n. 3, p. 747-771, Mar 1996. ISSN 0014-2956. Available at: < <Go to ISI>://WOS:A1996UX16200001 >.

ROY. **Translational Regulation in Arabidopsis thaliana: Genetic and Functional Characterization of Eukaryotic Initiation Factor 3. PhD diss.** BIJOYITA. University of Tennessee 2010.

ROY, B.; COPENHAVER, G. P.; VON ARNIM, A. G. Fluorescence-Tagged Transgenic Lines Reveal Genetic Defects in Pollen Growth-Application to the Eif3 Complex. **Plos One,** v. 6, n. 3, p. 7, Mar 2011. ISSN 1932-6203. Available at: < <Go to ISI>://WOS:000288099800030 >.

ROZEN, S. et al. CSNAP Is a Stoichiometric Subunit of the COP9 Signalosome. **Cell Reports,** v. 13, n. 3, p. 585-598, Oct 2015. ISSN 2211-1247.

RUTLEY, N.; TWELL, D. A decade of pollen transcriptomics. **Plant Reproduction,** v. 28, n. 2, p. 73-89, Jun 2015. ISSN 2194-7953. Available at: < <Go to ISI>://WOS:000354500200001 >.

SCHWECHHEIMER, C. The COP9 signalosome (CSN): an evolutionary conserved proteolysis regulator in eukaryotic development. **Biochimica Et Biophysica Acta-Molecular Cell Research,** v. 1695, n. 1-3, p. 45-54, Nov 2004. ISSN 0167-4889.

SESEN, J. et al. The bad, the good and eIF3e/INT6. **Frontiers in Bioscience-Landmark,** v. 22, p. 1-20, Jan 2017. ISSN 1093-9946. Available at: < <Go to ISI>://WOS:000397908600001 >.

STUGER, R. et al. Messenger RNA-binding properties of nonpolysomal ribonucleoproteins from heat-stressed tomato cells. **Plant Physiology,** v. 120, n. 1, p. 23-31, May 1999. ISSN 0032-0889. Available at: < <Go to ISI>://WOS:000080329200004 >.

TWELL, D. Male gametogenesis and germline specification in flowering plants. **Sexual Plant Reproduction,** v. 24, n. 2, p. 149-160, Jun 2011. ISSN 0934-0882. Available at: < <Go to ISI>://WOS:000290800200007 >.

VON ARNIM, A. G.; CHAMOVITZ, D. A. Protein homeostasis: A degrading role for Int6/eIF3e. **Current Biology,** v. 13, n. 8, p. R323-R325, Apr 2003. ISSN 0960-9822. Available at: < <Go to ISI>://WOS:000182490000015 >.

WALSH, D.; MOHR, I. Coupling 40S ribosome recruitment to modification of a cap-binding initiation factor by eIF3 subunit e. **Genes & Development,** v. 28, n. 8, p. 835-840, Apr 2014. ISSN 0890-9369. Available at: < <Go to ISI>://WOS:000334585400004 >.

WANG, W. Y. et al. The Rice Eukaryotic Translation Initiation Factor 3 Subunit e (OseIF3e) Influences Organ Size and Pollen Maturation. **Frontiers in Plant Science,** v. 7, p. 14, Sep 2016. ISSN 1664-462X. Available at: < <Go to ISI>://WOS:000383437600001 >.

WEI, N.; SERINO, G.; DENG, X. W. The COP9 signalosome: more than a protease. **Trends in Biochemical Sciences,** v. 33, n. 12, p. 592-600, Dec 2008. ISSN 0968-0004.

XIA, C. A. et al. The Arabidopsis eukaryotic translation initiation factor 3, subunit F (AteIF3f), is required for pollen germination and embryogenesis. **Plant Journal,** v. 63, n. 2, p. 189-202, Jul 2010. ISSN 0960-7412. Available at: < <Go to ISI>://WOS:000279750800002 >.

YAHALOM, A. et al. Arabidopsis eIF3e is regulated by the COP9 signalosome and has an impact on development and protein translation. **Plant Journal,** v. 53, n. 2, p. 300-311, Jan 2008. ISSN 0960-7412. Available at: < <Go to ISI>://WOS:000252109500009 >.

_____. Arabidopsis eIF3e (INT-6) associates with both eIF3c and the COP9 signalosome subunit CSN7. **Journal of Biological Chemistry,** v. 276, n. 1, p. 334-340, Jan 2001. ISSN 0021-9258. Available at: < <Go to ISI>://WOS:000166280700046 >.